DYNAMIC STRESS-STRAIN MODELS FOR SOIL

USING WAVE PROPAGATION

By

MICHAEL FRED KOCHER

Bachelor of Science
University of Nebraska-Lincoln
Lincoln, Nebraska
1979

Master of Science
University of Nebraska-Lincoln
Lincoln, Nebraska
1983

Submitted to the Faculty of the
Graduate College of the
Oklahoma State University
in partial fulfillment of
the requirements for
the Degree of
DOCTOR OF PHILOSOPHY
May, 1986

DYNAMIC STRESS-STRAIN MODELS FOR SOIL

USING WAVE PROPAGATION

Thesis Approved:

Thesis Adviser

Dean of the Graduate College

ACKNOWLEDGEMENTS

Although my name is the only one on the cover, this dissertation is certainly not the result of my work alone. Much of the credit should go to other people, especially Dr. James D. Summers, my research adviser, and the rest of my committee members. I would like to thank Dr. Summers for his friendship, support and encouragement, as well as all the help he has provided in each phase of this research project. Thanks also to Professor David Batchelder, who served as chairman of my graduate committee until his retirement, Dr. Richard Whitney, who took over chairmanship of the committee, and Dr. John Solie and Dr. John Stone who also served on my graduate committee. I would also like to thank Oklahoma State University and the Agricultural Engineering Department for the monetary support in terms of project funds, a one-semester teaching assistantship and a research assistantship. Without that support this project would never have started.

Additional thanks to Galen McLaughlin at the Oklahoma Cotton Research Station in Chickasha for all his help in obtaining the soil samples used in this work. Galen's ideas and help made that task much easier and faster than I anticipated. Norvil Cole, Robert Harrington and Cliff Riley were instrumental in helping with the design and building the soil sampler, and I thank them. Richard Greenwell also spent more than a few hours helping me process all the data (98 floppy disks full) and I owe him thanks.

I would also like to thank my many friends among the faculty, staff and graduate students in the Agricultural Engineering Department. Without their friendship and help this doctoral program would have been much less lively and enjoyable.

Last but not least, I would like to thank my wife, Jodi, for all her love, support and understanding during this program. She has patiently suffered through my grumpy days when things haven't gone well, days when I've been too preoccupied with qualifying exams and the like, and shared the happy times when things have gone well. I would also like to thank Mom and Dad Kocher, Grandpa Kocher, Mom and Dad Wolford, Grandpa Wolford, Grandpa Innes, Eric, Bruce and Joan, Jeanne, Carrie, Steve, Danna and Megan, Greg, Pam and Adam and the rest of my extended family for their support and understanding through this program.

TABLE OF CONTENTS

LIST OF TABLES

LIST OF FIGURES

Figure Page

LIST OF SYMBOLS

A - Cross sectional area of the soil sample

C_1, C_2 - Constant coefficients that satisfy the wave equation

dx - Length of a small element of the soil sample

E - Static stress-strain modulus

E' - Complex stress-strain proportionality constant

j - Imaginary number

k' - As defined in text

L - Length of soil sample

m - Mass of thin disk and accelerometer at top of soil sample

M - Mass of a small cross-sectional element of the soil sample

t - Time

u - Displacement of a point in the soil sample

x - Distance from bottom of soil sample to point of interest

X - A function of x that satisfies the wave equation

X'' - The second derivative of X with respect to x

α - Parameter in proposed stress-strain model

β - Coefficient for viscous damping per unit length

δ - Storage modulus in the complex modulus stress-strain model

ε - Strain

λ - Magnitude of maximum displacement at bottom of soil sample

ξ - Parameter in proposed stress-strain model

ρ - Soil sample mass density at time of dynamic test

σ - Stress

ϕ' - As defined in text

ω - Vibration frequency

CHAPTER I

INTRODUCTION AND OBJECTIVES

Introduction

Soil is an important part of agriculture, and the feeding of the world's population. Most plant material grown to meet the demand for food is planted in soil. Soil serves plants as a structural base and a medium for supplying plant nourishing materials.

In today's agriculture, man uses machines to change the soil towards conditions more suitable for plant growth and maximum yield. Tractors pull tools or implements through the soil. Therefore, soil must have adequate strength to support tractors and resist tractive forces for tractor propulsion. The soil must also yield to forces exerted by tillage tools and change to a condition suitable for plant growth.

Designers of tillage and tractive devices need to know the relationships between soil properties and strength. Gill and Vanden Berg (1968) concluded the obvious way to describe soil strength was by using stress-strain equations to describe the interaction between forces and displacements. The importance of stress-strain relationships then, is to provide designers of tillage and tractive devices a method to predict performance of designs. Designs which do the best job can then be produced and used. A soil stress-strain model which can be used to predict soil displacement has not been developed.

Objectives

The overall objectives of this research were to develop a test using one-dimensional wave propagation and evaluate four proposed dynamic soil stress-strain models. The specific objectives were:

1. Derive and solve the differential equation describing one-dimensional wave propagation through a cylindrical soil sample assuming a second-order viscoelastic stress-strain model.
2. Develop a method for attaching soil samples to a shaker head, and accelerometers to soil samples.
3. Develop a probe for extracting soil samples which will minimize sample disturbance during extraction.
4. Determine appropriate frequency and acceleration ranges for the test.
5. Determine which of the stress-strain models best describes the dynamic behavior of the soil.
6. Determine if the dynamic stress-strain behavior of the soil is independent of the original orientation of the sample in the field.

7. Validate the stress-strain model by comparing model predictions with measured stress data.

CHAPTER II

LITERATURE REVIEW

Soil-Machine System Performance Prediction

Designers of machines that work soil need methods of predicting machine performance so design parameters can be optimized to get the "best" machine. Reaves and Schafer (1971) wrote that three methods are used for designing machines that manipulate soil: trial and error, theoretical analysis and model theory. The trial and error method was not recommended because it is expensive and requires experience with the particular system and experimental methods to obtain good results. Analytical methods were described as difficult to use because of the complexity of the analyses required. A major drawback to model theory is the requirement that all pertinent soil properties must be known. Frietag et al. (1969) and Reaves and Schafer (1971) indicated soil properties relating to soil-machine systems are not well understood, measured or predicted. Despite this, researchers have worked to obtain useable methods for predicting soil-machine system performance from soil properties.

Methods for predicting tractive effort have been developed, but are not satisfactory for design. Wismer and

Luth (1974) used similitude studies to arrive at a tractive force prediction equation that included both soil and wheel characteristics. The soil parameter involved was the ASAE standard penetrometer cone index value. Their work in laboratory soils has been difficult to use in the field to predict tractive effort (Bloome et al., 1983, Clark, 1984 and Hayes and Ligon, 1977).

Upadhaya et al. (1984) developed a finite element model of the soil-tire interface to predict tractive forces. The majority of the model involved modeling the cords, plies, lugs and layers of the tire. Soil was represented as a linearized spring. This was noted as the weak point of the model. They anticipated improving representation of the soil to improve model prediction capabilities.

Stress-Strain Models

The main difficulties researchers have experienced have been related to descriptions of soil behavior, or soil mechanics. Vanden Berg (1961) wrote:

> An accurate soil mechanics requires accurate stress-strain relationships. The word 'mechanics' itself implies stress and strain since it is defined as that part of physical sciences which treats the action of forces on bodies. The results of these actions in the case of soils are deformations. Since stress is a measure of forces in soil and strain is a measure of deformation, soil mechanics should include both quantities.

Vanden Berg (1961) also wrote that accurate stress-strain relationships for a general soil mechanics must be developed. Kitani and Persson (1967) placed importance on development of stress-strain relationships for soil.

Classical soil mechanics texts such as Lambe and Whitman (1979) do not emphasize use of stress-strain relationships for soil. Instead they use other methods such as limit analysis based on failure criterion (Mohr-Coulomb failure law). Stress-strain relationships probably will not be used in place of these other methods until sucessful applications of the stress-strain relationships have proved their worth.

Attempts have been made to develop appropriate stress-strain relationships for soils. Both elastic and plastic theories have been used. Taylor and Vanden Berg (1966) developed a stress-strain relationship to predict maximum shearing stress as a function of normal stress and displacement. This is more of a limit approach rather than a stress-strain relationship.

Duncan (1980) reported on a hyperbolic stress-strain model which used tangent values for Young's modulus that varied with magnitude of stress, and values for bulk modulus that varied with confining stress. A limitation for this model is that it is based on Hooke's law (elasticity) so it is useful only for predicting movements in stable masses.

Salencon (1977) discussed applications of plastic theory in soil mechanics. Soil behavior does not follow true plastic behavior. A truly plastic material will not deform until the yield criterion is met, and then it flows according to the flow rule. Use of plastic theory substitutes yield criterion and flow rules for stress-strain relationships.

Christian (1966) used incremental plastic theory where the strain rate is a function of the existing stresses and the stress rate. This theory can be further divided into perfectly plastic and strain hardening categories. Several different approaches and tests were conducted with the theory implemented in a computer model. Christian (1966) emphasized the usefulness of computer models and recommended more theoretical research aimed at general stress-strain relationships.

Dynamic Stress-Strain Models

Gill and Vanden Berg (1968), Persson (1969) and Johnson et al. (1972) agreed that stress-strain behavior of soil is a function of time. Persson (1969) concluded that constitutive equations did not include rate of deformation. Flenniken et al. (1977) found soil strengths in dynamic unconfined compression 3 to 5 times greater than quasi-static strength. Stafford and Tanner (1983) found that peak cohesion varied as the logarithm of the deformation rate. They also noted little increase in shear strength at deformation rates above 1 m/s. These studies show that dynamic tests should be used to determine dynamic response of soil.

Bernhard and Finelli (1954) and DeRoock and Cooper (1967) used impact methods for determining the velocity of compressive waves through soil. Bernhard and Finelli were interested in predicting the dynamic modulus of elasticity, while DeRoock and Cooper were interested in relating wave velocity to soil strength. Both efforts yielded reliable results. DeRoock and Cooper recommended energy dissipation in soil be measured.

Richart et al. (1970) and Hardin and Richart (1963) cited examples of vibratory tests for measuring strength of foundation soils. Richart et al. (1970) noted the magnitude of damping in the test soils (mostly sands) did not justify adopting viscoelastic theory. For that reason their analyses were based on elastic theory.

McNiven and Brown (1963) noted that it may not have been proper for Hardin and Richart (1963) to use the differential equations of motion for elastic bodies to determine wave velocities of non-elastic materials. Relative wave velocities of different materials were said to be a function of effective moduli and damping characteristics.

Viscoelastic Dynamic Stress-Strain Models

Vanden Berg (1961) wrote that neither elastic nor plastic theory provided useable models of soil behavior. Gill and Vanden Berg (1968) concluded elastic and plastic theories do not describe time dependency of soil deformation. They cited work McMurdie (1963) accomplished using viscoelastic theory as showing promise. Mohsenin (1970) described viscoelasticity as, "a combined liquid-like and solid-like behavior in which the stress-strain relationship is time dependent." Thus, it appears that viscoelastic theory may work well to describe the stress-strain-time relationship of soil.

McMurdie (1963) used a four element viscoelastic model to describe creep behavior in soil. He did not think the model described creep behavior properly, but did recommend further investigation into the viscoelastic behavior of soil.

Ram and Gupta (1972), Gupta and Pandya (1967) and Aref et al. (1975) used viscoelastic stress-strain equations in their work. Ram and Gupta (1972) used creep tests to develop a relationship between total compressive strain, strain rate at yield point, creep retardation time, yield stress, instantaneous and delayed elastic moduli, and a flow constant. Use of this equation requires evaluation of 6 parameters and a simpler relationship is desireable.

Gupta and Pandya (1967) were successful in predicting the average compressive stress on a vertical plate pulled through soil. Their prediction equation related compressive stress to the velocities of the plate and the compression wave, rather than relating stress directly to strain. Strain rate is indirectly included in the equation as the plate velocity.

Aref et al. (1975) used triaxial compression tests at strain rates of 0.018 and 0.254 percent per minute to determine a dynamic stress-strain model for soil. The model related stress directly to a linear combination of strain and strain rate. They hinted that the relationship should be tested at strain rates more closely resembling actual field conditions.

Theoretical Mechanics Approach

Results from several experiments have shown a viscoelastic stress-strain equation may be used to model dynamic behavior of soil. Viscoelastic theory has been used with success in stress-strain models for other materials. The approach used by Smith et al. (1978) is a theoretical mechanics approach based on assumptions of possible stress-strain relationships. Smith et al. (1978) evaluated complex modulus, viscous and first-order viscoelastic stress-strain models for the dynamic behavior of prosthetic urethane compounds. The one-dimensional wave equation was solved analytically for the displacement. The displacement equation was then used to determine the stress resulting from sinusoidal extension of a specimen. Measurements of dynamic stress were compared with predicted values from the three models. The first-order viscoelastic model fit the experimental data best. A further modification to include a dependency on the frequency of excitation provided a good representation of the experimental data.

The approach used by Smith et al. (1978) has sound basis in theoretical mechanics. Application of their methods to soils for development of a stress-strain model is promising. A viscoelastic stress-strain model shows potential for describing dynamic behavior of soil.

CHAPTER III

THEORY

The test procedure selected for evaluation of dynamic soil stress-strain models was a simple dynamic system involving a prismatic rod (cylindrical soil sample) in longitudinal oscillation (Figure 1). One end of the soil sample was attached to an electromagnetic shaker which induced sinusoidal displacement. Attached to the other end of the soil sample was a mass consisting of a thin disk and an accelerometer.

A free body diagram of a small cross section of the soil sample is shown in Figure 2. By Newton's second law, the sum of the forces acting on the element is equal to the mass times the acceleration of the element.

$$A(\sigma + \frac{\partial \sigma}{\partial x} dx) - A\sigma = M \frac{\partial^2 u}{\partial t^2} \tag{1}$$

The displacement of the element in the x direction is denoted as u. The mass of the element is equal to the mass density multiplied by the cross sectional area and the length of the element. Substituting into equation (1) and simplifying yields:

$$\frac{\partial \sigma}{\partial x} = \rho \frac{\partial^2 u}{\partial t^2} \tag{2}$$

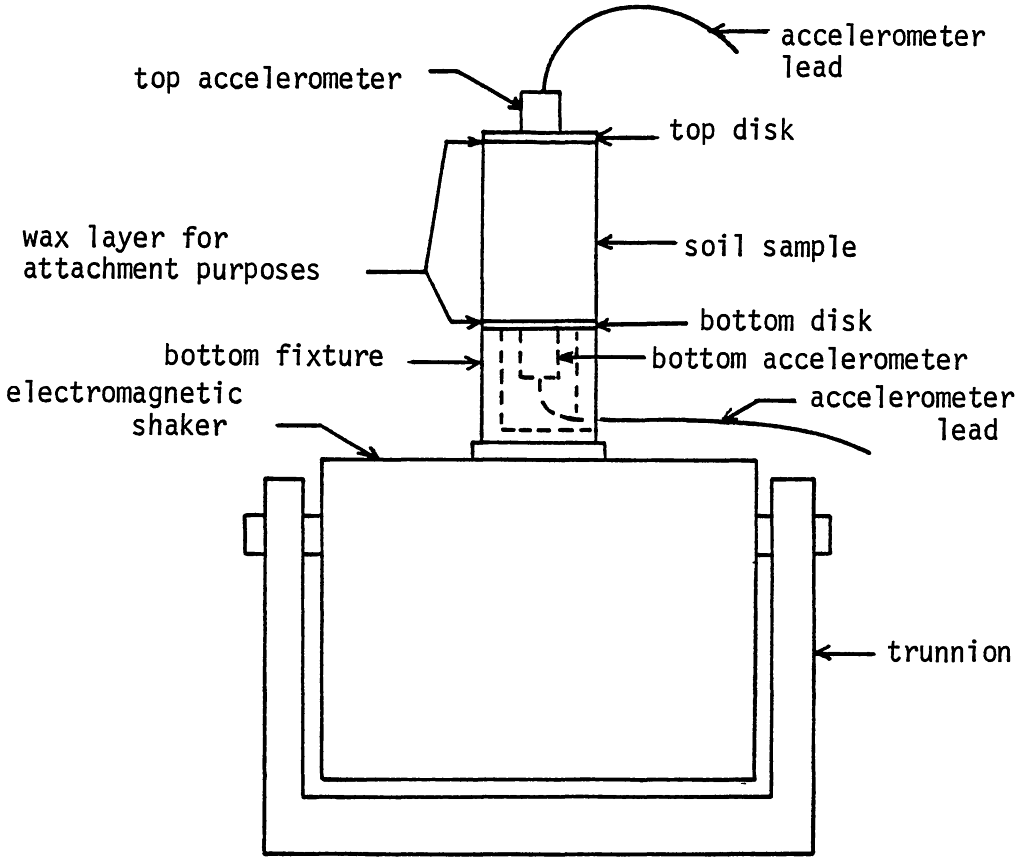

Figure 1. Schematic of the Dynamic Test System

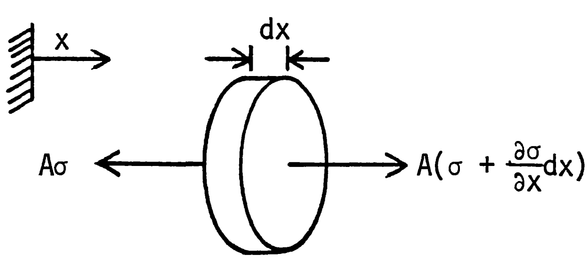

Figure 2. Free Body Diagram of a Small Element of a Prismatic Rod in Longitudinal Vibration

At this point a stress-strain model must be assumed to solve the equation. Assume for now that stress is proportional to strain by a complex proportionality constant E´:

$$\sigma = E'\varepsilon = E' \frac{\partial u}{\partial x} \tag{3}$$

Differentiating stress with respect to x and substituting in equation (2) yields the equation for one-dimensional longitudinal wave propagation:

$$E' \frac{\partial^2 u}{\partial x^2} = \rho \frac{\partial^2 u}{\partial t^2} \tag{4}$$

The steady state solution (after transients have died out) for the wave equation is:

$$u = Xe^{j\omega t} \tag{5}$$

where X is a function of x alone. The differentiations indicated in equation (4) are:

$$\frac{\partial^2 u}{\partial x^2} = X''e^{j\omega t} \tag{6}$$

$$\frac{\partial^2 u}{\partial t^2} = -\omega^2 \ Xe^{j\omega t} \tag{7}$$

Substituting equations (6) and (7) into equation (4) and rearranging yields:

$$e^{j\omega t} \ (X'' + \omega^2 \frac{\rho}{E'} X) = 0 \tag{8}$$

The exponential term cannot equal zero for all time, hence the part of the equation in the parenthesis must equal zero. The solution to this second-order linear homogeneous differential equation with constant coefficients is:

$$X = C_1 \cos(\omega \sqrt{\frac{\rho}{E'}}\, x) + C_2 \sin(\omega \sqrt{\frac{\rho}{E'}}\, x) \tag{9}$$

Setting

$$k' = \omega \sqrt{\frac{\rho}{E'}} \tag{10}$$

and substituting in equation (9) yields:

$$X = C_1 \cos k'x + C_2 \sin k'x \tag{11}$$

Substituting equation (11) in equation (5) yields the general solution to the wave equation.

$$u = (C_1 \cos k'x + C_2 \sin k'x)e^{j\omega t} \tag{12}$$

The boundary conditions shown in Figure 3 can be used to solve for the unknown coefficients. At the end of the soil sample attached to the shaker (x=0), the displacement is given by the electromagnetic shaker displacement function. This is equal to the expression obtained by substituting 0 for x in equation (12):

$$u(0,t) = \lambda \sin \omega t = \mathrm{Im}(\lambda e^{j\omega t}) = \mathrm{Im}(C_1 e^{j\omega t}) \tag{13}$$

Solving equation (13) for the first coefficient yields:

$$C_1 = \lambda \tag{14}$$

At the end of the soil sample attached to the disk and accelerometer (x=L), the force acting on the end of the

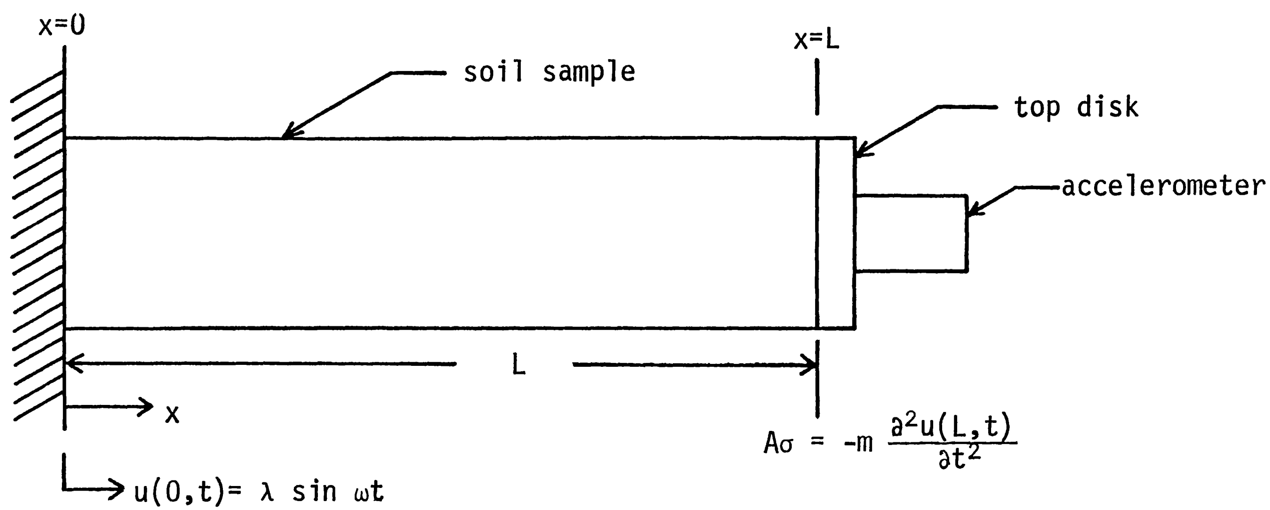

Figure 3. Boundary Conditions for the Prismatic Rod in Longitudinal Vibration

sample is equal to the attached mass times its acceleration, but in the opposite direction.

$$A\sigma = -m \frac{\partial^2 u(L,t)}{\partial t^2} \tag{15}$$

Substituting equation (3) into equation (15) yields:

$$AE' \frac{\partial u(L,t)}{\partial x} = -m \frac{\partial^2 u(L,t)}{\partial t^2} \tag{16}$$

Differentiating equation (12) appropriately and substituting into equation (16) yields:

$$AE'k'e^{j\omega t}(C_2 \cos k'L - \lambda \sin k'L) =$$

$$m\omega^2 e^{j\omega t}(\lambda \cos k'L + C_2 \sin k'L) \tag{17}$$

Rearranging equation (17) yields:

$$C_2 = \lambda \frac{AE'k' \sin k'L + m\omega^2 \cos k'L}{AE'k' \cos k'L - m\omega^2 \sin k'L} \tag{18}$$

Further simplification of equation (18) can be obtained by defining ϕ' as:

$$\phi' = \mathrm{Tan}^{-1} \left(\frac{m\omega^2}{AE'k'}\right) \tag{19}$$

Using the definition in equation (19), the formulas for the sine and cosine of the sum of two angles and equation (18) yields:

$$C_2 = \lambda \tan(k'L + \phi') \tag{20}$$

Substituting equations (20) and (14) into equation (12) yields the specific solution to equation (4):

$$u = \lambda e^{j\omega t}[\cos k'x + \tan(k'L + \phi')\sin k'x] \tag{21}$$

Equation (21) can be differentiated twice with respect to time to obtain an expression for the acceleration at any point x in the soil sample:

$$\frac{\partial^2 u}{\partial t^2} = -\omega^2 \lambda e^{j\omega t}[\cos k'x + \tan(k'L + \phi')\sin k'x] \tag{22}$$

The acceleration at x=0 is:

$$\frac{\partial^2 u(0,t)}{\partial t^2} = -\omega^2 \lambda e^{j\omega t} \tag{23}$$

The acceleration at x=L is:

$$\frac{\partial^2 u(L,t)}{\partial t^2} = -\omega^2 \lambda e^{j\omega t}[\cos k'L + \tan(k'L + \phi')\sin k'L] \tag{24}$$

The ratio of the acceleration at the top of the soil sample to the acceleration at the bottom is:

$$\frac{\text{top accel.}}{\text{bottom accel.}} = \cos k'L + \tan(k'L + \phi')\sin k'L \tag{25}$$

This theoretical value can be compared with the ratio determined experimentally from the accelerometers.

The acceleration ratio consists of two parts, magnitude and phase lag. The experimental measure of the magnitude is the ratio of the peak acceleration at the top of the sample to the peak acceleration at the bottom of the sample. This can be compared to the magnitude of the theoretical expression which is the square root of the sum of the squares of the real and imaginary parts.

The experimental measure of the phase lag is equal to the oscillation frequency multiplied by the time delay between the peak acceleration at the bottom of the soil sample and the peak acceleration at the top of the soil sample. This can be compared to the phase lag of the theoretical expression which is the inverse tangent of the imaginary part divided by the real part. Normal calculator and computer inverse tangent functions yield angles in the first and fourth quadrants, while phase lag angles are normally in the third and fourth quadrants. Hence, a computational check must be made to ensure the inverse tangent function returns appropriate phase lag angles.

Appropriate values for the parameters in the stress-strain model must be determined at each frequency to fit the model to the data. Once the model has been fit to the acceleration ratio data, it can be used to predict the magnitude of the peak stress at the top of the soil sample. Comparisons between measured and predicted peak stress at the top of the soil sample can then be used to validate the stress-strain model.

The theoretical expression for the stress at the top of the soil sample can be obtained from the stress-strain model and the appropriate differentiations of the displacement u (equation 21). The magnitude of the theoretical expression for stress is the square root of the sum of the squares of the real and imaginary parts. The magnitude of the measured peak stress at the top of the soil sample can be calculated from the measured peak acceleration at the top of the soil sample, the mass of the attached disk and accelerometer and the cross sectional area of the soil sample. The magnitude of the theoretical stress can then be compared to the magnitude of the measured stress to validate the model.

The four stress-strain models chosen for investigation in this study are given in Table I. The complex modulus, viscous and first-order viscoelastic models were evaluated by Smith et al. (1978) as models for the dynamic behavior of prosthetic urethane compounds. The second-order visco-elastic model was conceived for this work to account for anticipated additional complexity in the dynamic behavior of soil.

The four models can be substituted into the analysis presented at the beginning of this chapter by replacing equation (3) with the desired stress-strain model. No changes in the analysis result. The only changes occur in the functions k' and ϕ'. Table II gives the expressions for these functions for each of the four models.

The complex modulus model includes a static stress-strain component, E, and an imaginary loss factor which can be used to model the time lag between stress and strain. The viscous model includes the static stress-strain

TABLE I

PROPOSED STRESS-STRAIN MODELS

Model Name	Model Equation
Complex Modulus	$\sigma = E(1 + j\delta)\varepsilon$
Viscous	$\sigma = E\varepsilon - \frac{\beta}{A} \int_0^L \frac{\partial u}{\partial t}\, dx$
First-Order Viscoelastic	$\sigma = E\varepsilon + \alpha \frac{\partial \varepsilon}{\partial t}$
Second-Order Viscoelastic	$\sigma = E\varepsilon + \alpha \frac{\partial \varepsilon}{\partial t} + \xi \frac{\partial^2 \varepsilon}{\partial t^2}$

TABLE II

EXPRESSIONS FOR k´ AND ϕ´ FOR THE PROPOSED STRESS-STRAIN MODELS

Model Name	k'	ϕ'
Complex Modulus	$\omega\sqrt{\frac{\rho}{E(1+j\delta)}}$	$Tan^{-1}[\frac{m\omega}{A\sqrt{\rho E(1+j\delta)}}]$
Viscous	$\omega\sqrt{\frac{\rho}{E}(1-j\frac{\beta}{A\rho\omega})}$	$Tan^{-1}[\frac{m\omega}{A\sqrt{\rho E}}\sqrt{1-j\frac{\beta}{A\rho\omega}}]$
First-Order Viscoelastic	$\omega\sqrt{\frac{\rho}{E+j\omega\alpha}}$	$Tan^{-1}[\frac{m\omega}{A\sqrt{\rho(E+j\omega\alpha)}}]$
Second-Order Viscoelastic	$\omega\sqrt{\frac{\rho}{E-\xi\omega^2+j\omega\alpha}}$	$Tan^{-1}[\frac{m\omega}{A\sqrt{\rho(E-\xi\omega^2+j\omega\alpha)}}]$

component and a viscous damping term which models time lag between stress and strain as energy loss to factors proportional to velocity. The parameter β is a coefficient modeling viscous damping per unit sample length. The first-order viscoelastic model includes the static stress-strain component and a term including the first time derivative of strain to model the time lag between stress and strain. This model has been used successfully by Smith et al. (1978) to describe the dynamic stress-strain behavior of prosthetic urethane compounds. The second-order viscoelastic model includes the first-order viscoelastic model and a term with the second time derivative of strain. This term models dynamic behavior similar to the phenomenon known as creep.

The denominator of the real part of the k' term is analogous to the "spring rate" coefficient for the soil. The denominator of the real part of the second viscoelastic model k' shows that ξ interacts with the loading frequency to affect the soil "spring rate". If ξ is greater than zero the soil "spring rate" will decrease as the loading frequency increases. If ξ is less than zero the soil "spring rate" will increase as the loading frequency increases. This possibility is in agreement with creep where increasing loads are required to obtain a given displacement when the time under load is decreased.

CHAPTER IV

TEST APPARATUS

Static Measurements

Sample Diameter, Length, Density and Moisture Content

The soil sample diameters were measured to within 0.01 mm using a vernier caliper. Two flat porous stones of the type used in triaxial compression tests were placed on either side of the soil sample and the calipers used to measure the diameter plus the thickness of the two stones. The diameter of the soil sample was then equal to the measurement minus the thickness of the stones. Three diameters were measured for each soil sample each time the diameter was measured, and the average of the diameters was used to calculate the cross sectional area of the sample.

The sample length was measured in the same way the sample diameter was measured. Sample diameter and length were used to calculate sample volume. The mass of each sample was measured to within 0.01 g using an electronic scale. Sample density was then calculated from sample volume and sample mass.

Sample moisture content was determined by weighing the moist sample, drying it in an oven at 105 ^{o}C for 24 hours and weighing the dry sample. The moisture content was calculated on a precent dry weight basis.

Sample diameter, length and mass were measured before and after the dynamic test was performed. The values used in the model fitting programs for sample length, cross sectional area and density were the values calculated before the dynamic test. The length, diameter and mass data taken after the dynamic test were used to indicate whether the sample had changed significantly during the dynamic test. The difference between soil sample mass before and after the dynamic test was attributed to water loss from the sample, as negligible soil loss was observed. Some samples did not stay completely intact during the process of removal from the dynamic testing apparatus, so measurements taken after the dynamic test could not always be used to check for significant sample change.

The static stress-strain test was performed after the dynamic test. Sample moisture content was measured after the static stress-strain test as it was expected that oven drying the soil samples would cement and/or change the soil structure.

Static Stress-Strain Modulus

The static stress-strain test was an unconfined compression test. The test stand consisted of a plate with a threaded rod screwed into the plate (Figure 4). A mounting bracket was attached to the top of the threaded rod and a dial indicator bolted on the mounting bracket. The height of the mounting bracket was adjusted with height adjustment nuts on the threaded rod.

A porous stone was placed on each end of the sample for the static stress-strain test. The height of the dial indicator was adjusted for each soil sample so the dial indicator had approximately 5 mm of measurement travel remaining. The soil sample was then loaded with pairs of 5 g lead weights placed on the top porous stone at approximately 30 second intervals. Weights were used in pairs (one on each side of the dial indicator) to maintain a balanced load on the top porous stone, and thus on the top of the soil sample. Dial indicator readings were taken prior to placing each pair of additional weights on the top stone, and 30 seconds after the last pair of weights had been placed on the top stone. A total of 30 of the 5 g weights was placed on each sample. This was a maximum compression stress of approximately 1.5 kPa on each sample. (The maximum compressive stress during dynamic testing was approximately 1.0 kPa.)

Stress versus strain data were plotted for each sample to determine the static stress-strain modulus. No attempt was made to measure recovery in strain upon unloading the stress. It was noted that immediate strain recovery upon unloading was minimal for most samples. For this reason

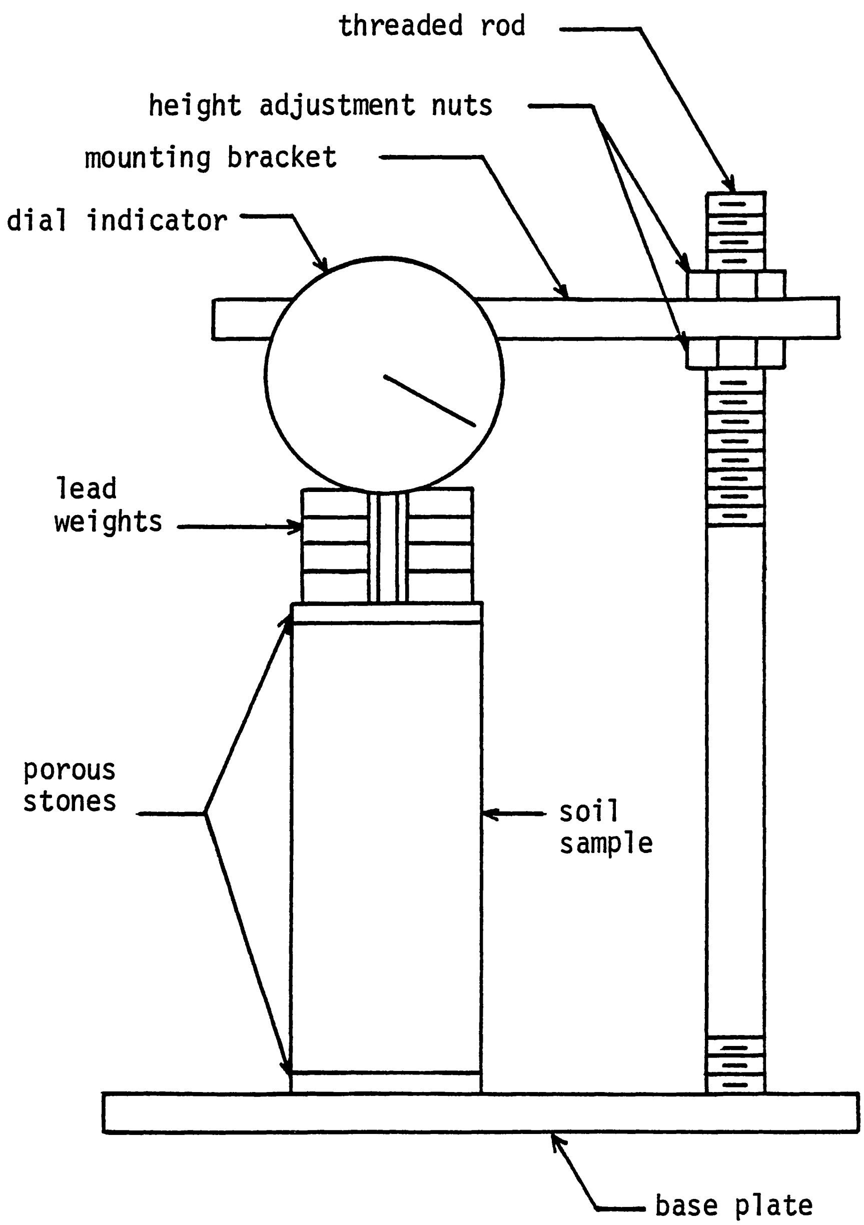

Figure 4. Schematic of the Static Stress-Strain Modulus Test Stand

the slope of the stress-strain line has been called the static stress-strain modulus in this work rather than the modulus of elasticity.

Field Capacity and Wilting Point Moisture Content

After the sample moisture content determinations, the soil samples were no longer considered to be in the same state as when they were removed from the field. Approximate field capacity and permanent wilting point moisture content determinations were performed for each soil sample, but it should be noted these determinations were for disturbed samples. Each sample was ground using a mortar and pestle and passed through a 2 mm square-hole sieve before being placed in rings on the ceramic pressure plate. The moisture content at a pressure differential of 1/3 bar was used as the approximate field capacity, and moisture content at a 15 bar pressure differential was used as the approximate permanent wilting point. The water extraction process followed was described in the U. S. Department of Agriculture publication Diagnosis and Improvement of Saline and Alkali Soils (1947).

Texture and Organic Matter Contents

Textural analysis (percent sand, silt and clay determinations) and organic matter content were the last tests performed on each soil sample. These tests were performed by the Oklahoma State University Agronomic Services Soil Testing Lab.

Dynamic Measurements

Shaker and Power Amplifier

The dynamic test procedure selected was a sinusoidal oscillation of a cylinder of soil. An electromagnetic shaker was selected as the oscillation device because electromagnetic shakers provide more accurate sinusoidal displacement functions than pneumatic or mechanical oscillators. Estimates of soil sample sizes were approximately 20 cm long and 3.6 cm in diameter with a maximum mass of approximately 1.2 kg. The estimate of maximum acceleration a soil sample could withstand was less than 5 times the acceleration of gravity (49 m/s^2). The minimum force required for the electromagnetic shaker was estimated at approximately 60 N. Previous data showed tillage operations in soil to have frequencies in the 9.5 to 63 rad/s range (Summers et al., 1985). As a result of this information, the electromagnetic shaker desired was to have the capability of continuously variable frequency adjustment in this frequency range. A Ling Dynamics model V-408 exciter with a model T-400 trunion base and a model PA-100 power amplifier were selected. This system provided approximately 100 N maximum force.

Instrumentation

Accelerometers and Charge Amplifiers. Accelerometers were needed to measure the accelerations at the top and bottom of the soil sample. Relatively small accelerometers were required so they could be attached to the top of the soil sample without much of a compressive load on the sample. The lowest natural frequency of the accelerometers needed to be greater than 10 times the highest operational frequency so accurate acceleration measurements could be made. Kistler model 8002 quartz accelerometers with a mass of 20 g each were used, along with Kistler model 5004 dual mode amplifiers to convert the charge produced by the accelerometers to voltages that could be measured with an oscilloscope. These accelerometers had natural frequencies of 251000 rad/s so accurate acceleration measurements could be made at frequencies up to 25100 rad/s.

Oscilloscope. A Nicolet 2090 digital oscilloscope with a model 206 module and a RS-232C port was used to capture, hold and display the voltage-time data from the accelerometers. The scope had dual trace capabilities with a 2048 by 2048 resolution screen. The number of data points per trace was 512.

Computer and Data Accessing Program. An IBM Personal Computer with two drives for double sided disks was used to interrogate the oscilloscope, download and store the data. The computer program used to access the voltage-time data from the scope was named NIC_PC.BAS (Appendix A). This program would access the voltage-time data from the scope, perform some basic communications error checking, and use the charge amplifier scale factor (input from the computer keyboard) to convert voltages to accelerations. The accelerometers were mounted on the sample in an orientation such that a negative signal from the top accelerometer indicated compression at the top accelerometer (deceleration). The bottom accelerometer was oriented in an opposite configuration so NIC_PC.BAS also changed the sign on the bottom acceleration to adjust for this orientation difference between the accelerometers.

Sample Attachment Method

An attachment method was required to hold the soil sample firmly in place on the electromagnetic shaker head and to hold the top disk and accelerometer firmly in place on top of the soil sample. These connections needed to be firm to ensure that accelerations measured by the accelerometers on the shaker head and top disk were equal to accelerations at the bottom and top of the soil sample, respectively. Tests were run on possible attachment meth-methods with no sample between the shaker head fixture and top disk.

Three different attachment methods were tested. The first attachment method consisted of shrinking a 5 cm piece of heat shrink tubing over the joint to be connected. The second attachment method used a hose clamp around the joint. The third attachment method was placing a thin layer of beeswax between the two pieces to be joined and gently seating one piece on the other.

Tests run at 6280 rad/s with the top disk attached directly to the shaker head showed the ratio of top acceleration to bottom acceleration was about 1.08 for the heat shrink tubing, 1.03 for the hose clamp, and 1.02 for the wax. The clamps could not be used on soil samples as the ends of the samples were expected to crumble under the stresses resulting from use of the clamps. The wax attachment method was preferred to the heat shrink tubing, provided the wax would hold the soil sample in place in the same way it held the top disk in place. Another test run with a soil sample showed the thin wax layer between the two surfaces to be joined worked well as an attachment method.

CHAPTER V

SOIL SAMPLES

Soil Description

The soil samples were obtained at the Oklahoma Cotton Research Station in Chickasha, Oklahoma. The soil was a McClain silt loam with the taxonomic description of Fine, Mixed, Thermic Pachic Argiustoll. Twenty-five penetrations with the ASAE standard cone penetrometer were taken and the data from 50 to 300 mm depths were averaged for each penetration. The average of the cone penetrometer readings in the area from which the samples were taken was 2561 kPa with a standard deviation of 345 kPa.

Soil is not normally considered a uniform, isotropic material so it is possible that original orientation of samples in the field may affect soil behavior. A cylindrical soil sample that originally had its longitudinal axis oriented in the vertical direction in the field (vertical sample) may not behave the same as a sample that originally had its longitudinal axis oriented horizontally (horizontal sample) in the field. Fifteen vertical samples and fifteen horizontal samples taken from the field were used in this research. Sample measurements and properties are given in Tables III and IV.

TABLE III

VERTICAL SOIL SAMPLE MEASUREMENTS AND PROPERTIES

Sample	Bulk Density (kg/m^3) wet[1]	Bulk Density (kg/m^3) dry	Moisture Content by Weight (% d.b.)	Sample Length[1] (mm)	Cross Section Area[1] (mm^2)	Water Loss (%)	Length Loss (%)	Static Stress-Strain Modulus (MPa)	Moisture Content at Pressure Differential 1/3 bar	Moisture Content at Pressure Differential 15 bar	Texture Determination[2] % Sand	% Silt	% Clay	% OM
V1	1928	1685	12.35	52.36	986	2.07	0.46	4.79	25.05	8.97	25	53	23	1.2
V2	1891	1651	11.78	50.92	978	2.76	0.39	6.12	21.81	7.58	29	50	22	1.0
V3	1918	1653	12.16	46.50	978	3.87	0.28	5.23	23.48	8.59	25	46	30	1.2
V4	1898	1643	12.41	49.18	968	3.11	0.37	6.90	22.79	8.24	21	48	32	0.9
V5	1897	1660	12.72	51.34	987	1.56	0.23	7.68	24.23	8.22	23	50	28	0.8
V6	1949	1671	13.12	52.74	972	3.52	0.21	7.93	24.24	8.52	21	46	34	1.0
V7	1874	1615	12.50	51.47	973	3.54	0.23	10.22	24.38	8.34	21	54	26	0.7
V8	1971	1710	11.32	41.39	981	3.94	-0.10	7.60	23.07	7.89	25	44	32	0.3
V9	1861	1631	11 62	47.35	972	2.48	NA[3]	6.01	24.32	8.22	27	50	24	0.4
V10	1896	1638	12 24	51.10	969	3.51	0.22	6.60	25.21	8.20	25	52	24	0.0
V11	1913	1641	12.67	53.49	973	3.91	0.11	11.56	22.65	7.89	23	52	26	0.0
V12	1847	1575	13.86	51.25	974	3.41	0.18	5.01	24.80	5.01	25	50	26	0.0
V13	1868	1630	11.46	41.96	979	3.14	0.05	8.99	25.63	7.99	25	53	23	0.9
V14	1924	1667	12.99	52.93	978	2.43	0.11	8.54	23.69	8.21	20	55	25	1.0
V15	1961	1675	14.34	52.56	974	2.73	0.23	5.79	27.16	10.16	32	43	25	0.8

[1] Prior to dynamic test.
[2] Total percentage may not equal 100 due to rounding methods.
[3] Data not available.

TABLE IV

HORIZONTAL SOIL SAMPLE MEASUREMENTS AND PROPERTIES

Sample	Bulk Density (kg/m^3) wet[1]	Bulk Density (kg/m^3) dry	Moisture Content by Weight (% d.b.)	Sample Length[1] (mm)	Cross Section Area[1] (mm^2)	Water Loss (%)	Length Loss (%)	Static Stress-Strain Modulus (MPa)	Moisture Content at Pressure Differential 1/3 bar	Moisture Content at Pressure Differential 15 bar	Texture Determination[2] % Sand	% Silt	% Clay	% OM
H1	1934	1691	10.84	51.03	970	3.53	0.24	5.98	22.58	8.00	21	57	23	0.0
H2	1844	1611	11.28	52.94	974	3.18	0.04	6.70	22.96	7.93	27	51	23	0.0
H3	2016	1755	12.57	53.00	975	2.30	0.28	4.89	24.18	8.70	27	49	25	0.1
H4	2020	1755	12.13	51.95	969	2.97	0.29	5.31	24.26	8.47	31	47	23	0.0
H5	1975	1722	10.88	55.25	977	3.81	0.22	5.07	23.02	7.87	23	55	23	0.1
H6	1938	1690	12.22	50.90	980	2.45	0.22	7.19	24.18	8.25	21	55	25	0.0
H7	1859	1625	10.82	50.83	973	3.58	NA[3]	6.24	23.21	8.16	19	55	27	1.5
H8	1884	1644	9.81	44.08	972	4.79	0.23	6.70	23.96	8.16	23	55	23	0.9
H9	1911	1655	11.59	52.46	974	3.88	0.30	6.55	24.93	8.42	23	55	23	1.9
H10	1932	1677	11.70	53.92	975	3.51	NA[3]	6.20	24.32	9.23	23	55	23	1.0
H11	1860	1609	11.14	48.90	965	4.46	0.18	6.22	24.49	8.17	23	59	19	0.4
H12	1954	1684	12.08	50.78	972	3.95	0.12	7.48	24.44	7.33	25	59	17	1.6
H13	1963	1703	12.07	52.82	971	3.20	0.27	5.53	24.17	7.09	NA[3]	NA[3]	NA[3]	NA[3]
H14	1992	1708	12.78	53.04	971	3.85	0.32	4.48	26.41	7.83	27	57	17	0.9
H15	1964	1721	10.93	50.81	969	3.19	0.26	7.06	23.55	7.84	27	57	17	1.0

[1] Prior to dynamic test.
[2] Total percentage may not equal 100 due to rounding methods.
[3] Data not available.

Soil Sampler

Buchele (1961) discussed a powered soil sampler to obtain undisturbed soil samples. Raper and Erbach (1985) modified this sampler slightly and studied soil bulk density as an indication of sample disturbance. Raper and Erbach (1985) concluded their powered auger sampler disturbed soil samples less than a pushed sampler. A sampler similar to the one discussed by Raper and Erbach (1985) was developed to obtain samples for this research.

The sampling device consisted of a hydraulically powered auger rotating around a non-rotating sleeve. The sampler was pushed into the ground by a hydraulic cylinder, while a belt drive from a hydraulic motor drove the auger. The cutting edge of a cutting tip attached to the non-rotating sleeve provided initial contact with undisturbed soil to cut a circular cylinder from the soil. The tip of the double auger 3 mm above the cutting edge of the cutting tip (Figure 5) removed soil from around the sampler to relieve compression by the intruding sampler and prevent compaction of soil beneath the cutting tip. The inside of the cutting tip was tapered outward so that only the cutting edge of the tip contacted the soil sample. This prevented friction between the sample and the inside edges of the cutting tip which would have resulted in compaction of the soil sample at its circumference. The sleeve was also of a larger diameter than the cutting edge to prevent

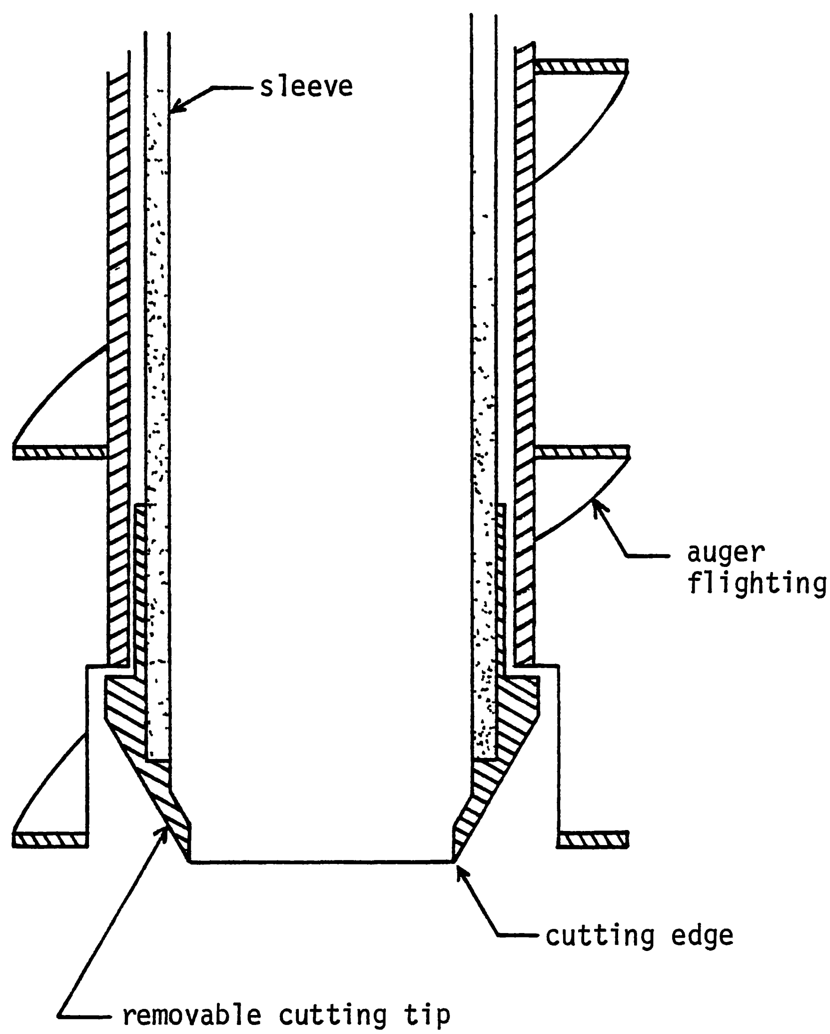

Figure 5. Schematic Cross Section of the Cutting End of the Soil Sampler

friction between the sample and sleeve from compacting the soil sample at its circumference.

The cutting edge of the cutting tip was 35 mm in diameter so samples obtained could be used in a standard triaxial compression testing apparatus if necessary. It was desired to obtain a 400 mm long sample in approximately 2 minutes with approximately one auger revolution per mm of sample length. Anticipated torque requirements resulted in use of a 0.75 kW motor operating at 300 rpm to power the belt drive for the auger.

The soil sampler was attached to a hydraulic cylinder on the frame used for the penetrometer. The frame was attached to a tractor via the three point hitch, and hydraulic power provided by the tractor.

Extra work was required before using the sampler to extract the horizontal samples. A steel box with a hole in one end was driven into the ground (Figure 6). Soil was removed from around the box, and a shovel driven under the box to help separate the soil in the box from the soil under the box. The box was then turned so the longitudinal axis of the box, which had been horizontal, was rotated to the vertical. The soil sampler could then be operated vertically through the hole in the end of the box to obtain a horizontal sample.

To obtain a sample, the tractor was driven to the spot where a sample was to be taken, and the auger drive started. The hydraulic cylinder that pushed the sampler into

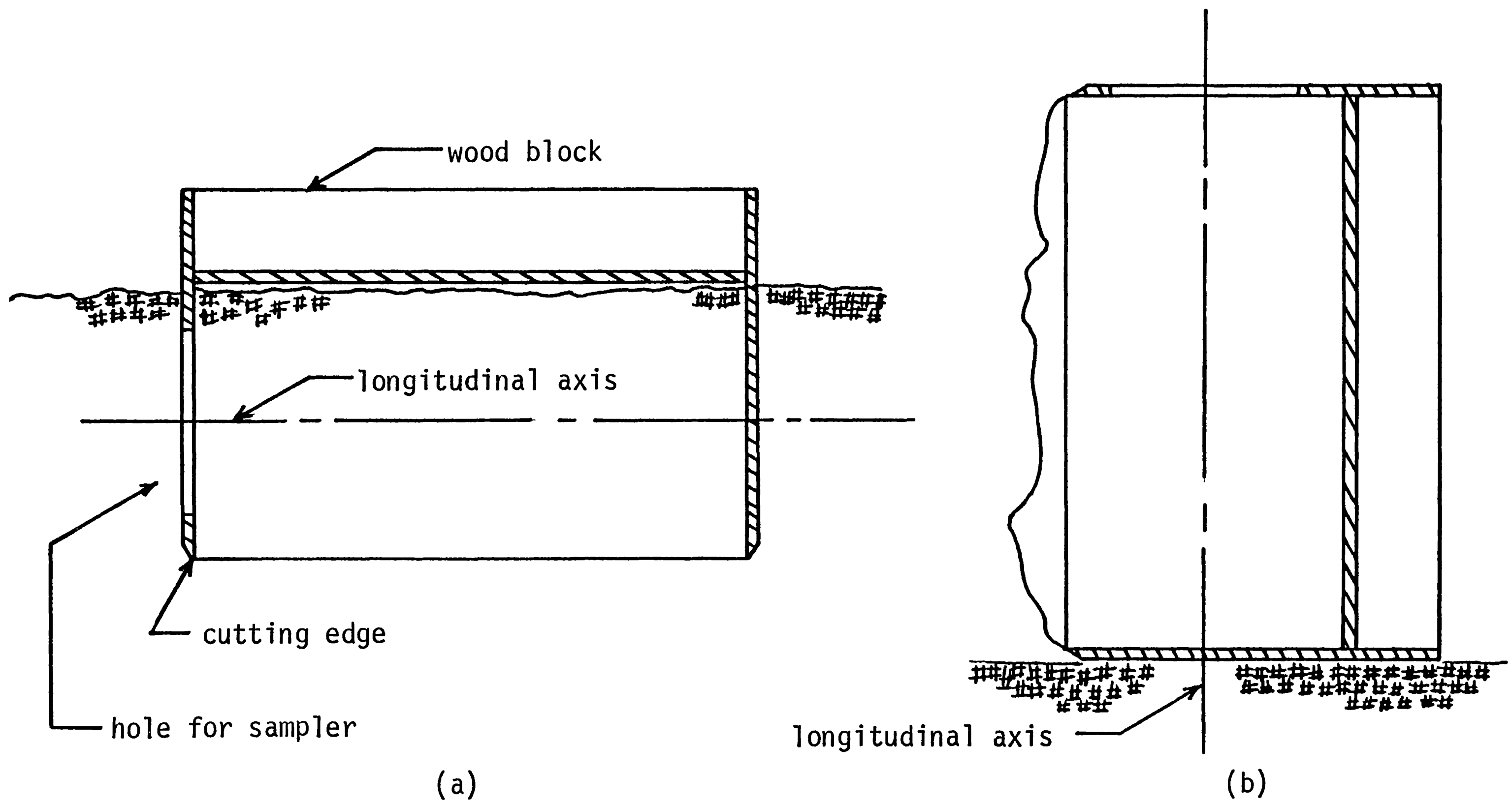

Figure 6. Schematic of Steel Box Used in Obtaining Horizontal Samples: a) Schematic of Box Driven Into Ground, b) Schematic of Box Rotated Into Position for Operation of the Sampler

the soil was then operated slowly to prevent disturbing the soil sample or exceeding power limitations on the auger belt drive. The auger drive was stopped when the sampler had reached the desired depth (approximately 300 to 400 mm) and the sampler was raised. The cutting tip of the sampler was disconnected but left in place, and the sampler was removed from its drive system. The sleeve, soil sample and cutting tip were removed from inside the auger, and placed so the longitudinal axis of the soil sample was parallel to the ground. The disconnected cutting tip was removed and the sleeve slowly tipped up so the soil sample could be gently removed from inside the sleeve.

The sample was then cut into lengths about 75 mm long with a knife, if it had not already broken. Pieces shorter than about 75 mm were discarded. Each of the individual pieces saved was rolled in a plastic bag, placed inside a second plastic bag and the outside bag was closed with a twist-tie to reduce moisture loss. The bagged samples were placed on packing material (plastic sheets with air bubbles) inside a cardboard box for transportation to the Agricultural Engineering Laboratory at Stillwater. The samples and packing material were moved from the cardboard box into a refrigerator for storage. Temperature in the refrigerator was maintained between 12 and 14 ^{o}C to reduce moisture loss from the samples.

Sample Preparation

Before the dynamic test was run, the ends of the test sample were trimmed to form a right circular cylinder. A jig to hold the sample during trimming was constructed from a short length of pipe. The pipe was cut in half lengthwise and a hinge welded onto the two halves. The inside of the pipe was then reamed slightly larger than the 35 mm sample diameter. The jig was then placed in a lathe and both ends squared.

To trim a sample, the sample was wrapped with a paper towel to take up the clearance between sample diameter and the inside diameter of the jig. The sample was positioned so one end could be trimmed flush with the end of the jig. A knife was used to whittle away the majority of the excess soil on the end of the sample. A putty knife with a wide blade was then used to finish trimming the end of the sample flush with the squared end of the jig. The sample was then removed from the jig and switched end-for-end so the other end of the sample could be trimmed. The sample was positioned in the jig so the trimmed sample would be approximately 5 cm long. If the end of the sample crumbled or had pieces pull out, the end was retrimmed so a flat surface was obtained.

The sample was then mounted on the electromagnetic shaker for the dynamic test. A thin layer of beeswax was applied to the end of the fixture on the shaker head, and the sample was gently seated on this wax layer. Another thin layer of beeswax was applied to the top disk, and the disk and accelerometer were gently seated on top of the soil sample.

CHAPTER VI

TEST RESULTS

Static Stress-Strain Modulus

The static stress-strain relationship was highly linear for the soil samples. Plots of stress versus strain for all samples are shown in Figures 7 through 14. The slopes of the stress-strain graphs are given as the static stress-strain modulus in Tables III and IV.

Dynamic Tests

Frequency and Acceleration Test Levels

Preliminary tests with a soil sample showed the sample behaved as a rigid body for frequencies in the 15 to 200 rad/s range. Non-rigid behavior began in the vicinity of 600 rad/s. Preliminary tests with 5 soil samples showed the soil samples definitely exhibited dynamic behavior above approximately 1250 rad/s. System measurement errors were determined as the ratio of top acceleration to bottom acceleration with the top disk and accelerometer attached to the bottom disk with a thin layer of beeswax. System measurement errors were within 3 percent for frequencies between 1250 and 12500 rad/s.

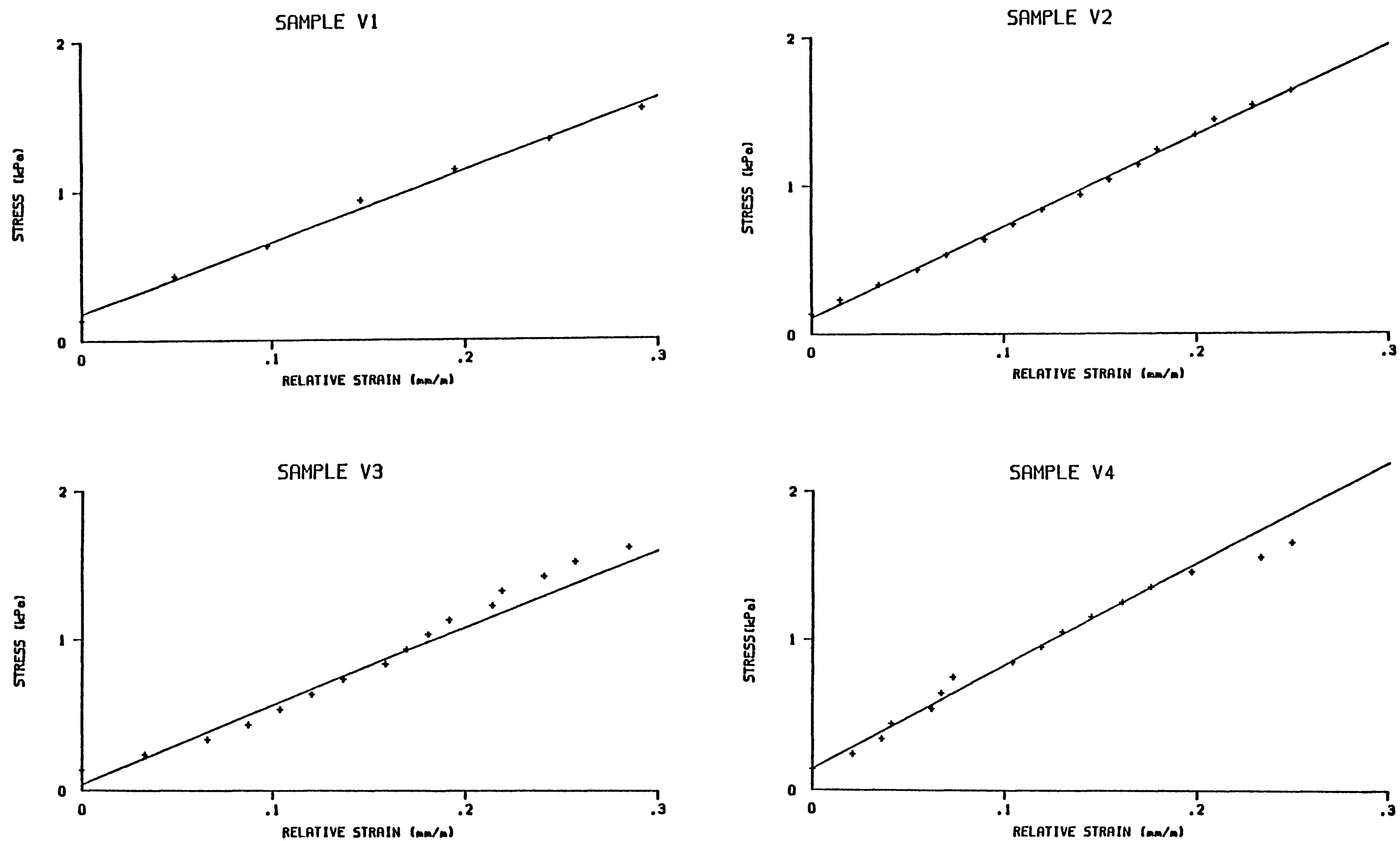

Figure 7. Static Stress-Strain Modulus Curves for Samples V1, V2, V3 and V4

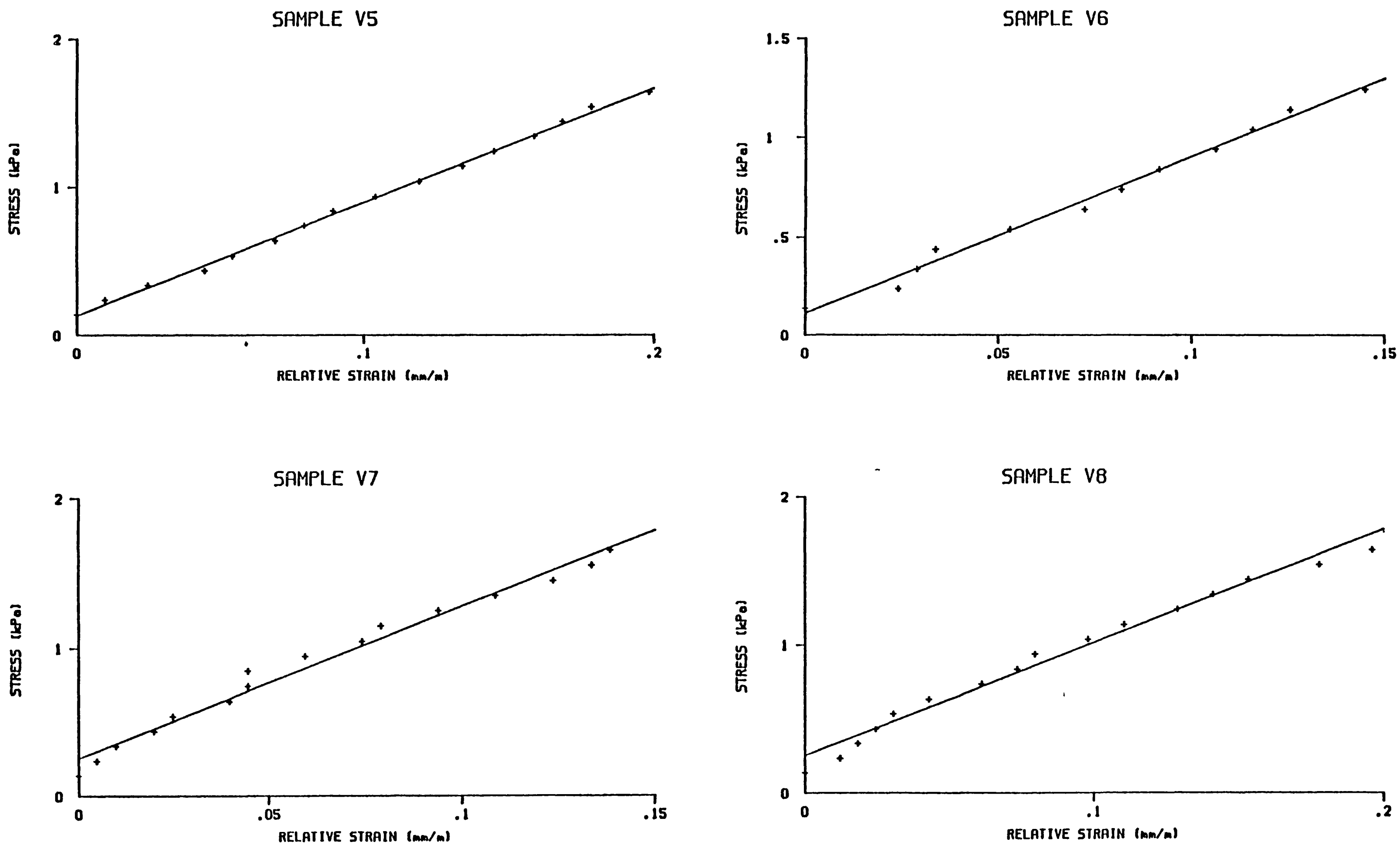

Figure 8. Static Stress-Strain Modulus Curves for Samples V5, V6, V7 and V8

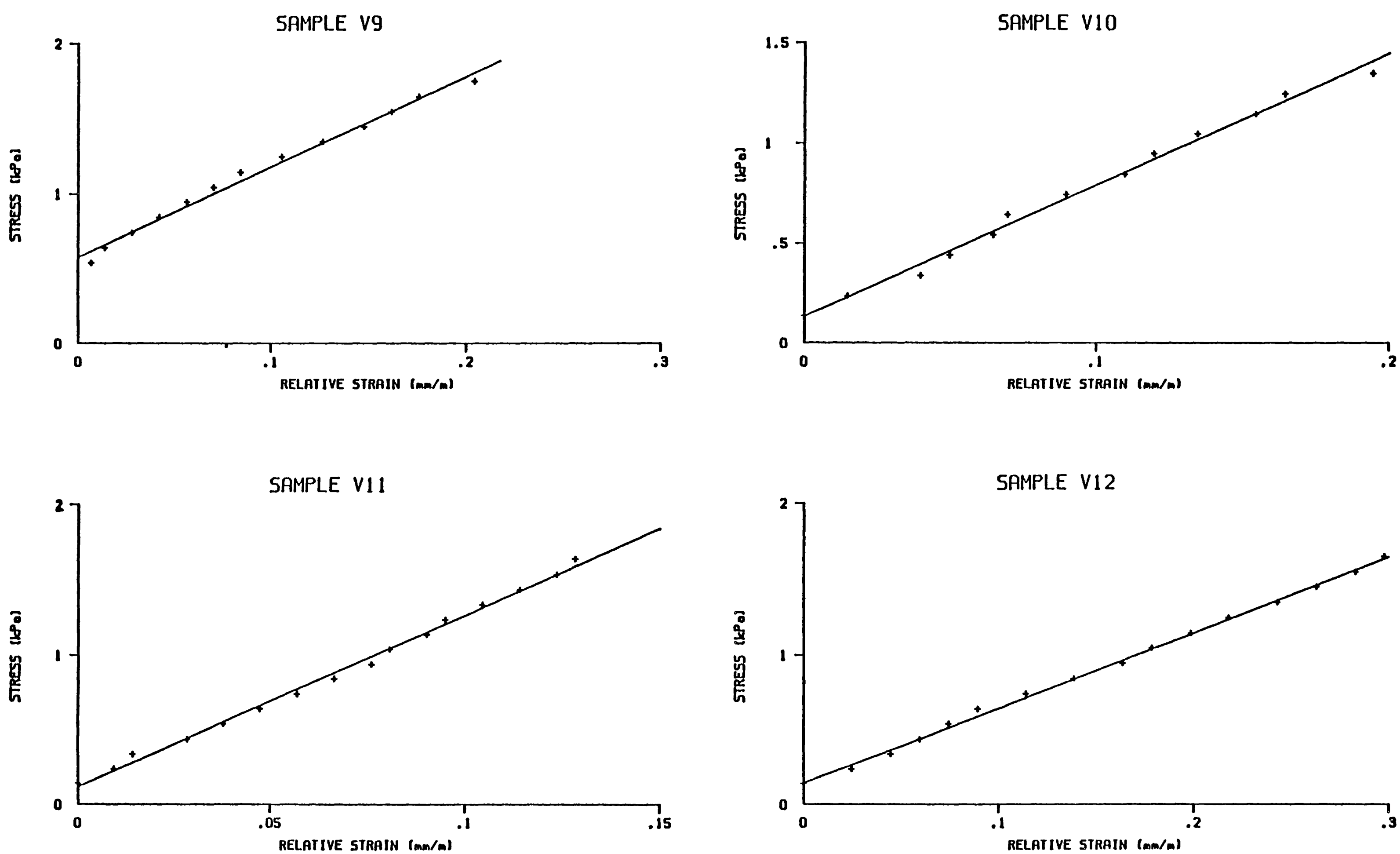

Figure 9. Static Stress-Strain Modulus Curves for Samples V9, V10, V11 and V12

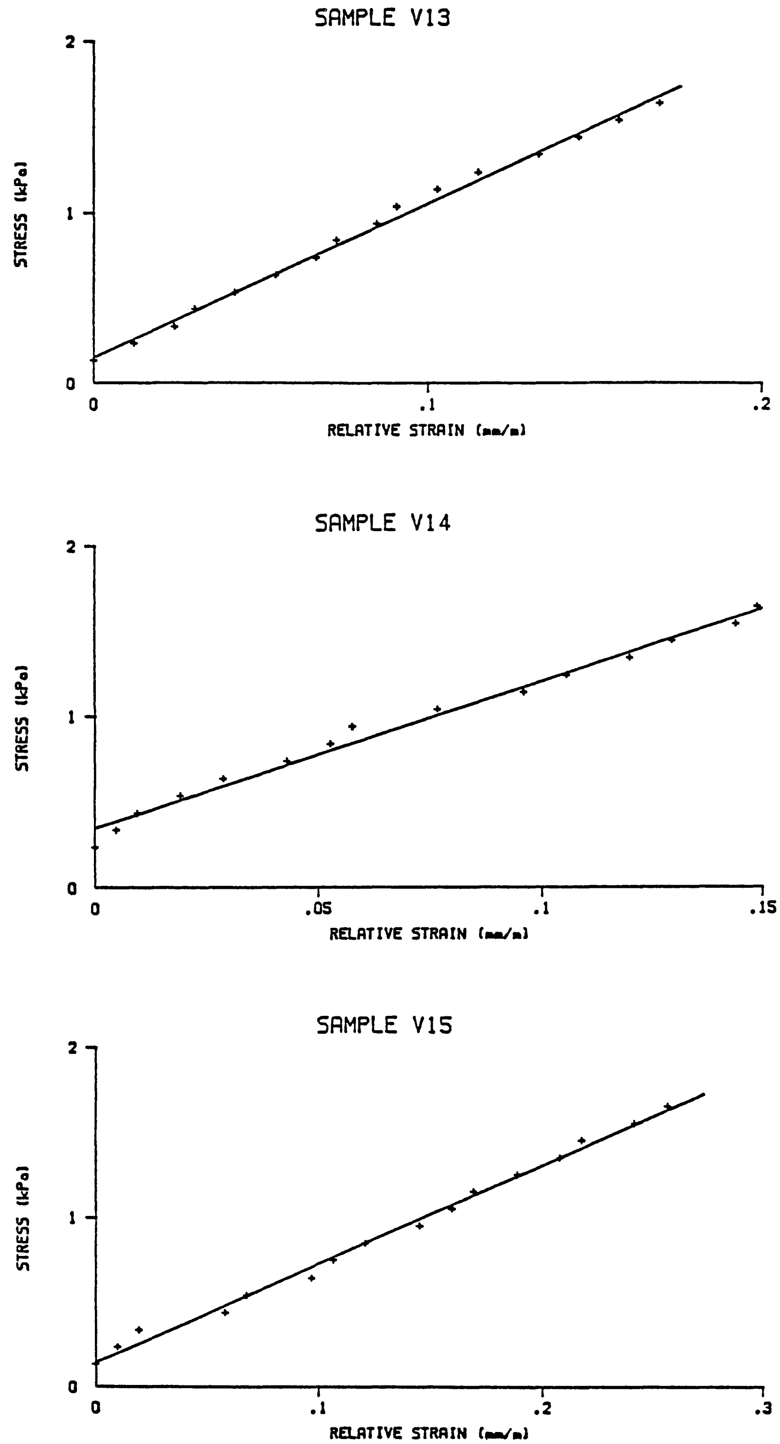

Figure 10. Static Stress-Strain Modulus Curves for Samples V13, V14 and V15

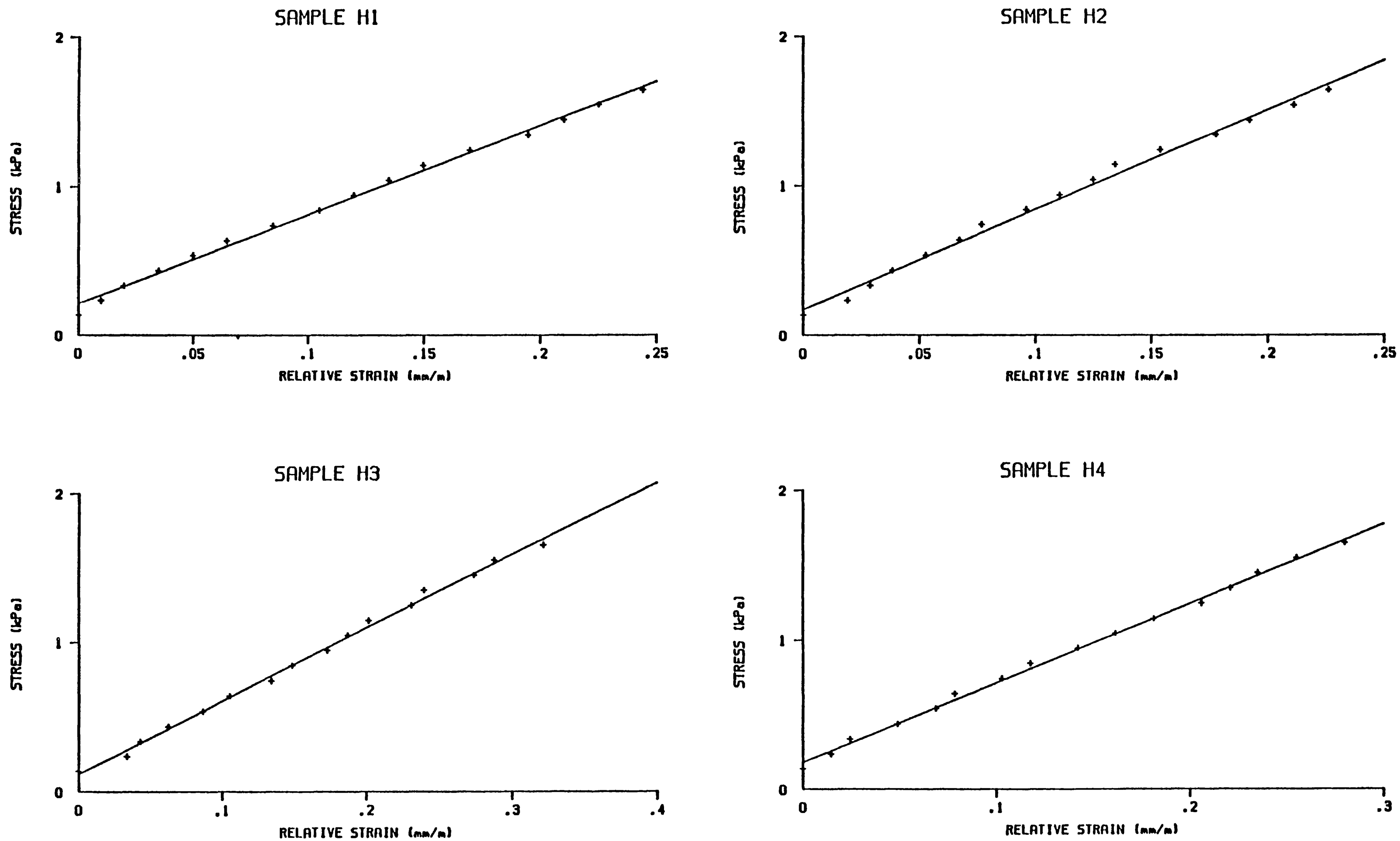

Figure 11. Static Stress-Strain Modulus Curves for Samples H1, H2, H3 and H4

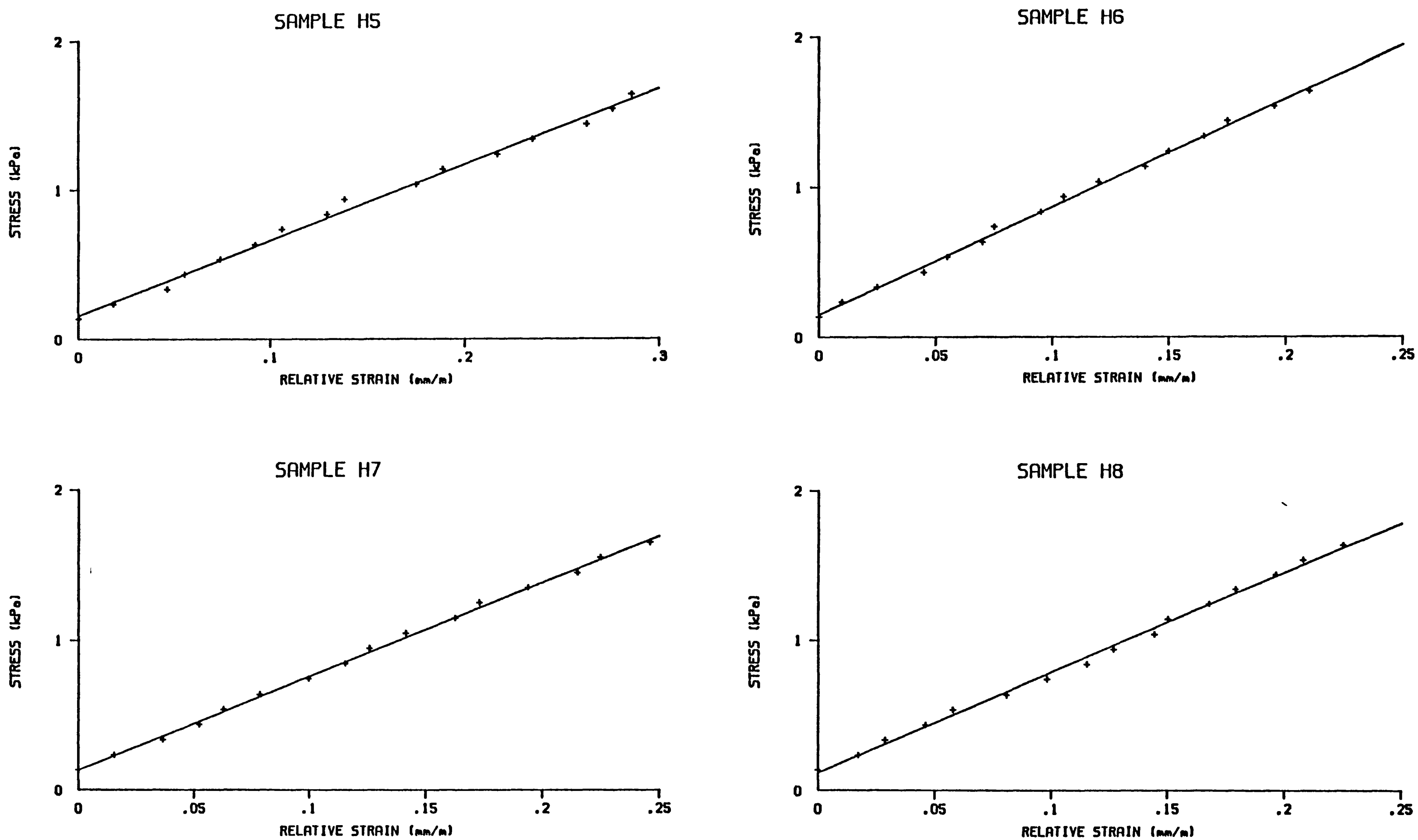

Figure 12. Static Stress-Strain Modulus Curves for Samples H5, H6, H7 and H8

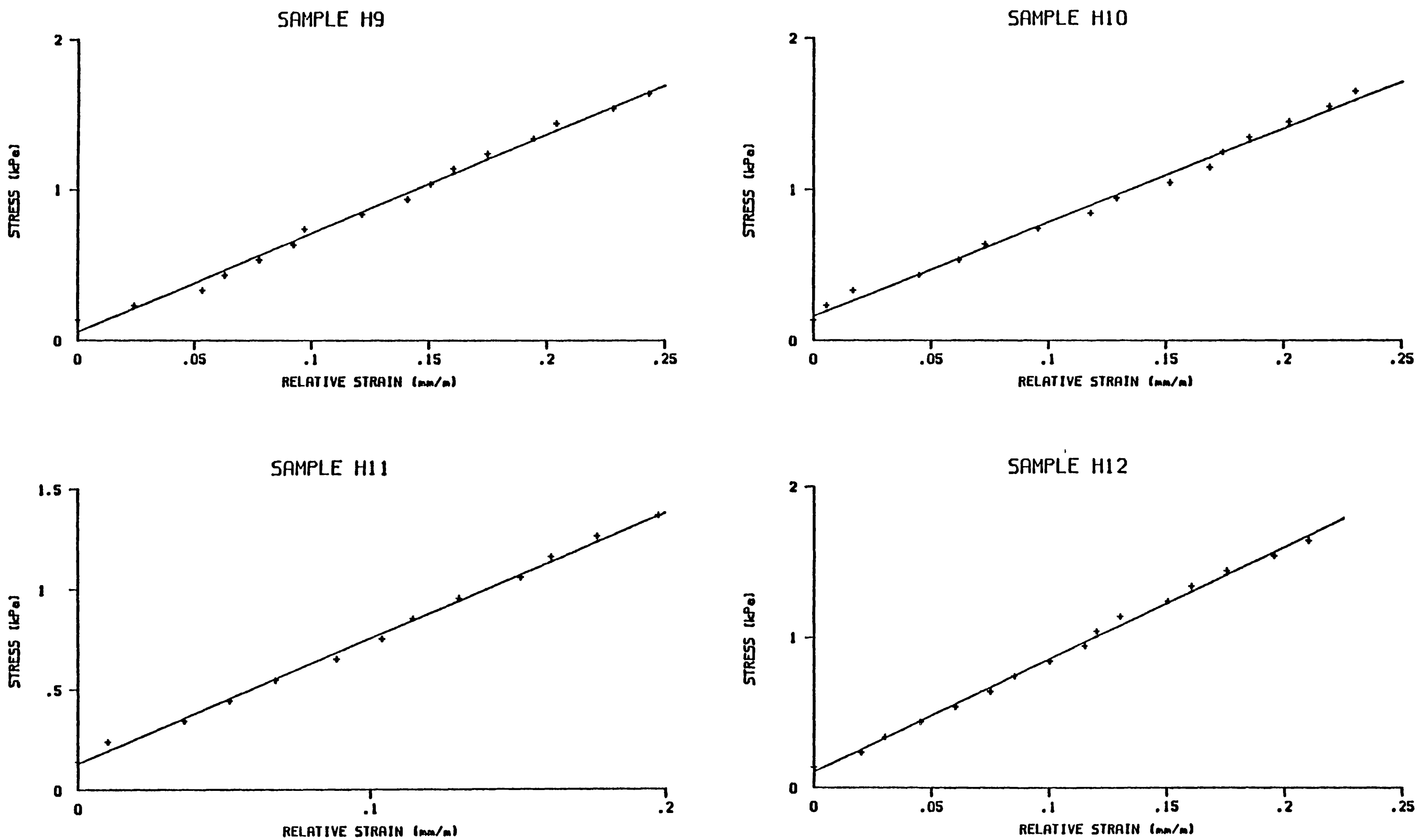

Figure 13. Static Stress-Strain Modulus Curves for Samples H9, H10, H11 and H12

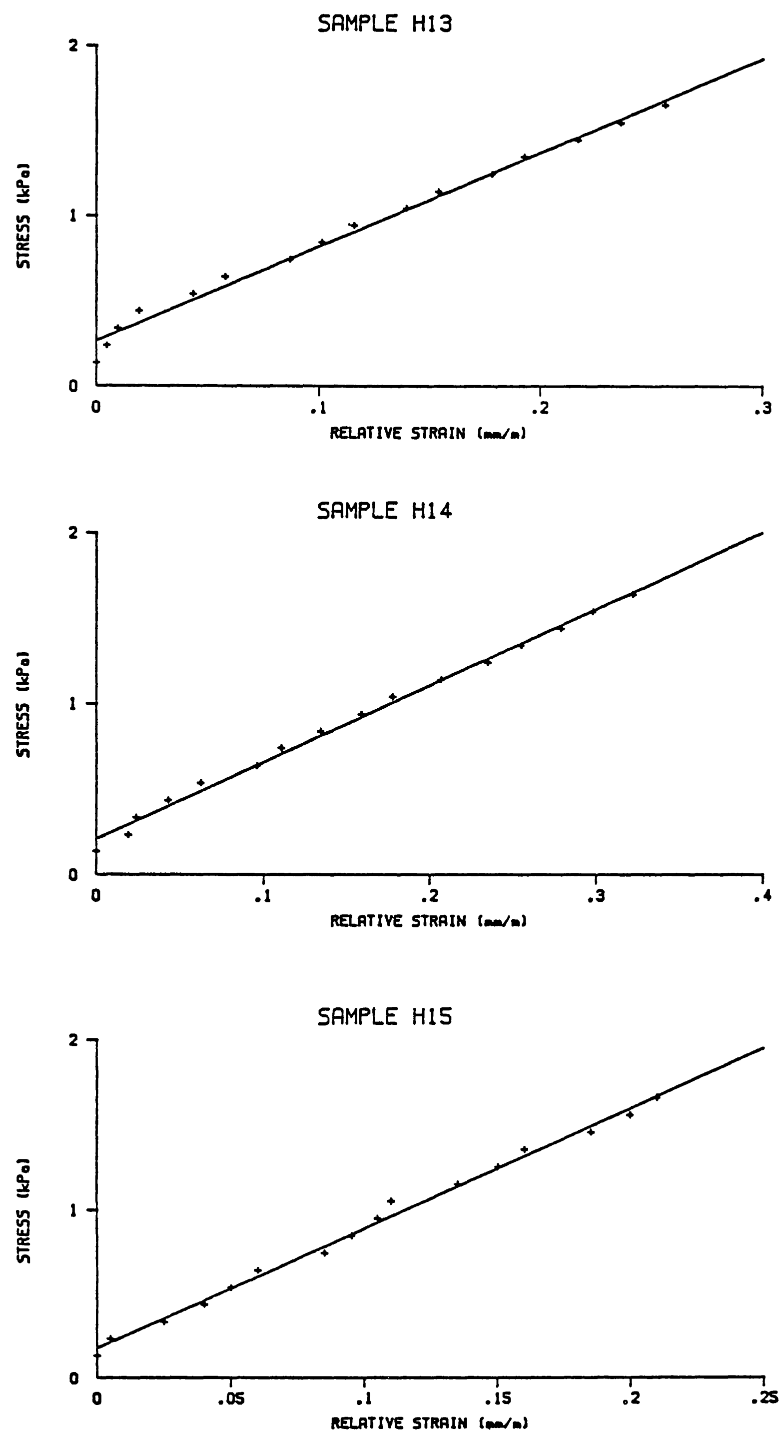

Figure 14. Static Stress-Strain Modulus Curves for Samples H13, H14 and H15

An attempt was made to run the dynamic test at 14 evenly spaced frequencies between 1250 and 9500 rad/s. The acceleration ratio changed greatly over some of these frequency intervals, resulting in large gaps between acceleration ratio data points in these regions. It was decided to increase the frequency range to between 1250 and 12500 rad/s. Particular frequencies for the dynamic test were selected to include more acceleration ratio data points in regions where the change in acceleration ratio was great. The frequencies selected for the dynamic test were: 1260, 1880, 2510, 3140, 3770, 4080, 4400, 4710, 5030, 5650, 5970, 6280, 6600, 6910, 7230, 7540, 7850, 8170, 8480, 8800, 9110, 9420, 10050, 10680, 11310, 11940 and 12570 rad/s. Tests could not be run at exactly these frequencies, but the frequency was adjusted to be within 60 rad/s of these frequencies.

Preliminary tests with a soil sample showed dust flew from the sample when the acceleration was above approximately 98 m/s^2. To prevent the majority of the soil samples from losing soil or disintegrating, the maximum acceleration used in the dynamic tests was approximately 25 m/s^2. The oscilloscope had a range switch which could be used to magnify the signal shown on the screen. The 4 times magnification switch setting was used so that magnified acceleration traces of ± 25 m/s^2 appeared as full scale on the screen.

Model Fits

The dynamic test data were written to floppy disks by the program NIC_PC.BAS which acquired the data from the oscilloscope and converted voltages to accelerations. One data file containing time and bottom acceleration data points and another file containing time and top acceleration data points were written to the disk for each frequency in the dynamic test.

The program MANIP.BAS (Appendix B) read the bottom acceleration data file and determined starting and stopping points for a full sine wave. The average acceleration value for the full cycle was determined and used as the average value of drift or bias introduced to the data from the measurement system. This average was subtracted from each point in the cycle to eliminate the drift or bias. The maximum acceleration for the bottom was determined and output to a printout. All acceleration values in the cycle were divided by this maximum acceleration value to normalize the data. The test frequency was then determined by an iterative procedure.

The top acceleration file was then read and the starting point of a full sine wave was found. The same number of points as were used for the bottom acceleration cycle were read for use as the top acceleration cycle. The average acceleration was calculated and subtracted from each acceleration value to remove the drift or bias. The maximum acceleration in the cycle was determined and output to printout. The acceleration values in the cycle were normalized, dividing each by the maximum value. The phase lag between the bottom and top acceleration cycles was determined using the difference in time between the starting points of the bottom and top acceleration cycles multiplied by the frequency. Frequency, acceleration ratio and phase lag were then written to a data file for use in programs matching the stress-strain models to the dynamic test data.

Once the frequency, acceleration ratio and phase lag were known for each frequency, stress-strain models were fit to the dynamic test data. This amounted to selection of a value for model parameters at each frequency to "best" fit the model predictions to the measured data. The acceleration ratio data was considered as a vector consisting of the acceleration ratio magnitude at the phase lag angle. The measure of best fit used was minimizing the magnitude of the vector difference between the predicted and measured acceleration ratio vectors.

The technique used in the computer programs to determine the value of the paramter which yielded the best fit of predicted and measured data at a certain frequency was the same for the complex modulus, viscous and first-order viscoelastic models. Initially, the parameter was set to zero, and the error (magnitude of the vector difference between predicted and measured data) was calculated. The parameter was then increased, and the new error calculated.

If the new error was smaller then the old error, a larger increase of the parameter was implemented. If the new error was larger than the old error, a smaller decrease in the parameter was implemented. This iterative approach was used until the error was very small, or the change in the parameter was so small it was concluded the error had been minimized.

The technique used to determine the best fit values for the two parameters in the second-order viscoelastic model was the same technique used for the other three models. The main difference was that the first parameter was held constant while the second parameter was varied until the error was minimized. Then the second parameter was held constant and the first parameter varied until the error was minimized. This procedure was repeated until the error was considered to be negligible.

COMPAR.FOR (Appendix C) was used to determine the best fit of the parameter in the complex modulus model and the parameter in the first-order viscoelastic model. VISPAR.FOR (Appendix D) was used to determine the best fit of the parameter in the viscous model. ATXA.FOR (Appendix E) was used to determine the best fit of the two parameters in the second-order viscoelastic model.

Results from fitting the complex modulus, viscous and first-order viscoelastic models to the acceleration ratio data for the first vertical sample are shown in Figure 15. Note that these models do not fit the data satisfactorily.

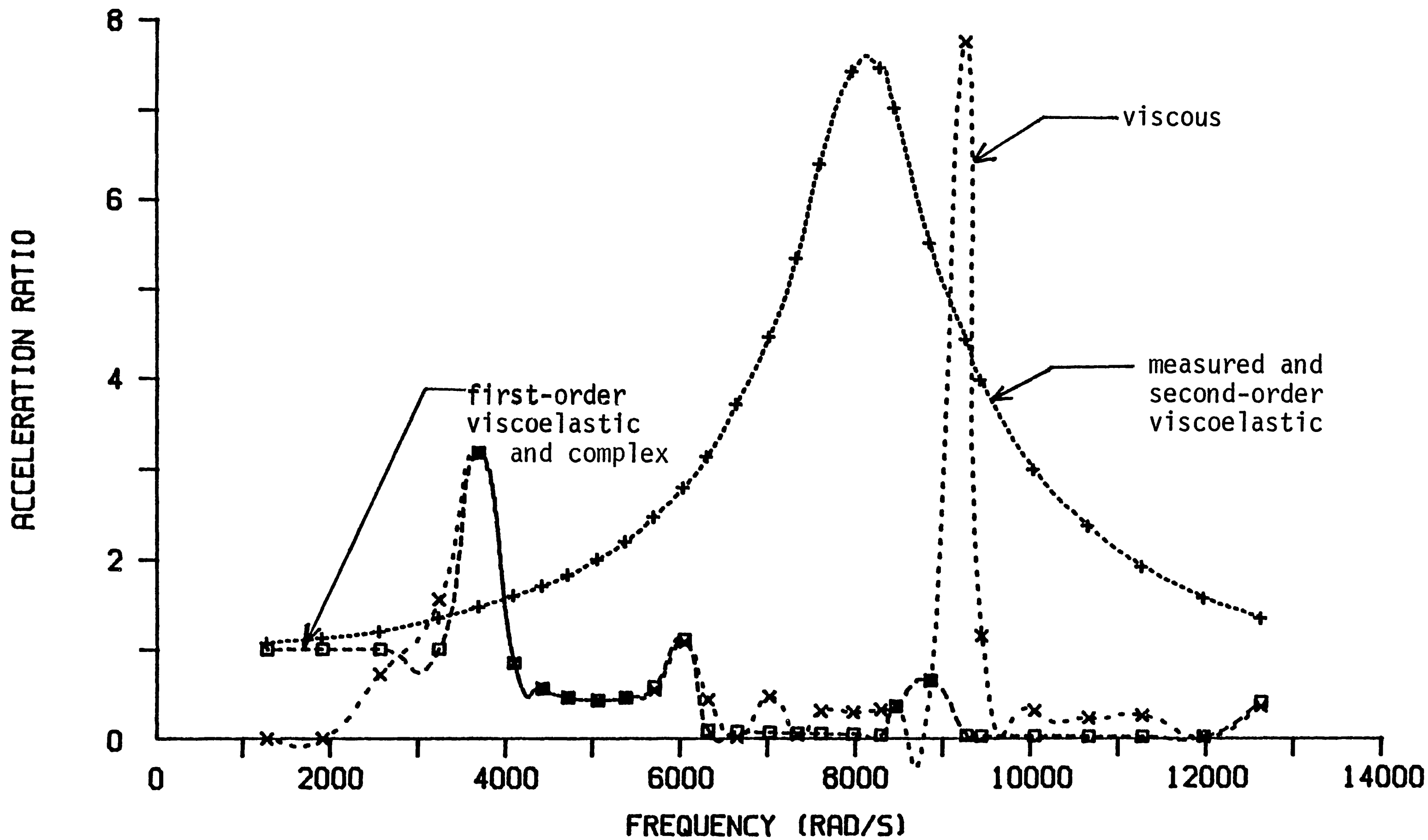

Figure 15. Stress-Strain Model Predictions of Acceleration Ratio for Sample V1

The reason these models do not fit the data is the creep-like phenomenon of the dynamic behavoir of the soil.

The acceleration ratio magnitude and phase lag angle can be thought of as denoting a vector in the imaginary plane. This vector has a real part consisting of the acceleration ratio magnitude multiplied by the cosine of the phase lag angle. The imaginary part of the vector consists of the acceleration ratio magnitude multiplied by the sine of the phase lag angle. In order to match the predicted vector and the measured vector, both the real and imaginary parts of the two vectors must match. The complex modulus, viscous and first-order viscoelastic models had only one parameter which could be varied, but two parts of the vectors to match. These models could not be fit to any generalized vectors, but only to ones whose real and imaginary parts varied in the same manner as the variation in the real and imaginary parts of the predicted vector due to changes in the one parameter.

The second-order viscoelastic model had two parameters which could be varied to match predicted and measured acceleration ratio magnitude and phase lag data with negligible error. The values for the model parameters are given for each sample in Appendix F. The values for the parameters α, alpha, (the first-order parameter) and ξ, xi, (the second-order parameter) were not constants for each soil sample, but varied with frequency. Figure 16 shows the parameters had the form of power functions.

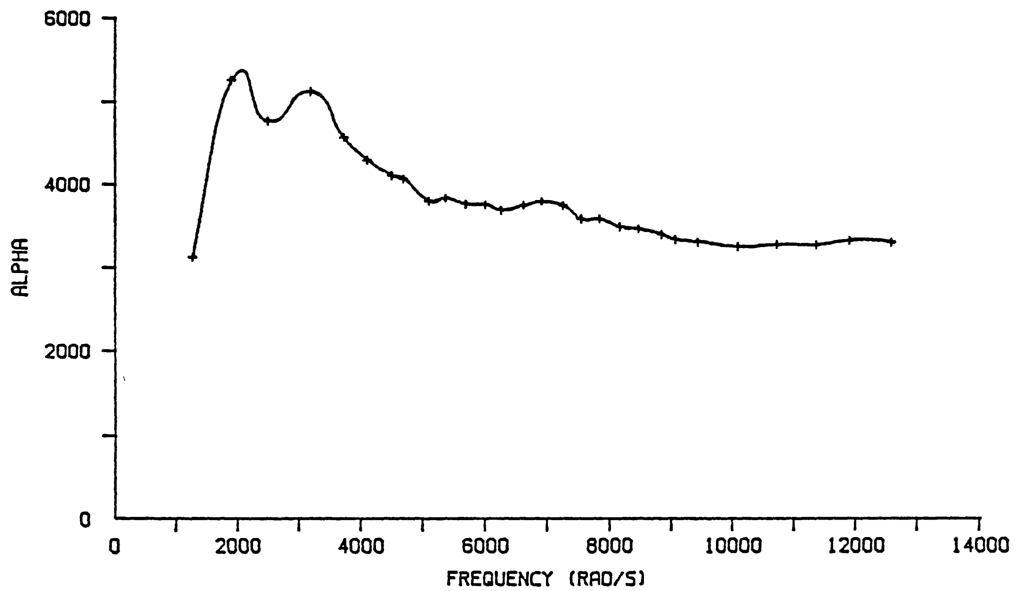

(a)

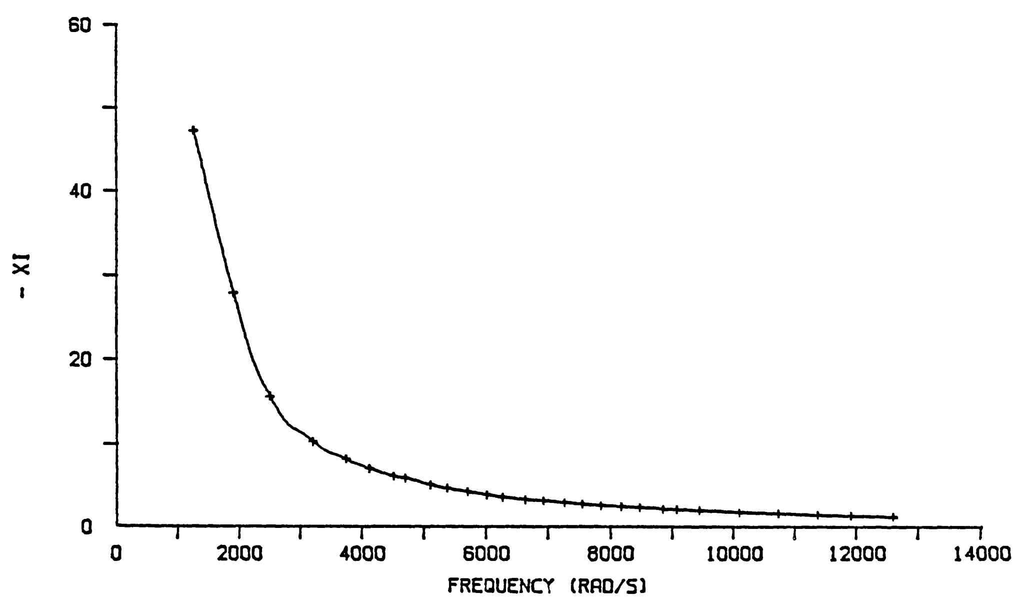

(b)

Figure 16. Values for the Parameters a) Alpha and b) X_1 Fitting the Second-Order Viscoelastic Model to the Acceleration Ratio Data for Sample V7

The variation in α at low frequencies did not fit a power curve function. Resolution and noise errors in the phase lag measurement were used to determine the sensitivity of α to those errors. This sensitivity is shown in Figure 17. The curves for measured α plus and minus noise and resolution errors were considered as boundaries of the expected value for α. The boundary is very wide at low frequencies, where the phase lag is small. Measurements of resolution and noise errors showed these errors were a major portion of the phase angle at low frequencies. Values for α were ignored for frequencies with phase lag angles less than 0.1 rad to reduce the impact of noise and resolution errors on the decription of α as a power function of frequency.

Sample Orientation Differences

A standard regression program was used to minimize the sum of the squared errors in fitting the best power functions to α and ξ for each sample. An average value for each coefficient was determined separately for 12 vertical samples and 12 horizontal samples (Tables V and VI). A two-tailed t test for comparing two means from independent samples with equal variances showed that three of the four mean coefficients for the power functions of the horizontal samples were different from the mean coefficients for the power functions of the vertical samples (Table VII). The one exception was that the mean coefficient for the

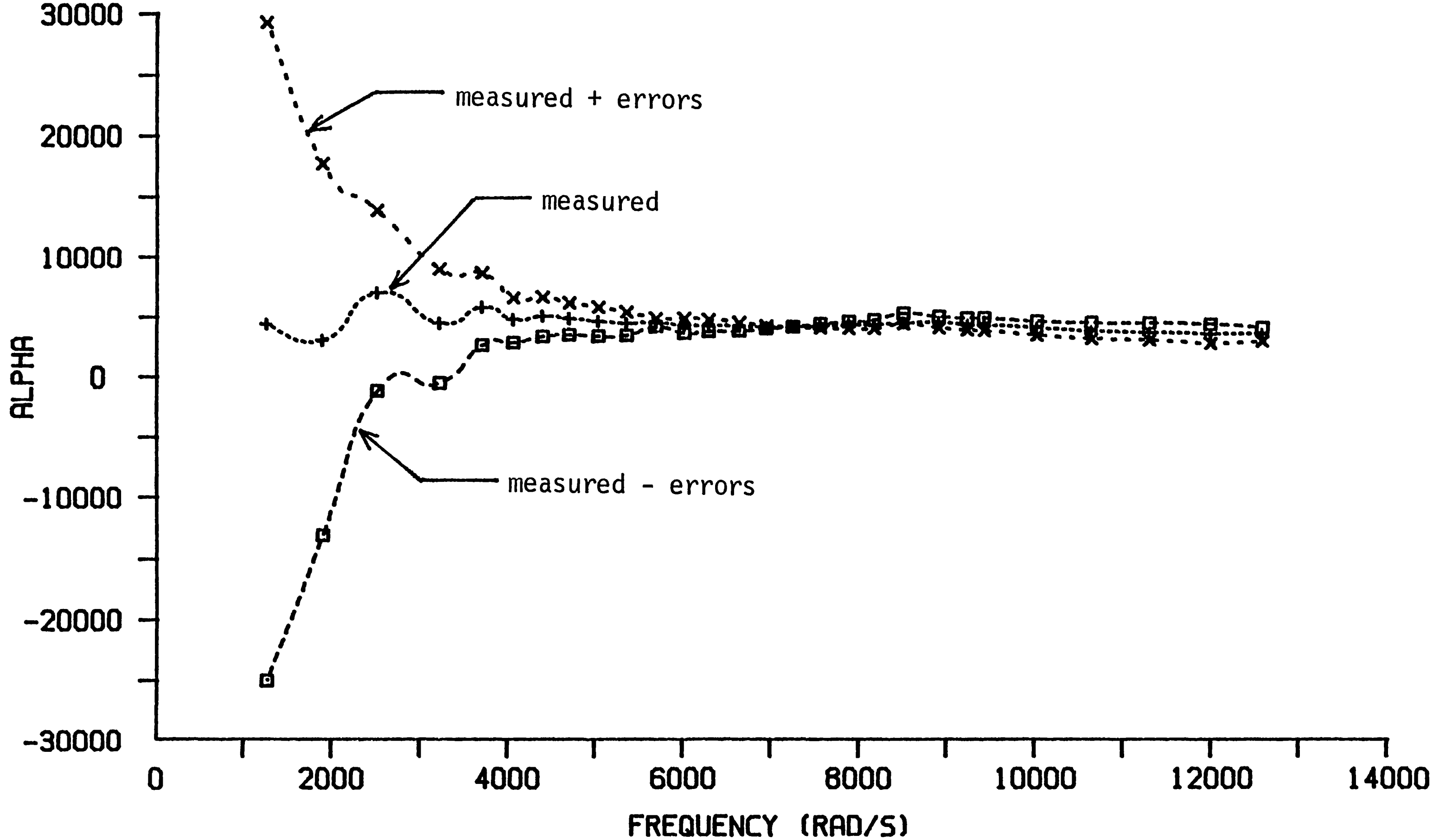

Figure 17. Sensitivity of Alpha to Noise and Resolution Errors in the Measurement of Phase Lag Angles (Sample V3)

exponent of the power function for α for horizontal samples was not significantly different than for the vertical samples. Since at least one coefficient mean value was dependent on sample orientation, the conclusion was drawn that original orientation of the sample in the field affected dynamic behavior of the soil sample.

TABLE V

SECOND-ORDER VISCOELASTIC MODEL PARAMETER POWER FUNCTION COEFFICIENTS FOR THE VERTICAL SAMPLES

Sample No.	Alpha		Xi	
	a_1	b_1	a_2	b_2
V1	11.51	-0.324	15.48	-1.565
V2	10.17	-0.235	14.41	-1.524
V3	10.64	-0.257	15.18	-1.570
V4	10.62	-0.260	14.89	-1.539
V5	10.95	-0.276	15.49	-1.577
V6	10.54	-0.241	15.58	-1.601
V7	10.51	-0.261	15.32	-1.605
V8	11.51	-0.324	15.00	-1.524
V9	10.86	-0.296	13.96	-1.453
V10	10.27	-0.231	15.21	-1.598
V11	11.41	-0.359	15.19	-1.575
V12	11.55	-0.399	14.86	-1.567
V13	12.20	-0.453	15.06	-1.581
V14	13.10	-0.540	15.10	-1.578
V15	12.77	-0.468	15.92	-1.619
Mean	10.88	-0.289	15.05	-1.558
Std. Dev.	0.503	0.0530	0.473	0.0429

Alpha = e^{a_1} (frequency)^{b_1}. Xi = e^{a_2} (frequency)^{b_2}. Mean and standard deviation are for the first 12 samples.

TABLE VI

SECOND-ORDER VISCOELASTIC MODEL PARAMETER POWER FUNCTION COEFFICIENTS FOR THE HORIZONTAL SAMPLES

Sample No.	Alpha		Xi	
	a_1	b_1	a_2	b_2
H1	11.68	-0.340	15.67	-1.575
H2	11.92	-0.184	16.35	-1.675
H3	10.44	-0.184	17.09	-1.721
H4	11.08	-0.243	16.64	-1.661
H5	12.26	-0.414	16.80	-1.705
H6	11.26	-0.302	16.19	-1.652
H7	11.22	-0.321	15.45	-1.602
H8	11.50	-0.320	15.57	-1.565
H9	11.15	-0.299	15.68	-1.624
H10	12.27	-0.440	16.08	-1.671
H11	10.96	-0.308	15.32	-1.602
H12	11.40	-0.306	15.90	-1.603
H13	11.85	-0.367	16.24	-1.648
H14	12.05	-0.361	16.38	-1.637
H15	11.71	-0.341	15.94	-1.607
Mean	11.43	-0.322	16.06	-1.638
Std. Dev.	0.537	0.0702	0.566	0.0503

Alpha = e^{a_1} (frequency)^{b_1}. Xi = e^{a_2} (frequency)^{b_2}. Mean and standard deviation are for the first 12 samples.

TABLE VII

STUDENT'S t TEST COMPARING THE VERTICAL AND HORIZONTAL SAMPLE PARAMETER POWER FUNCTION COEFFICIENT MEANS

Statistic	Alpha		Xi	
	a_1	b_1	a_2	b_2
S_{Y1-Y2}	0.212	0.0254	0.213	0.0191
t	2.589*	1.300	4.743*	4.192*

* Statistically significant at the 0.05 level.

Confidence intervals were calculated for the parameter power function coefficient means for use in sensitivity studies (Table VIII). New parameter power function coefficients were also calculated for the samples after the phase lag data had been changed to reflect an increase in phase lag (high phase) or a decrease (low phase) due to noise and resolution errors. Differences between the high and low phase power function coefficient means for α were much larger than the 95 percent confidence interval. Differences between the high and low phase power function coefficient means for ξ were approximately the same size as the 95 percent confidence intervals. This shows the α coefficients are much more sensitive to errors in phase lag measurement than the ξ coefficients. Hence, a small increase in measurement accuracy for the phase lag would have greatly decreased the differences between the high and low phase power function coefficient means for α.

Figures 18 through 21 show effects of changes in the parameter power function coefficients on fit of the second-order viscoelastic model to the acceleration ratio magnitude and phase lag data. Figure 18 shows use of a power function that yields higher values for α reduces the peak predicted acceleration ratio magnitude. Figure 19 shows use of a power function that yields high values for ξ shifts the peak predicted acceleration ratio from lower to higher frequencies. Figure 20 shows use of a power function that yields higher values for α increases the predicted frequency range over which the dramatic phase change occurs. Figure 21 shows use of a power function that yields higher values for ξ shifts the predicted area of dramatic phase change from low frequencies to high frequencies. In general, α determines the peak of the predicted acceleration ratio magnitude curve and the size of the predicted frequency range over which the dramatic phase change occurs, while ξ determines the frequency at which the peak predicted acceleration ratio magnitude and the frequency at which the predicted dramatic phase change will occur.

TABLE VIII

NINETY FIVE PERCENT CONFIDENCE INTERVALS FOR THE PARAMETER POWER FUNCTION COEFFICIENT MEANS FOR TWELVE VERTICAL AND TWELVE HORIZONTAL SOIL SAMPLES

Coefficient	Sample Orientation	
	Vertical	Horizontal
Alpha		
a_1	(10.56,11.20)	(11.09,11.77)
b_1	(-0.323,-0.255)	(-0.367,-0.277)
Xi		
a_2	(14.75,15.35)	(15.70,16.42)
b_2	(-1.585,-1.531)	(-1.670,-1.606)

Alpha = e^{a_1} (frequency)^{b_1}. Xi = e^{a_2} (frequency)^{b_2}.

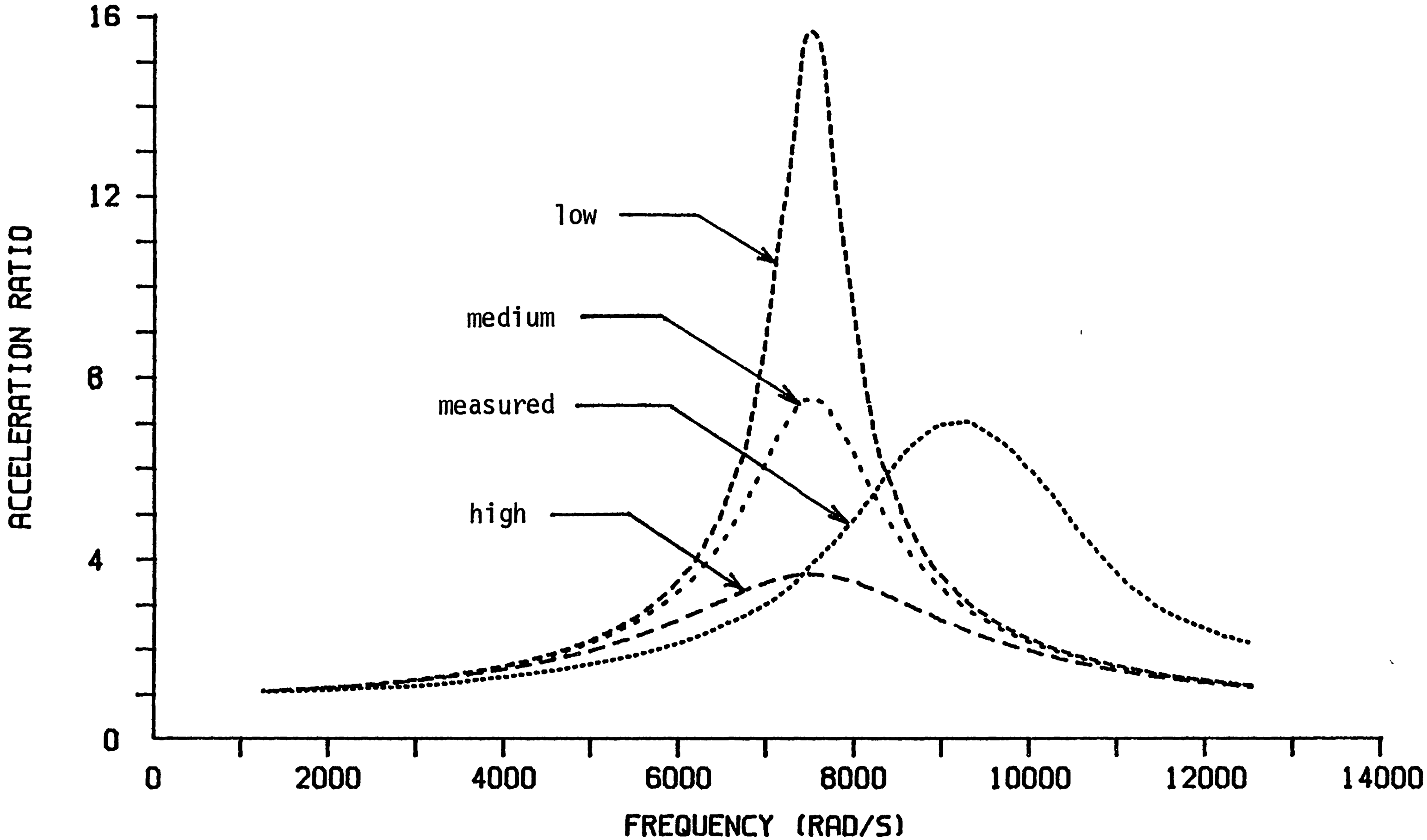

Figure 18. Sensitivity of the Acceleration Ratio Magnitude to Changes in Alpha
(Sample H14)

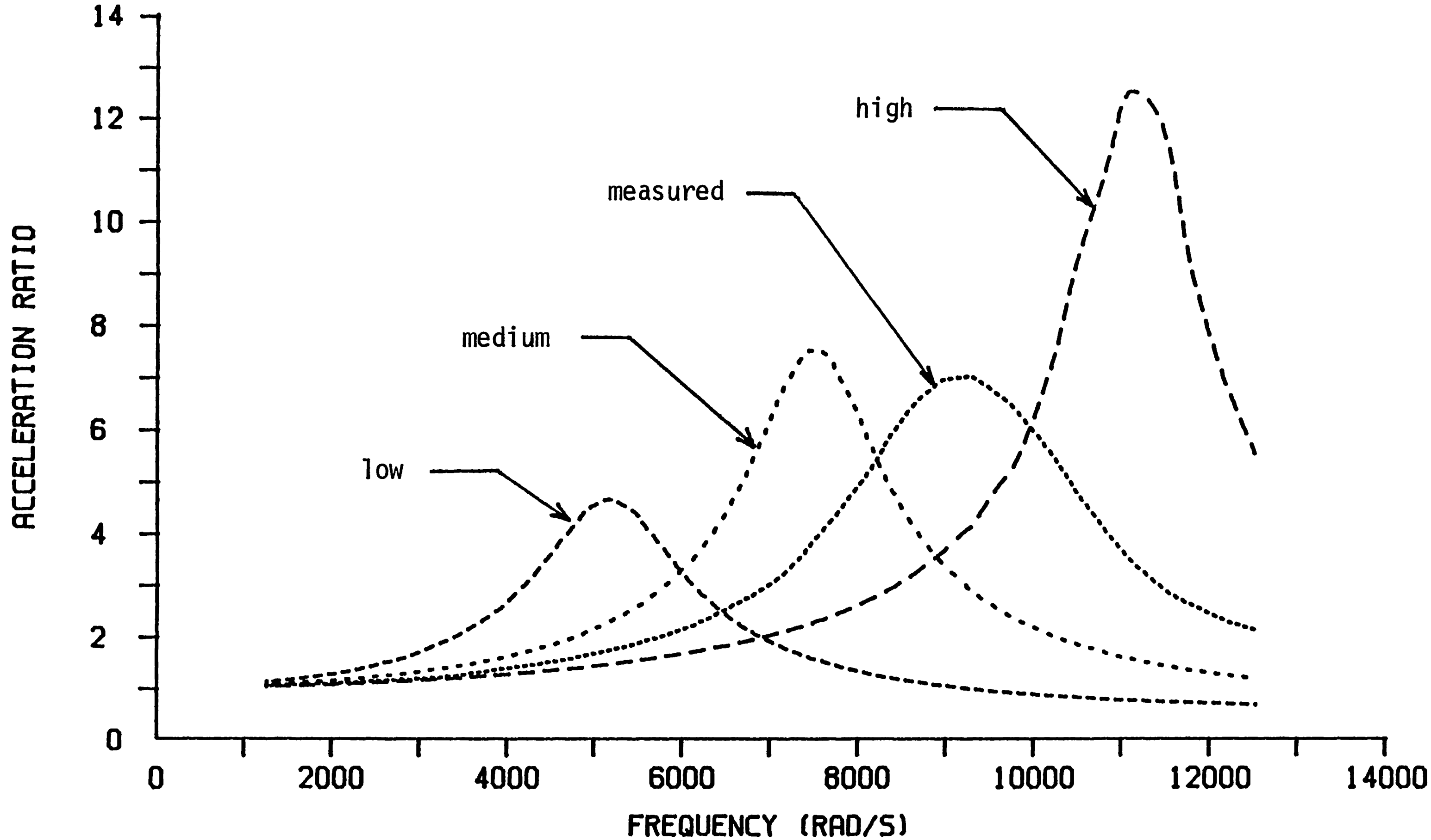

Figure 19. Sensitivity of the Acceleration Ratio Magnitude to Changes in Xi (Sample H 14)

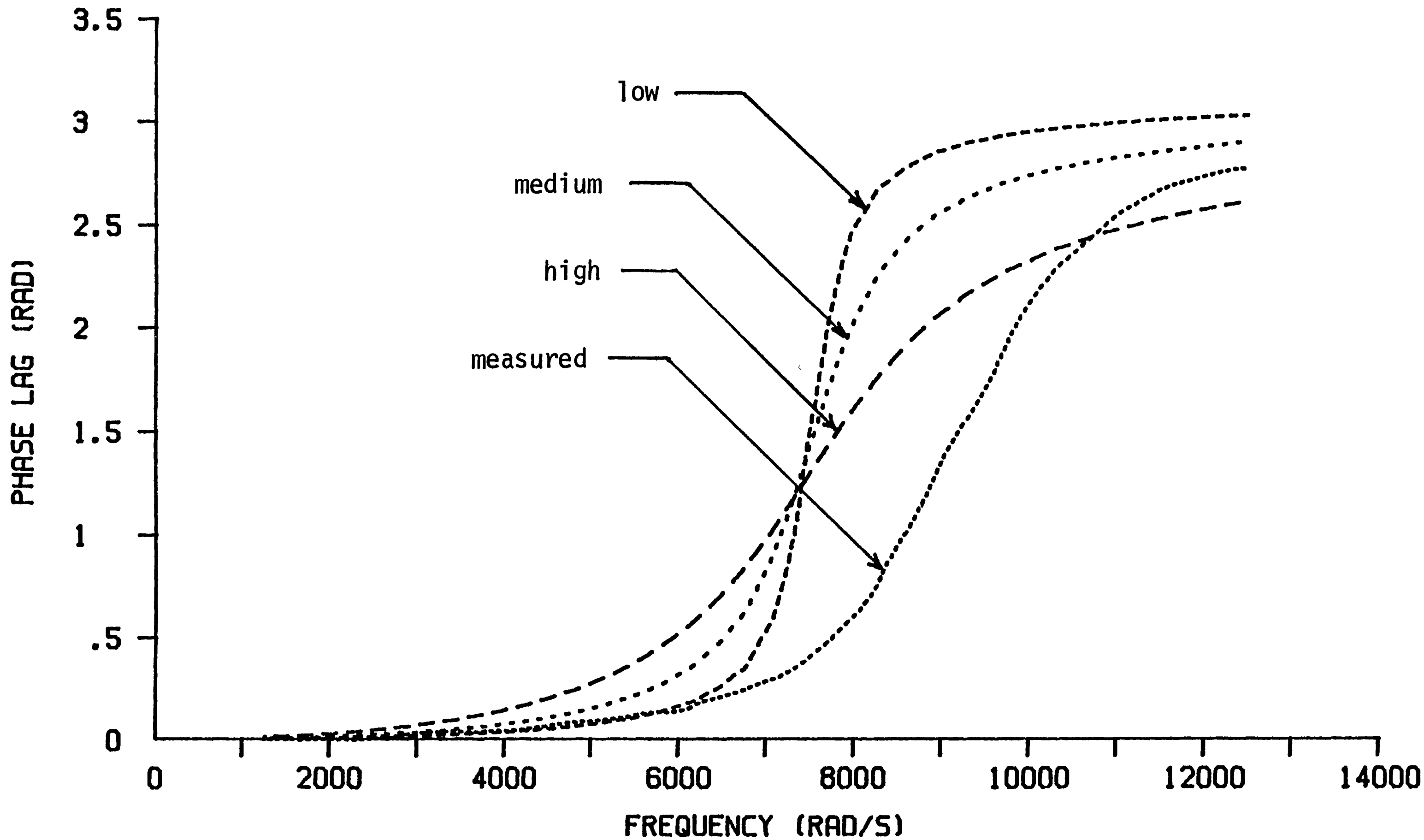

Figure 20. Sensitivity of the Acceleration Ratio Phase Lag Angle to Changes in Alpha (Sample H14)

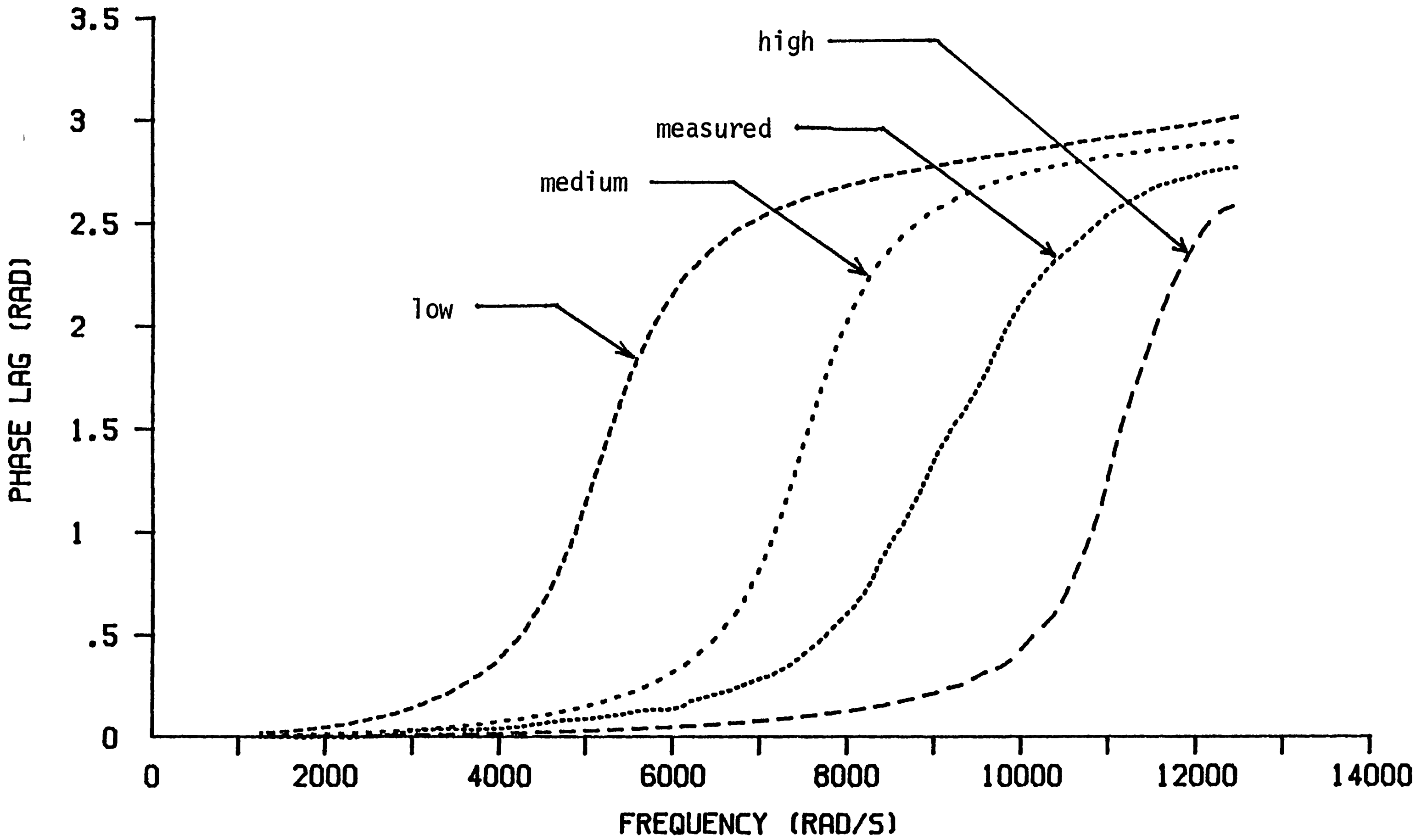

Figure 21. Sensitivity of the Acceleration Ratio Phase Lag Angle to Changes in Xi (Sample H14)

CHAPTER VII

MODEL VALIDATION

Dynamic Stress Prediction Capability

Values for the parameters in the second order visco-elastic stress-strain model were selected to fit the model to the acceleration ratio data. The stress prediction capability of the model was validated by comparison of measured and predicted stress.

Development of the theoretical expression for the stress at the top of the soil sample was outlined in Chapter III. This expression was used in the program PREDSTRS.FOR (Appendix G) to calculate the predicted stress at the top of the soil sample. The measured stress at the top of the soil sample was equal to the mass of the disk and accelerometer attached to the top of the sample multiplied by the acceleration at the top of the sample. Values for the α and ξ power function coefficients were entered from the keyboard so the coefficients that best fit the acceleration ratio data for that sample could be used in the stress predictions.

Vertical samples V13, V14 and V15 and horizontal samples H13, H14, and H15 were used to validate dynamic stress prediction capability. Figures 22 and 23 show the

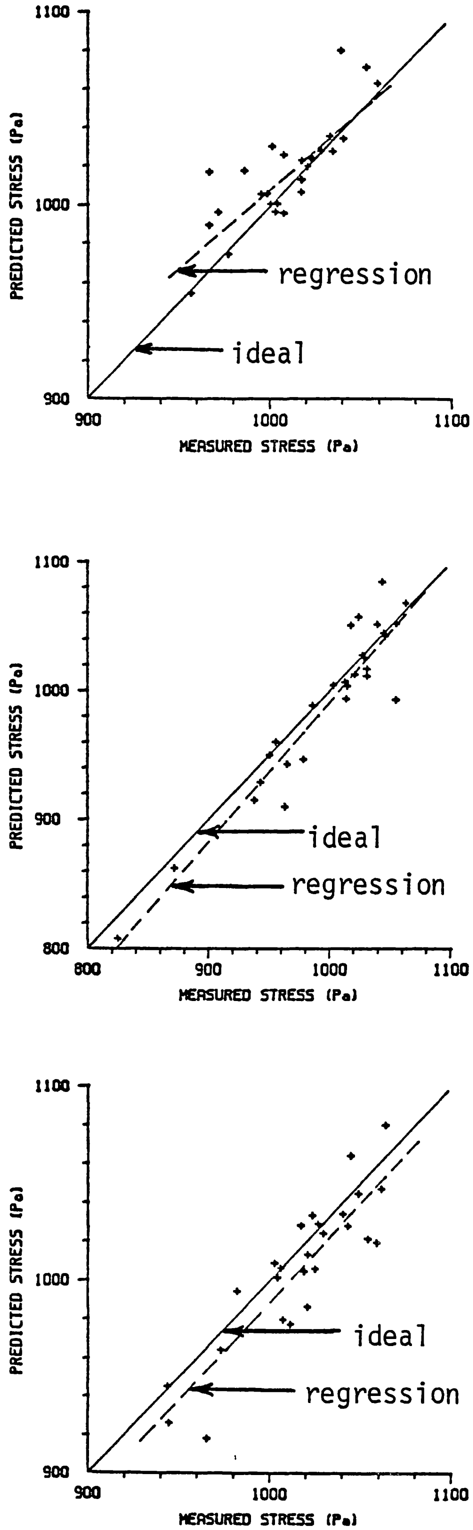

Figure 22. Comparison of Predicted and Measured Stress at the Top of Vertical Samples V13, V14 and V15

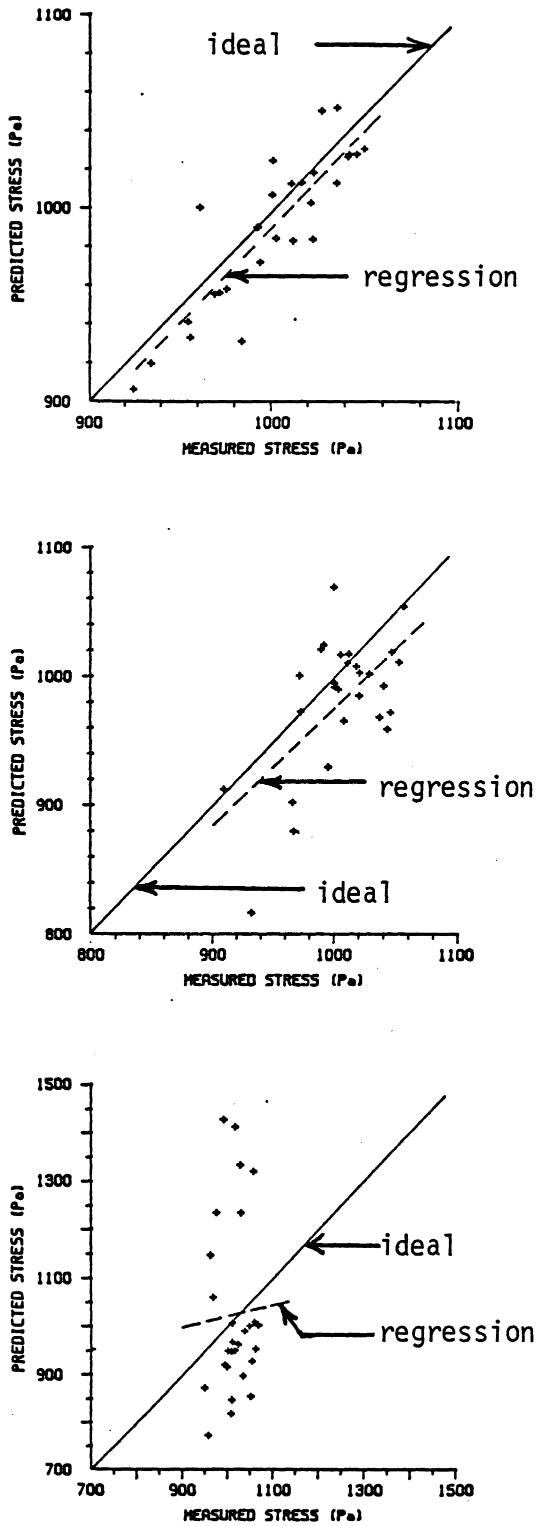

Figure 23. Comparison of Predicted and Measured Stress at the Top of Horizontal Samples H13, H14 and H15

second-order viscoelastic stress-strain model did a reasonable job of predicting the stress at the top of the soil sample, except for sample H15. Regression equation coefficients and statistics for the comparison of predicted and measured stresses at the top of the soil samples are given in Table IX. The intercepts and slopes were reasonably close to 0 and 1 respectively, while the coefficients of determination (R^2) showed the effect of scatter in the data. Root Mean Square (RMS) errors were calculated as the standard error of the estimate for the regression divided by the mean of the observed values. Note the RMS errors were also reasonable except for sample H15. Overall, it can be concluded the second-order viscoelastic stress-strain model did a reasonable job of predicting dynamic stress at the top of the soil samples.

TABLE IX

REGRESSION EQUATION COEFFICIENTS AND STATISTICS COMPARING PREDICTED TO MEASURED STRESS AT THE TOP OF THE SOIL SAMPLES

Sample	Intercept	Slope	R^2	RMS Error, Percent
V13	185.49	0.823	0.660	1.54
V14	-99.23	1.093	0.889	2.22
V15	-39.72	1.029	0.784	1.82
H13	-10.11	1.000	0.763	1.98
H14	56.52	0.920	0.373	4.38
H15	790.51	0.231	0.00184	17.79

Stress Prediction Envelopes

The 3 vertical samples and 3 horizontal samples used in this validation test were the samples remaining after the 12 horizontal and 12 vertical samples had been used to develop the mean parameter coefficients. The 95 percent confidence limit values for the parameter coefficients from the 12 vertical and 12 horizontal samples were used to predict 95 percent confidence envelopes for the stress at the top of the remaining 3 vertical and 3 horizontal samples. Measured stress at the top of the samples was enclosed by the confidence envelopes for all 3 vertical and 3 horizontal samples (Figures 24 and 25) indicating the dynamic stress-strain behavior of these 3 vertical and 3 horizontal samples was bounded by the confidence interval of the parameter coefficient means. This reinforces the idea that the second-order viscoelastic stress-strain model is a reasonable model for the soil investigated.

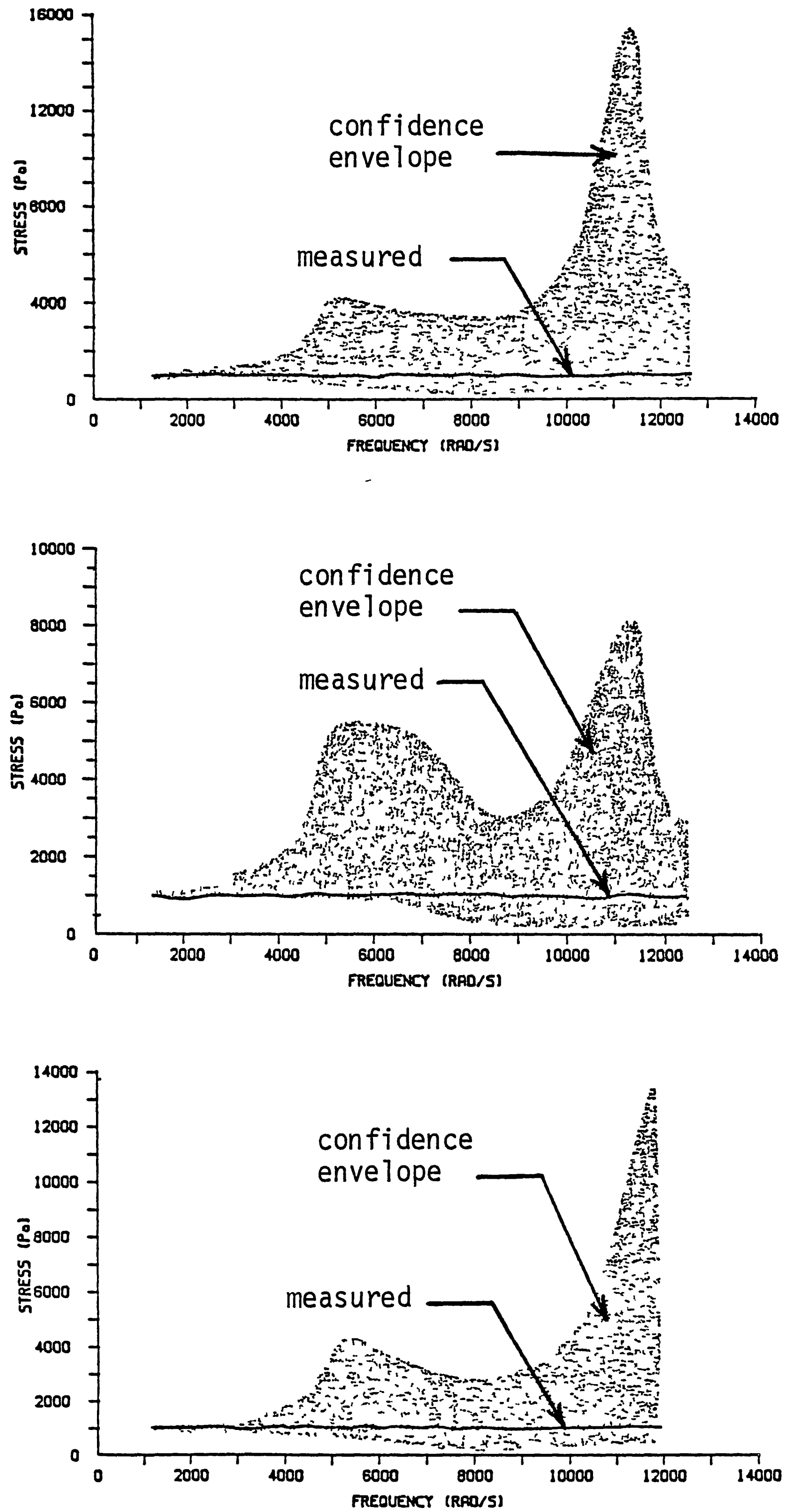

Figure 24. Ninety Five Percent Confidence Envelopes for the Stress at the Top of Vertical Samples V13, V14 and V15

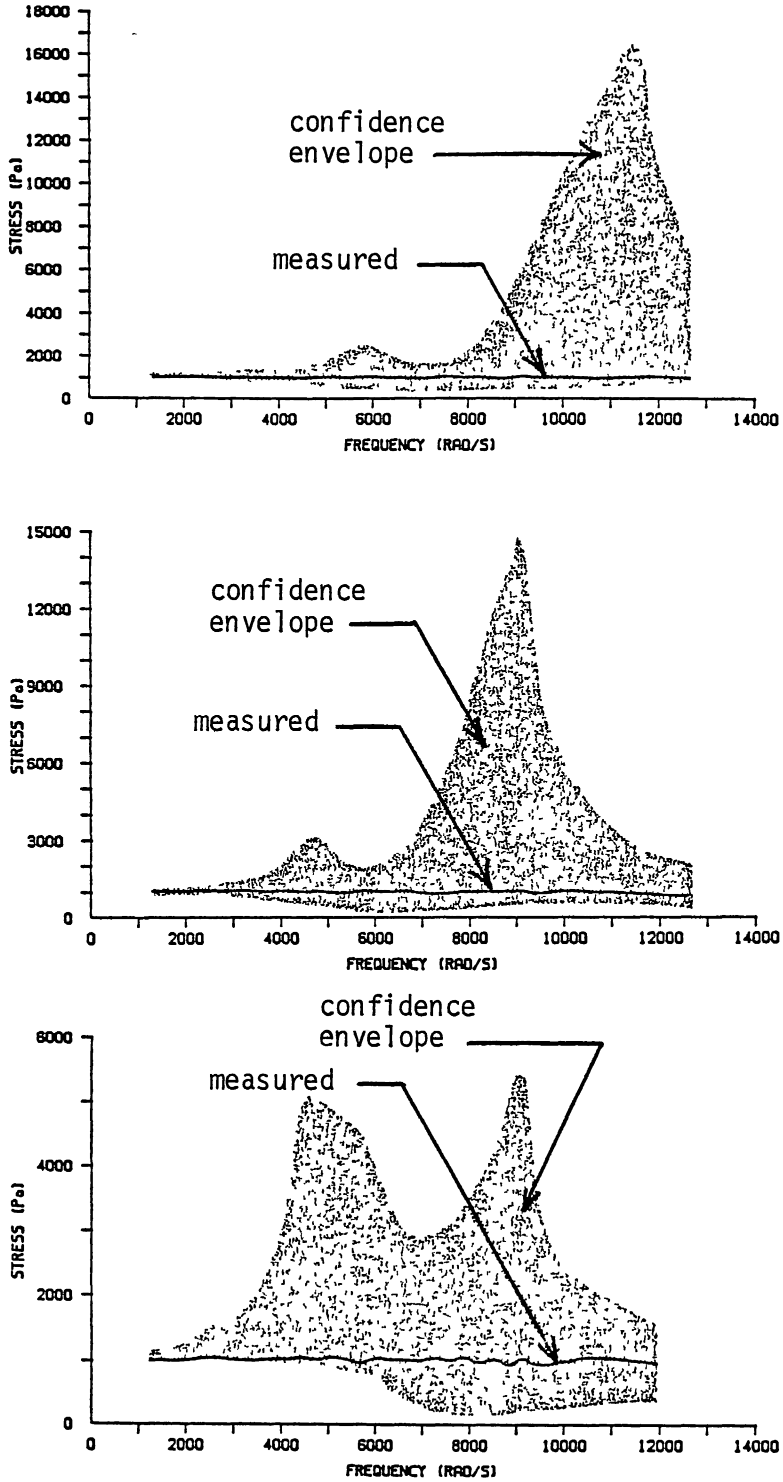

Figure 25. Ninety Five Percent Confidence Envelopes for the Stress at the Top of Horizontal Samples H13, H14 and H15

CHAPTER VIII

CONCLUSIONS

A test using one-dimensional wave propagation techniques was developed to allow evaluation of dynamic stress-strain models for soil. The test consisted of measuring the acceleration at the top and bottom of a right circular cylindrical soil sample as it was given a sinusoidal displacement by an electromagnetic shaker. Four proposed dynamic stress-strain models were evaluated with this test. Specific conclusions were:

1. A second-order viscoelastic stress-strain model was used in solving the differential equation describing one-dimensional wave propagation through a cylindrical soil sample.
2. Beeswax was determined to be a good material for attaching soil samples to a shaker head and accelerometers to soil samples.
3. Miminally disturbed soil samples were obtained using a sampler with an outer auger.
4. Frequencies between 1250 and 12500 rad/s and accelerations between 0 and 25 m/s^2 were determined to be appropriate for the dynamic test.

5. The second-order viscoelastic stress-strain model originated in this work best described the dynamic stress-strain behavior of the soil samples.
6. Original sapmle orientation (vertical or horizontal) influenced dynamic behavior.
7. Predicted stress using the second-order viscoelastic model compared well with the measured stress for five of six soil samples.

CHAPTER IX

RECOMMENDATIONS FOR FURTHER RESEARCH

Experimental Technique Improvements

Tables III and IV show that water loss during dynamic testing ranged from 1.5 to 5 percent of sample dry weight. While the effect of this water loss on test results is not known, attempts to reduce water loss or understand the effects on results are recommended.

Some increase in the accuracy of the phase lag measurement can be obtained by a change in experimental technique. During the dynamic testing, the time-per-point switch on the oscilloscope was set so that at least one and one half acceleration cycles fit on the screen at each frequency. This was necessary to measure the acceleration ratio, but resulted in reduced resolution for the phase lag measurement especially at low phase angles. A possible solution to this problem is to use two sets of time-acceleration data at each frequency. The first set could be at one time-per-point switch setting that would be appropriate for measuring the acceleration ratio. The second data set could be taken with a shorter time-per-point setting to increase the resolution for measuring the phase lag. This procedure would slow down the dynamic test and increase the amount of data to be stored on computer disks.

Additional Research

This research on dynamic stress-strain in soil has shown promise for use in tillage, traction and compaction work. Applications of this research in design of vibratory tillage tools appears especially promising. Suggestions for further work along this line are:

1. Determine the effect of moisture content and soil type on the α and ξ parameter coefficients.
2. Determine if displacement functions other than sinusoidal show the dynamic stress-strain relationship for soil to be dependent on the type of displacement or forcing function.
3. Differentiate the expression for stress with respect to frequency, set that equal to zero and solve for the frequency at which the stress in the soil is maximized. Comparison with experimental measurements would provide another indication of the validity of the model. The frequency at which stress in the soil is maximized may indicate optimum operation frequency for vibratory tillage.
4. Differentiate the expression for stress with respect to x, set that equal to zero and solve for the length at which the stress is maximized. Comparison with experimental measurements would

provide another indication of the validity of the model. The length at which the stress is maximized may indicate the size of soil particles resulting from vibratory tillage.

LITERATURE CITED

Aref, K. E., W. J. Chancellor and D. R. Nielsen. 1975. Dynamic shear strength properties of unsaturated soils. TRANSACTIONS of the ASAE 17(5):818-823.

Bernhard, R. K. and J. Finelli. 1954. Pilot studies on dynamic testing of soils. Part II. Propagation velocity and dynamic moduli of elasticity. ASTM symposium on soil mechanics. ASTM Publication No. 156.

Bloome, P. D., J. D. Summers, A. Khalilian and D. G. Batchelder. 1983. Ballasting recommendations for two-wheel and four-wheel drive tractors. ASAE Paper No. 83-1067. ASAE, St. Joseph, MI 49085.

Buchele, W. F. 1961. A power sampler of undisturbed soils. TRANSACTIONS of the ASAE 4(2):185-187,191.

Christian J. T. 1966. Plane strain deformation analysis of soil. Report No. 3-129. U.S. Army Engineer Waterways Experiment Station, Vicksburg, MS 39180.

Clark, R. L. 1984. Tractive modeling and field data requirements to predict traction. ASAE Paper No. 84-1055. ASAE, St. Joseph, MI 49085.

DeRoock, B. and A. W. Cooper. 1967. Relation between propagation velocity of mechanical waves through soil and soil strength. TRANSACTIONS of the ASAE 10(4):471-474.

Duncan, J. M. 1980. Hyperbolic stress-strain relationships. Proceedings of the workshop on limit equilibrium, plasticity and generalized stress-strain in geotechnical engineering. ASCE, New York, NY 10017.

Flenniken, M., R. E. Hefner and J. A. Weber. 1977. Dynamic soil strength parameters from unconfined compression tests. TRANSACTIONS of the ASAE 20(1):21-25,29.

Frietag, D. R., R. L. Schafer and R. D. Wismer. 1969. Similitude studies of soil-machine systems. TRANSACTIONS of the ASAE 13(2):201-213.

Gill, W. R. and G. E. Vanden Berg. 1968. Soil dynamics in tillage and traction. USDA-ARS Agriculture Handbook No. 316. U.S. Government Printing Office, Washington, DC 20402.

Gupta, C. P. and A. C. Pandya. 1967. Behavior of soil under dynamic loading: its application to tillage implements. TRANSACTIONS of the ASAE 10(3):352-358, 363.

Hardin, B. O. and F. E. Richart. 1963. Elastic wave velocities in granular soils. Proc. of ASCE, Journal of the Soil Mech. and Found. Div. 89(SM1): 33-65.

Hayes, J. C. and J. T. Ligon. 1977. Prediction of traction using soil physical properties. ASAE Paper No. 77-1054. ASAE, St. Joseph, MI 49085.

Johnson, C. E., G. Murphy, W. G. Lovely and R. L. Schafer. 1972. Identifying soil dynamic parameters for soil-machine systems. TRANSACTIONS of the ASAE 15(1): 9-13.

Kitani, O. and S. P. E. Persson. 1967. Stress-strain relationships for soil with variable lateral strain. TRANSACTIONS of the ASAE 10(6):738-741,745.

Lambe, T. W. and R. V. Whitman. 1979. Soil mechanics, SI version. John Wiley and Sons, Inc. New York, NY 10016.

McMurdie, J. L. 1963. Some characteristics of the soil deformation process. Soil Sci. Soc. of Am. Proc. 27(3):251-254.

McNiven, H. D. and C. B. Brown. 1963. (Discussion of) Elastic wave velocities in granular soil. Proc. of ASCE, Journal of Soil Mech. and Found. Div. 89(SM5): 103,106-109.

Mohsenin, N. N. 1970. Physical properties of plant and animal materials. Gordon and Breach Science Publishers, New York, NY 10011.

Persson, S. P. E. 1969. Gaps and limitations in existing traction theories. ASAE Paper No. 69-134. ASAE, St. Joseph, MI 49085.

Ram, R. B. and C. P. Gupta. 1972. Relationship between rheological coefficients and soil parameters in compression test. TRANSACTIONS of the ASAE 15(6): 1054-1058.

Raper, R. L. and D. C. Erbach. 1985. Accurate bulk density measurements using a core sampler. ASAE Paper No. 85-1542. ASAE, St. Joseph, MI 49085.

Reaves, C. A. and R. L. Schafer. 1971. Soil measurements related to the performance of soil-machine systems. SAE Paper No. 710512. SAE, Warrendale, PA 15096.

Richart, F. E, J. R. Hall and R. D. Woods. 1970. Vibrations of soils and foundations. Prentice-Hall, Inc., Englewood Cliffs, NJ 07632.

Salencon, J. 1977. Applications of the theory of plasticity in soil mechanics. John Wiley and Sons, Inc., New York, NY 10016.

Smith, G. M., Y. C. Pao and J. D. Fickes. 1978. Determination of a dynamic model for urethane prosthetic compounds. Experimental Mechanics 18(10):389-395.

Stafford, J. V. and D. W. Tanner. 1983. Effect of rate on soil shear strength and soil-metal friction. I. Shear strength. Soil Tillage Res. 3(3):245-260.

Summers, J. D., M. F. Kocher and J. B. Solie. 1985. Frequency analysis of tillage tool forces. Proceedings of the International Conference on Soil Dynamics. 2:377-383.

Taylor J. H. and G. E. Vanden Berg. 1966. Role of displacement in a simple traction system. TRANSCATIONS of the ASAE 9(1):10-13.

Upadhaya, S. K., R. Hamidi, F. Shafigh-Nobari and R. W. Hooley. 1984. Tractive ability of pnuematic tires: a finite element model. ASAE Paper No. 84-1052. ASAE, St. Joseph, MI 49085.

USDA. 1947. Diagnosis and improvement of saline and alkali soils. USDA Agricultural Research Administration, Bureau of Plant Industry, Soils and Agricultural Engineering, Division of Soils, Fertilizers and Irrigation. US Regional Salinity Laboratory, Riverside CA.

Vanden Berg, G. E. 1961. Requirements for a soil mechanics. TRANSACTIONS of the ASAE 4(2):234-238.

Wismer, R. D. and H. J. Luth. 1974. Off-road traction prediction for wheeled vehicles. TRANSACTIONS of the ASAE 17(1):8-10,14.

APPENDIXES

APPENDIX A

NIC_PC.BAS

```
10 REM*  THIS PROGRAM WILL ALLOW AN IBM PERSONAL COMPUTER TO GET DIGITAL DATA
20 REM*  FROM THE NICOLET 2090 MODEL 604 OSCILLOSCOPE   IN PARTICULAR, IT WILL
30 REM*  GET ACCELERATION DATA OBTAINED FROM THE LING DYNAMICS MODEL 408
40 REM*  SHAKER.  THE SCOPE SHOULD BE OPERATED IN THE + OR - 10 V SCALE WITH
50 REM*  THE Q1 MEMORY, AN APPROPRIATE TIME PER POINT SO ROUGHLY 2 TO 4 CYCLES
60 REM*  SHOW ON THE SCREEN,  THE ACCELEROMETER AT THE BOTTOM OF THE SAMPLE
70 REM*  ATTACHED TO THE FIRST CHANNEL, AND THE ACCELEROMETER AT THE TOP OF THE
80 REM*  SAMPLE ATTACHED TO THE SECOND CHANNEL   ENTER BASIC ON THE PC WITH THE
90 REM*  COMMAND BASIC/C:50000    THIS ALLOWS USE OF A COMMUNICATIONS BUFFER
100 REM* FOR INTERFACING WITH THE NICOLET   MICHAEL F  KOCHER
110 REM* OKLAHOMA STATE UNIVERSITY DEPARTMENT OF AGRICULTURAL ENGINEERING
120 REM* MARCH 11, 1985
130 REM**********************************************************************
140 DIM BOT(512),TOP(512),TBOT(512),TTOP(512)
150 INPUT "ENTER FILENAME FOR BOTTOM ACCELEROMETER DATA ";B$
160 INPUT 'ENTER FILENAME FOR TOP ACCELEROMETER DATA ";T$
170 REM**********************************************************************
180 REM  PREPARE PORT FOR OPERATION AT 9600 BAUD, PARITY BIT ALWAYS A SPACE,
190 REM  7 BITS PER DATA WORD, 1 STOP BIT
200 REM**********************************************************************
210 OPEN "COM1:9600,S,7,1" AS #1
220 REM**********************************************************************
230 REM  SEND CNTL-A TO ACTIVATE SCOPE RS-232C PORT   SEND CR/LF DELIMITERS,
240 REM  RESET DATA ADDRESS TO START, SEND ASCII DATA, AUTOMATICALLY ADVANCING
250 REM  THE DATA ADDRESS, SEND 1024 DATA POINTS, START TRANSMISSION
260 REM**********************************************************************
270 PRINT #1,CHR$(1)
280 PRINT #1,"E1D1D001024"+CHR$(2)
290 REM**********************************************************************
300 REM  INPUT BOTTOM AND TOP ACCELERATION
310 REM**********************************************************************
320 FOR I=0 TO 511
330 INPUT #1,BOT(I)
340 INPUT #1,TOP(I)
350 PRINT I,BOT(I),TOP(I)
360 NEXT I
370 REM**********************************************************************
380 REM  CHECK FOR ERRORS DURING TRANSMISSION
390 REM**********************************************************************
400 INPUT #1,E1$
410 PRINT "E1$ =",E1$
420 IF E1$<>"|@" THEN PRINT "ERROR DURING RECALL"
430 REM**********************************************************************
440 REM  GET OSCILLOSCOPE SCALE FACTOR DATA
450 REM  SEND CNTL-A TO ACTIVATE SCOPE RS-232C PORT
460 REM**********************************************************************
470 PRINT #1,CHR$(1)
480 REM**********************************************************************
490 REM  SEND CR/LF DELIMITERS, SEND ORIGINAL NORMALIZING NUMBERS, OUTPUT 2
500 REM  NORMALIZING SETS, START TRANSMISSION
510 REM**********************************************************************
520 PRINT #1,"E1N100002 +CHR$(2)
530 INPUT #1,N1$
540 PRINT "N1$ =',N1$
550 REM**********************************************************************
560 REM  CHECK FOR ERRORS DURING TRANSMISSION
570 REM**********************************************************************
580 INPUT #1,N2$
590 PRINT "N2$ =",N2$
600 INPUT #1,E2$
610 PRINT "E2$ =",E2$
620 IF E2$<>"|@" THEN PRINT"ERROR DURING NORMALIZATION RECALL"
630 CLOSE
640 REM**********************************************************************
650 REM  CONVERT NORMALIZATION DATA TO SCALE FACTORS FOR BOTTOM ACCELERATION
660 REM**********************************************************************
670 VNB1=VAL(MID$(N1$,1,1))
680 HNB1=VAL(MID$(N1$,2,1))
690 MF1=VAL(MID$(N1$,3,1))
700 VZ1=VAL(MID$(N1$,4,5))
710 HZ1=VAL(MID$(N1$,9,5))
720 VN1=VAL(MID$(N1$,14,3))
730 VN1E=VAL(MID$(N1$,18,3))
740 HN1=VAL(MID$(N1$,21,3))
750 HN1E=VAL(MID$(N1$,25,3))
760 REM**********************************************************************
770 REM  CONVERT NORMALIZATION DATA TO SCALE FACTORS FOR TOP ACCELERATION
780 REM**********************************************************************
790 VNB2=VAL(MID$(N2$,1,1))
800 HNB2=VAL(MID$(N2$,2,1))
810 MF2=VAL(MID$(N2$,3,1))
820 VZ2=VAL(MID$(N2$,4,5))
830 HZ2=VAL(MID$(N2$,9,5))
840 VN2=VAL(MID$(N2$,14,3))
850 VN2E=VAL(MID$(N2$,18,3))
860 HN2=VAL(MID$(N2$,21,3))
870 HN2E=VAL(MID$(N2$,25,3))
880 IF MF1<>8 OR MF2<>8 THEN PRINT"RESET SCOPE MEMORY TO Q1, USE TWO INPUTS "
890 PRINT "INPUT CHARGE AMPLIFIER SCALE FACTOR (G/VOLT)"
900 INPUT SF
910 REM**********************************************************************
920 REM  WRITE BOTTOM TIME AND ACCELERATION DATA TO DISK
930 REM**********************************************************************
940 OPEN "B:'+B$+" DAT" FOR OUTPUT AS #2
950 WRITE #2, TIME (S), BOTTOM ACCELERATION (M/S**2)'
960 REM**********************************************************************
970 REM  CONVERT SCOPE DATA TO ACCELERATION DATA FOR THE BOTTOM ACCELEROMETER
980 REM**********************************************************************
990 FOR I=0 TO 511
1000 TBOT(I)=HN1*(10^HN1E)*I
1010 BOT(I)=(BOT(I)-VZ1)*VN1*(10^VN1E)*SF*9 810001*(-1I)
1020 NEXT I
1030 FOR I=0 TO 511
1040 WRITE #2,TBOT(I),BOT(I)
1050 NEXT I
1060 CLOSE
1070 REM**********************************************************************
1080 REM  WRITE TOP TIME AND ACCELERATION DATA TO DISK
1090 REM**********************************************************************
1100 OPEN "B:"+T$+" DAT" FOR OUTPUT AS #3
1110 WRITE #3,'TIME (S), TOP ACCELERATION (M/S**2)"
1120 REM**********************************************************************
1130 REM  CONVERT SCOPE DATA TO ACCELERATION DATA FOR THE TOP ACCELEROMETER
1140 REM**********************************************************************
1150 FOR I=0 TO 511
1160 TTOP(I)=HN2*(10^HN2E)*I
1170 TOP(I)=(TOP(I)-VZ2)*VN2*(10^VN2E)*SF*9 810001
1180 NEXT I
1190 FOR I=0 TO 511
1200 WRITE #3,TTOP(I),TOP(I)
1210 NEXT I
1220 CLOSE
1230 END
```

APPENDIX B

MANIP.BAS

```
10 REM THIS PROGRAM WILL READ ACCELERATION DATA TAKEN WITH THE NICOLET
20 REM 2090 SCOPE AND STORED IN TWO FILES ON FLOPPY DISK   THE PROGRAM
30 REM WILL NORMALIZE THE ACCELERATION DATA AND CALCULATE THE FRFQUENCY
40 REM *TIME VARIABLE FOR COMPARISON WITH A SINE FUNCTION   THIS PROGRAM
50 REM MODIFIES DATA FOR USE WITH THE SINE REGRESSION PROGRAM   PROGRAM
60 REM DEVELOPED AT THE OKLAHOMA STATE UNIVERSITY DEPARTMENT OF AGRICULTURAL
70 REM ENGINEERING.  SEPTEMBER 27, 1985   MICHAEL F  KOCHER
80 REM**********************************************************************
90 DIM T(520),Y(520),XB(520),YB(520),XT(620),YT(520)
100 PRINT "PUT DATA DISK IN DRIVE B'
110 INPUT "ENTER DATA FILENAME ",B$
120 INPUT 'ENTER SAMPLE NUMBER ",SN$
130 LPRINT
140 LPRINT
150 A6$= DATA: " + B$
160 A6=CINT((LEN(A6$))/2)
170 LPRINT SPC(40-A6);A6$
180 REM*********************************************************************
190 REM     START READING THE BOTTOM ACCELERATION DATA FILE
200 REM*********************************************************************
210 OPEN 'B:B" + B$ + " DAT" FOR INPUT AS #1
220 INPUT #1,L$
230 INPUT #1, T(0),Y(0)
240 INPUT #1, T(1),Y(1)
250 I=1
260 I=I+1
270 INPUT #1, T(I),Y(I)
280 REM*********************************************************************
290 REM     FIND THE START OF A SINE WAVE
300 REM*********************************************************************
310 IF Y(I-2)>0 GOTO 260
320 IF Y(I-1)<0 GOTO 260
330 IF Y(I-1)>0 GOTO 400
340 IF Y(I)<0 GOTO 260
350 IF Y(I)=0 GOTO 380
360 I0=I-1
370 GOTO 480
380 I0=I
390 GOTO 480
400 IF Y(I)<=0 GOTO 260
410 IF ABS(Y(I-1)) > ABS(Y(I-2)) GOTO 440
420 I0=I-1
430 GOTO 480
440 I0=I-2
450 REM*********************************************************************
460 REM     FIND THE MIDDLE OF THE SINE WAVE (PI)
470 REM*********************************************************************
480 I=I+1
490 INPUT #1,T(I),Y(I)
500 IF Y(I-2)<0 GOTO 480
510 IF Y(I-1)>0 GOTO 480
520 IF Y(I-1)<0 GOTO 560
530 IF Y(I)>0 GOTO 480
540 I1=I-1
550 GOTO 610
560 IF Y(I)>=0 GOTO 480
570 I1=I-2
580 REM*********************************************************************
590 REM      FIND THE END OF THE SINE WAVE (2*PI)
600 REM*********************************************************************
610 I=I+1
620 INPUT #1,T(I),Y(I)
630 IF Y(I-2)>0 GOTO 610
640 IF Y(I-1)<0 GOTO 610
650 IF Y(I-1)>0 GOTO 690
660 IF Y(I)<0 GOTO 610
670 I2=I-1
680 GOTO 770
690 IF Y(I)<=0 GOTO 610
700 IF ABS(Y(I-1)) > ABS(Y(I-2)) GOTO 730
710 I2=I-1
720 GOTO 770
730 I2=I-2
740 REM*********************************************************************
750 REM     STOP READING THE BOTTOM DATA FILE
760 REM*********************************************************************
770 CLOSE
780 REM*********************************************************************
790 REM   FIND THE AVERAGE ACCELERATION OVER THE 2*PI CYCLE
800 REM*********************************************************************
810 SUM=0
820 FOR I=I0 TO I2
830      SUM=SUM+Y(I)
840 NEXT I
850 N=I2+1-I0
860 AVE=SUM/N
870 REM*********************************************************************
880 REM   REMOVE THE BIAS OF THE AVERAGE ACCELERATION FROM THE DATA
890 REM   FIND THE MAXIMUM ACCELERATION OVER THE 2*PI CYCLE
900 REM   SCALE THE ACCELERATION DATA TO BETWEEN -1 AND 1
910 REM*********************************************************************
920 AB=0
930 FOR I=I0 TO I2
940      Y(I)=Y(I)-AVE
950      IF ABS(Y(I)) <= AB GOTO 970
960      AB=ABS(Y(I))
970 NEXT I
980 FOR I=I0 TO I2
990      YB(I-I0)=Y(I)/AB
1000 NEXT I
1010 REM********************************************************************
1020 REM    ITERATE TO FIND THE EXCITATION FREQUENCY
1030 REM********************************************************************
1040 W=6 283185/(T(I2)-T(I0))
1050 TS=T(I0)-(YB(0)/W)
1060 TE=T(I2)-(YB(I2-I0)/W)
1070 WN=6 283185/(TE-TS)
1080 IF ABS(WN-W) <  001 GOTO 1110
1090 W=WN
1100 GOTO 1050
1110 F=1!/(TE-TS)
```

```
1120 REM*********************************************************************
1130 REM     ADJUST THE TIME VALUES TO THE REAL START OF THE SINE WAVE AND
1140 REM     CHANGE THE TIME VALUES TO ANGLE VALUES (W*T)
1150 REM*********************************************************************
1160 FOR I=I0 TO I2
1170      XB(I-I0)=(T(I)-TS)*W
1180 REM*********************************************************************
1190 REM     PRINT THE RESULTS FOR THE BOTTOM ACCELERATION DATA FILE
1200 REM*********************************************************************
1210 NEXT I
1220 LPRINT
1230 LPRINT
1240 LPRINT "             FREQUENCY = ";
1250 LPRINT USING "#### ##";F;
1260 LPRINT " Hz  = ";
1270 LPRINT USING "##### ##";W;
1280 LPRINT " RAD/SEC"
1290 LPRINT
1300 LPRINT
1310 LPRINT "             AVERAGE BOTTOM ACCELERATION OVER 2*PI = ";
1320 LPRINT USING "# #####";AVE;
1330 LPRINT " (M/S**2)"
1340 LPRINT
1350 LPRINT "             MAXIMUM BOTTOM ACCELERATION OVER 2*PI = ";
1360 LPRINT USING "### ####";AB;
1370 LPRINT " (M/S**2)"
1380 LPRINT
1390 LPRINT
1400 REM*********************************************************************
1410 REM   WRITE A DATA SET TO DISK FOR REGRESSION AGAINST A SINE WAVE
1420 REM*********************************************************************
1430 OPEN "B:CB" + B$ + ".DAT" FOR OUTPUT AS #2
1440 WRITE #2,N
1450 FOR I=0 TO I2-I0
1460      WRITE #2,XB(I),YB(I)
1470      NEXT I
1480 REM*********************************************************************
1490 REM    START READING THE TOP ACCELERATION DATA FILE
1500 REM*********************************************************************
1510 CLOSE
1520 OPEN "B:T" + B$ + ".DAT" FOR INPUT AS #3
1530 INPUT #3,L$
1540 IT=CINT(I0/2)
1550 FOR I=0 TO IT
1560      INPUT #3,T(I),Y(I)
1570 NEXT I
1580 INPUT #3, T(I),Y(I)
1590 REM*********************************************************************
1600 REM     FIND THE START OF A SINE WAVE
1610 REM*********************************************************************
1620 I=I+1
1630 INPUT #3,T(I),Y(I)
1640 IF Y(I-2) > 0 GOTO 1620
1650 IF Y(I-1) < 0 GOTO 1620
1660 IF Y(I-1) > 0 GOTO 1730
1670 IF Y(I) < 0 GOTO 1620
1680 IF Y(I)=0 GOTO 1710
1690 I02=I-1
1700 GOTO 1820
1710 I02=I
1720 GOTO 1820
1730 IF Y(I) <= 0 GOTO 1620
1740 IF ABS(Y(I-1)) > ABS(Y(I-2)) GOTO 1770
1750 I02=I-1
1760 GOTO 1820
1770 I02=I-2
1780 REM*********************************************************************
1790 REM     READ THE SAME NUMBER OF POINTS FOR THE TOP ACCELERATION CYCLE
1800 REM     AS WERE IN THE BOTTOM SINE WAVE
1810 REM*********************************************************************
1820 FOR J=I+1 TO N+I02-1
1830      INPUT #3,T(J),Y(J)
1840 NEXT J
1850 REM*********************************************************************
1860 REM     FIND THE AVERAGE TOP ACCELERATION OVER THE 2*PI CYCLE
1870 REM*********************************************************************
1880 SUM=0
1890 FOR I=I02 TO I02+N-1
1900      SUM=SUM+Y(I)
1910 NEXT I
1920 CLOSE
1930 AVE=SUM/N
1940 LPRINT "             AVERAGE TOP ACCELERATION OVER 2*PI = ";
1950 LPRINT USING "# #####";AVE;
1960 LPRINT " (M/S**2)"
1970 LPRINT
1980 REM*********************************************************************
1990 REM   REMOVE THE AVERAGE ACCELERATION BIAS FROM THE DATA
2000 REM   FIND THE MAXIMUM ACCELERATION OVER THE 2*PI CYCLE
2010 REM*********************************************************************
2020 AT=0
2030 FOR I=I02 TO I02+N-1
2040      Y(I)=Y(I)-AVE
2050      IF ABS(Y(I)) <= AT GOTO 2070
2060      AT=ABS(Y(I))
2070 NEXT I
2080 LPRINT "             MAXIMUM TOP ACCELERATION OVER 2*PI = ";
2090 LPRINT USING "### ####';AT;
2100 LPRINT " (M/S**2)'
2110 LPRINT
2120 REM*********************************************************************
2130 REM   SCALE THE ACCELERATION DATA TO BETWEEN -1 AND 1
2140 REM   ADJUST THE TIME VALUES TO THE REAL START OF THE SINE WAVE
2150 REM   CHANGE THE TIME VALUES TO ANGLE VALUES (W*T)
2160 REM*********************************************************************
2170 FOR I=I02 TO I02+N-1
2180      YT(I-I02)=Y(I)/AT
2190      XT(I-I02)=((T(I)-T(I02))*W)+YT(0)
2200 NEXT I
```

```
2210 REM**********************************************************************
2220 REM   WRITE A DATA SET TO DISK FOR REGRESSION AGAINST A SINE WAVE
2230 REM**********************************************************************
2240 OPEN 'B:CT" + B$ + ".DAT' FOR OUTPUT AS #4
2250 WRITE #4,N
2260 FOR I=0 TO N-1
2270      WRITE #4,XT(I),YT(I)
2280 NEXT I
2290 CLOSE
2300 REM**********************************************************************
2310 REM   CALCULATE THE PHASE ANGLE BETWEEN THE BOTTOM AND TOP ACCELERATIONS
2320 REM**********************************************************************
2330 PHI=((T(I02)-T(I0))*W)-YT(0)+YB(0)
2340 PHI2=PHI*57 29578
2350 LPRINT
2360 LPRINT
2370 LPRINT "              PHASE LAG = ";
2380 LPRINT USING "# ####";PHI;
2390 LPRINT " RADIANS  = ";
2400 LPRINT USING "### ##";PHI2;
2410 LPRINT " DEGREES";
2420 ARATIO=AT/AB
2430 LPRINT
2440 LPRINT
2450 LPRINT "              ACCELERATION RATIO = ";
2460 LPRINT USING "## ####";ARATIO
2470 LPRINT
2480 LPRINT
2490 LPRINT
2500 REM**********************************************************************
2510 REM  WRITE THE FREQUENCY, ACCELERATION RATIO AND PHASE LAG TO A DISK
2520 REM  FILE FOR ANALYSIS BY OTHER PROGRAMS
2530 REM**********************************************************************
2540 OPEN "B:" + SN$ + ".DAT' FOR APPEND AS #5
2550 WRITE #5,W,ARATIO,-1!*PHI
2560 CLOSE
2570 END
```

APPENDIX C

COMPAR.FOR

```
C  THIS PROGRAM FINDS VALUES AT EACH FREQUENCY FOR THE PARAMETERS
C  IN THE FIRST-ORDER VISCOELASTIC AND COMPLEX MODULUS DYNAMIC
C  STRESS-STRAIN MODELS FOR SOIL   THE ERROR FUNCTION MINIMIZED IN
C  THIS ROUTINE IS THE VECTOR DIFFERENCE BETWEEN THE MEASURED AND
C  PREDICTED DATA   THIS PROGRAM USES THE PROFESSIONAL FORTRAN
C  COMPILER AVAILABLE FOR THE IBM PC   MICHAEL F. KOCHER
C  OKLAHOMA STATE UNIVERSITY AGRICULTURAL ENGINEERING DEPARTMENT.
C  OCTOBER 26, 1985
C
      CHARACTER*3 SNO
      CHARACTER*10 DATFN
      REAL M,RO,L,A,FREQ,AR,DEL,TRM,ERN,ERR
      REAL E,ALPHA,PH,PHTR,STEP,AL,BET
      COMPLEX Z1,Z,W,PHI,THETA,TR,CAR
      INTEGER I,K
C
C  OPEN DATA FILES FOR EASY PLOTTING OF THE MAGNITUDE OF THE
C  PREDICTED ACCELERATION RATIO, PHASE ANGLE AND LOSS
C  FACTORS VERSUS EXCITATION FREQUENCY.
C
      OPEN(UNIT=1,FILE='A:COMPLEX.DAT')
      OPEN(UNIT=2,FILE='A:VISCO1 DAT')
      OPEN(UNIT=3,FILE='A:MAGCOMV1 DAT')
      OPEN(UNIT=4,FILE='A:PHCOMV1.DAT')
      OPEN (UNIT=9,FILE='LPT1')
C
C  M IS THE MASS OF THE ATTACHED ACCELEROMETER AND DISK AT THE TOP
C  OF THE SOIL SAMPLE DURING THE DYNAMIC TESTS
C
      M=0.0413
C
C  INPUT THE SAMPLE DATA
C
      PRINT *,' ENTER SAMPLE NUMBER AS ''XXX'' '
      READ *,SNO
      WRITE(9,10)SNO
   10 FORMAT(' COMPLEX AND VISCOELASTIC MODELS FOR SAMPLE ',A3)
      PRINT *,' ENTER SAMPLE LENGTH (m) '
      READ *,L
      PRINT *,' ENTER SAMPLE CROSS SECTIONAL AREA (m**2) '
      READ *,A
      PRINT *,' ENTER SAMPLE WET BULK DENSITY (kg/m**3) '
      READ *,RO
      PRINT *,' ENTER SAMPLE ELASTIC MODULUS (Pa) '
      READ *,E
C
C  OUTPUT SAMPLE DATA TO PRINTER FOR HARDCOPY OF RESULTS
C
      WRITE(9,11)L,A,RO,E
   11 FORMAT('                  LENGTH = ',F7 4,' m',/,
     $ ' CROSS SECTIONAL AREA = ',E10 3,' m**2',/,
     $ '      WET BULK DENSITY = ',F7 1,' kg/m**3',/,
     $ '       ELASTIC MODULUS = ',E10 3,' Pa')
      WRITE (9,12)
   12 FORMAT('    FREQ',7X,'AR',7X,'TR',5X,'PH(AR)   PH(TR)',3X,
     $ 'DELTA',3X,'ALPHA')
C
C  GET THE FILENAME OF THE DYNAMIC TEST DATA
C
      PRINT *,' ENTER DYNAMIC TEST DATA FILENAME AS ''A:XXX.DAT'' '
      READ *,DATFN
      OPEN(UNIT=5,FILE=DATFN)
C
C  READ THE NUMBER OF FREQUENCIES AT WHICH THE SAMPLE WAS TESTED
C
      READ(5,*)I
C
C  START ITERATION PROCESS FOR A PARTICULAR FREQUENCY
C  GET THE DATA FOR THIS FREQUENCY
C
      DO 300 K=1,I
      READ(5,*)FREQ,AR,PH
C
C  START WITH LOSS FACTOR EQUAL TO ZERO AND STEP FORWARDS WHILE
C  KEEPING TRACK OF THE ERROR
C  AL IS USED TO ACCELERATE FORWARDS
C  BET IS USED TO DECELERATE  BACKWARDS
C
      STEP=1 0
      AL=3 0
      BET=-0.5
      DEL=0.0
C
C  CAR IS THE MEASURED ACCELERATION RATIO VECTOR
C  TR IS THE PREDICTED ACCELERATION RATIO VECTOR
C
      CAR=CMPLX(AR*COS(PH),AR*SIN(PH))
C
C  USE THE COMPLEX MODULUS MODEL TO FIND THE PREDICTED ACCELERATION
C  RATIO
C
      Z1=CSQRT(E*CMPLX(1.0,DEL))
      Z=M*FREQ/(A*SQRT(RO)*Z1)
      W=CLOG((CMPLX(0 0,1 0)+Z)/(CMPLX(0.0,1.0)-Z))
      PHI=CMPLX(0 0,0 5)*W
      THETA=L*FREQ*SQRT(RO)/Z1
      TR=CCOS(THETA)+CSIN(THETA)*CSIN(THETA+PHI)/
     $ CCOS(THETA+PHI)
C
C  THE ERROR IS THE VECTOR DIFFERENCE BETWEEN THE PREDICTED AND
C  MEASURED ACCELERATION RATIO
C
      ERR=CABS(CAR-TR)
C
C  TAKE A STEP FORWARD AND CALCULATE THE ERROR AT THIS NEW
C  VALUE FOR THE LOSS FACTOR
C
  200 DEL=DEL+STEP
```

```
      Z1=CSQRT(E*CMPLX(1 0,DEL))
      Z=M*FREQ/(A*SQRT(RO)*Z1)
      W=CLOG((CMPLX(0 0,1 0)+Z)/(CMPLX(0 0,1.0)-Z))
      PHI=CMPLX(0 0,0 5)*W
      THETA=L*FREQ*SQRT(RO)/Z1
      TR=CCOS(THETA)+CSIN(THETA)*CSIN(THETA+PHI)/
     * CCOS(THETA+PHI)
      ERN=CABS(CAR-TR)
C
C  IF THE ERROR AT THE NEW DEL VALUE IS GREATER THAN THE OLD ERROR
C  THEN CHANGE SEARCH DIRECTIONS AND DECREASE THE STEP SIZE CHANGE
C  IN THE DEL VALUE
C
      IF(ERN .GE. ERR) GO TO 210
C
C  THE NEW DEL VALUE HAS A SMALLER ERROR THAN THE OLD VALUE SO
C  RESET THE ERROR
C
      ERR=ERN
C
C  GO TO PRINTOUT THE RESULTS IF THE DEL VALUE IS GETTING
C  INFINITELY LARGE
C
      IF(DEL .GT. 10 0**10 0) GO TO 900
C
C  THE DEL VALUE IS NOT GETTING INFINITELY LARGE YET SO INCREASE
C  THE STEP SIZE AND GO BACK TO TRY A NEW DEL VALUE
C
      STEP=STEP*AL
      GO TO 200
C
C  GET READY TO PRINTOUT THE RESULTS IF THE STEP SIZE IS LESS THAN
C  ONE
C
  210 IF(ABS(STEP) .LE. 1 0) GO TO 890
C
C  DECREASE THE SIZE AND DIRECTION OF THE STEP FOR DEL
C  GO BACK TO TRY THE NEW DEL VALUE
C
      STEP=STEP*BET
      GO TO 200
C
C  THE NEW DEL VALUE HAS THE SAME SIZE OR LARGER ERROR THAN THE
C  OLD VALUE SO GO BACK TO THE OLD DEL VALUE
C
  890 DEL=DEL-STEP
      Z1=CSQRT(E*CMPLX(1 0,DEL))
      Z=M*FREQ/(A*SQRT(RO)*Z1)
      W=CLOG((CMPLX(0 0,1 0)+Z)/(CMPLX(0,0,1.0)-Z))
      PHI=CMPLX(0 0,0 5)*W
      THETA=L*FREQ*SQRT(RO)/Z1
      TR=CCOS(THETA)+CSIN(THETA)*CSIN(THETA+PHI)/
     * CCOS(THETA+PHI)
C
C  GET THE RESULTS READY FOR PRINTOUT
C
  900 TRM=CABS(TR)
      PHTR=ATAN(AIMAG(TR)/REAL(TR))
      IF(PHTR  LE. 0 0) GO TO 910
      PHTR=PHTR-3.1415926
C
C  CALCULATE THE LOSS FACTOR FOR THE FIRST-ORDER VISCOELASTIC
C  MODEL
C
  910 ALPHA=DEL*E/FREQ
C
C  OUTPUT THE RESULTS AT THIS FREQUENCY TO THE PRINTER
C
      WRITE(9,13)FREQ,AR,TRM,PH,PHTR,DEL,ALPHA
   13 FORMAT(F9 2,4F9 3,F8 0,F10 0,F9 3)
C
C  OUTPUT THE RESULTS AT THIS FREQUENCY TO DISK FILES FOR
C  EASY PLOTTING OF THE COMPLEX MODULUS LOSS FACTOR, FIRST-
C  ORDER VISCOELASTIC LOSS FACTOR AND MAGNITUDE AND PHASE OF
C  THE PREDICTED ACCELERATION RATIO VERSUS THE EXCITATION
C  FREQUENCY
C
      WRITE(1,14)FREQ,DEL
      WRITE(2,14)FREQ,ALPHA
      WRITE(3,15)FREQ,TRM
      WRITE(4,15)FREQ,PHTR
   14 FORMAT(1X,F9 2,1X,F10 1)
   15 FORMAT(1X,F9 2,1X,F7.3)
C
C  GO BACK TO ITERATE FOR ANOTHER FREQUENCY IF NECESSARY
C
  300 CONTINUE
      CLOSE(UNIT=1)
      CLOSE(UNIT=2)
      CLOSE(UNIT=3)
      CLOSE(UNIT=4)
      CLOSE(UNIT=5)
      CLOSE(UNIT=9)
      STOP
      END
```

APPENDIX D

VISPAR.FOR

```
C  THIS PROGRAM FINDS VALUES AT EACH FREQUENCY FOR THE PARAMETERS
C  IN THE VISCOUS DYNAMIC STRESS-STRAIN MODEL FOR SOIL   THE
C  ERROR FUNCTION MINIMIZED IN THIS ROUTINE IS THE VECTOR
C  DIFFERENCE BETWEEN THE MEASURED AND PREDICTED ACCELERATION RATIO
C  DATA   THIS PROGRAM USES THE PROFESSIONAL FORTRAN COMPILER
C  AVAILABLE FOR THE IBM PC   MICHAEL F  KOCHER   OKLAHOMA STATE
C  UNIVERSITY AGRICULTURAL ENGINEERING DEPARTMENT.  OCTOBER 29, 1985
C
      CHARACTER*3 SNO
      CHARACTER*10 DATFN
      REAL M,RO,L,A,FREQ,AR,BETA,TRM,ERN,ERR
      REAL E,PH,PHTR,STEP,AL,BET
      COMPLEX Z1,Z,W,PHI,THETA,TR,CAR
      INTEGER I,K
C
C  OPEN DATA FILES FOR EASY PLOTTING OF THE MAGNITUDE OF THE
C  PREDICTED ACCELERATION RATIO, PHASE ANGLE AND LOSS FACTORS
C  VERSUS EXCITATION FREQUENCY
C
      OPEN(UNIT=1,FILE='A:VISCOUS DAT')
      OPEN(UNIT=2,FILE='A:MAGVIS DAT')
      OPEN(UNIT=3,FILE='A:PHVIS DAT')
      OPEN (UNIT=9,FILE='LPT1')
C
C  M IS THE MASS OF THE ATTACHED ACCELEROMETER AND DISK AT THE TOP
C  OF THE SOIL SAMPLE DURING THE DYNAMIC TESTS
C
      M=0.0413
C
C  INPUT THE SAMPLE DATA
C
      PRINT *,' ENTER SAMPLE NUMBER AS ''XXX'' '
      READ *,SNO
      WRITE(9,10)SNO
   10 FORMAT(' VISCOUS MODEL FOR SAMPLE ',A3)
      PRINT *,' ENTER SAMPLE LENGTH (m) '
      READ *,L
      PRINT *,' ENTER SAMPLE CROSS SECTIONAL AREA (m**2) '
      READ *,A
      PRINT *,' ENTER SAMPLE WET BULK DENSITY (kg/m**3) '
      READ *,RO
      PRINT *,' ENTER SAMPLE ELASTIC MODULUS (Pa) '
      READ *,E
C
C  OUTPUT SAMPLE DATA TO PRINTER FOR HARDCOPY OF RESULTS
C
      WRITE(9,11)L,A,RO,E
   11 FORMAT('              LENGTH = ',F7 4,' m',/,
     $ ' CROSS SECTIONAL AREA = ',E10 3,' m**2',/,
     $ '     WET BULK DENSITY = ',F7 1,' kg/m**3',/,
     $ '      ELASTIC MODULUS = ',E10 3,' Pa')
      WRITE (9,12)
   12 FORMAT('   FREQ',7X,'AR',7X,'TR',5X,'PH(AR)   PH(TR)',3X,
     $ 'BETA')
C
C  GET THE FILENAME OF THE DYNAMIC TEST DATA
C
      PRINT *,' ENTER DYNAMIC TEST DATA FILENAME AS ''A:XXX DAT'' '
      READ *,DATFN
      OPEN(UNIT=4,FILE=DATFN)
C
C  READ THE NUMBER OF FREQUENCIES AT WHICH THE SAMPLE WAS TESTED
C
      READ(4,*)I
C
C  START ITERATION PROCESS FOR A PARTICULAR FREQUENCY
C  GET THE DATA FOR THIS FREQUENCY
C
      DO 300 K=1,I
      READ(4,*)FREQ,AR,PH
C
C  START WITH LOSS FACTOR EQUAL TO ZERO AND STEP FORWARDS WHILE
C  KEEPING TRACK OF THE ERROR
C  AL IS USED TO ACCELERATE FORWARDS
C  BET IS USED TO DECELERATE  BACKWARDS
C
      STEP=1 0
      AL=3 0
      BET=-0 5
      BETA=0 0
C
C  CAR IS THE MEASURED ACCELERATION RATIO VECTOR
C  TR IS THE PREDICTED ACCELERATION RATIO VECTOR
C
      CAR=CMPLX(AR*COS(PH),AR*SIN(PH))
C
C  USE THE VISCOUS MODEL TO FIND THE PREDICTED ACCELERATION RATIO
C
      Z1=CSQRT(CMPLX(1 0,-BETA/(A*RO*FREQ)))
      Z=M*FREQ*Z1/(A*SQRT(RO*E))
      W=CLOG((CMPLX(0 0,1 0)+Z)/(CMPLX(0 0,1.0)-Z))
      PHI=CMPLX(0 0,0 5)*W
      THETA=L*FREQ*SQRT(RO/E)*Z1
      TR=CCOS(THETA)+CSIN(THETA)*CSIN(THETA+PHI)/
     $ CCOS(THETA+PHI)
C
C  THE ERROR IS THE VECTOR DIFFERENCE BETWEEN THE PREDICTED AND
C  MEASURED ACCELERATION RATIO
C
      ERR=CABS(CAR-TR)
C
C  TAKE A STEP FORWARD AND CALCULATE THE ERROR AT THIS NEW
C  VALUE FOR THE LOSS FACTOR
C
  200 BETA=BETA+STEP
      Z1=CSQRT(CMPLX(1 0,-BETA/(A*RO*FREQ)))
      Z=M*FREQ*Z1/(A*SQRT(RO*E))
      W=CLOG((CMPLX(0 0,1 0)+Z)/(CMPLX(0 0,1 0)-Z))
      PHI=CMPLX(0 0,0 5)*W
      THETA=L*FREQ*SQRT(RO/E)*Z1
```

```
      TR=CCOS(THETA)+CSIN(THETA)*CSIN(THETA+PHI)/
     * CCOS(THETA+PHI)
      ERN=CABS(CAR-TR)
C
C  IF THE ERROR AT THE NEW BETA VALUE IS GREATER THAN THE OLD ERROR
C  THEN CHANGE SEARCH DIRECTIONS AND DECREASE THE STEP SIZE CHANGE
C  IN THE BETA VALUE
C
      IF(ERN  GE  ERR) GO TO 210
C
C  THE NEW BETA VALUE HAS A SMALLER ERROR THAN THE OLD VALUE SO
C  RESET THE ERROR
C
      ERR=ERN
C
C  GO TO PRINTOUT THE RESULTS IF THE BETA VALUE IS GETTING
C  INFINITELY LARGE
C
      IF(BETA  GT. 10 0**10 0) GO TO 900
C
C  THE BETA VALUE IS NOT GETTING INFINITELY LARGE YET SO INCREASE
C  THE STEP SIZE AND GO BACK TO TRY A NEW BETA VALUE
C
      STEP=STEP*AL
      GO TO 200
C
C  GET READY TO PRINTOUT THE RESULTS IF THE STEP SIZE IS LESS THAN
C  ONE
C
  210 IF(ABS(STEP)  LE. 1 0) GO TO 890
C
C  DECREASE THE SIZE AND DIRECTION OF THE STEP FOR BETA
C  GO BACK TO TRY THE NEW BETA VALUE
C
      STEP=STEP*BET
      GO TO 200
C
C  THE NEW BETA VALUE HAS THE SAME SIZE OR LARGER ERROR THAN THE
C  OLD VALUE SO GO BACK TO THE OLD BETA VALUE
C
  890 BETA=BETA-STEP
      Z1=CSQRT(CMPLX(1 0,-BETA/(A*RO*FREQ)))
      Z=M*FREQ*Z1/(A*SQRT(RO*E))
      W=CLOG((CMPLX(0 0,1 0)+Z)/(CMPLX(0 0,1 0)-Z))
      PHI=CMPLX(0 0,0 5)*W
      THETA=L*FREQ*SQRT(RO/E)*Z1
      TR=CCOS(THETA)+CSIN(THETA)*CSIN(THETA+PHI)/
     * CCOS(THETA+PHI)
C
C  GET THE RESULTS READY FOR PRINTOUT
C
  900 TRM=CABS(TR)
      PHTR=ATAN(AIMAG(TR)/REAL(TR))
      IF(PHTR  LE  0 0) GO TO 910
      PHTR=PHTR-3.1415926
C
C  OUTPUT THE RESULTS AT THIS FREQUENCY TO THE PRINTER
C
  910 WRITE(9,13)FREQ,AR,TRM,PH,PHTR,BETA
   13 FORMAT(F9 2,4F9 3,F8 0,F10 0)
C
C  OUTPUT THE RESULTS AT THIS FREQUENCY TO DISK FILES FOR EASY
C  PLOTTING OF THE VISCOUS LOSS FACTOR, AND MAGNITUDE AND PHADE
C  OF THE PREDICTED ACCELERATION RATIO VERSUS THE EXCITATION
C  FREQUENCY
C
      WRITE(1,14)FREQ,BETA
      WRITE(2,15)FREQ,TRM
      WRITE(3,15)FREQ,PHTR
   14 FORMAT(1X,F9 2,1X,F10 1)
   15 FORMAT(1X,F9 2,1X,F7.3)
C
C  GO BACK TO ITERATE FOR ANOTHER FREQUENCY IF NECESSARY
C
  300 CONTINUE
      CLOSE(UNIT=1)
      CLOSE(UNIT=2)
      CLOSE(UNIT=3)
      CLOSE(UNIT=4)
      CLOSE(UNIT=9)
      STOP
      END
```

APPENDIX E

ATXA.FOR

```
C  THIS PROGRAM FINDS VALUES AT EACH FREQUENCY FOR THE TWO
C  PARAMETERS IN THE SECOND-ORDER VISCOELASTIC STRESS-STRAIN MODEL
C  FOR SOIL.  THIS PROGRAM USES THE PROFESSIONAL FORTRAN COMPILER
C  AVAILABLE FOR THE IBM PC   MICHAEL F. KOCHER   OKLAHOMA STATE
C  UNIVERSITY AGRICULTURAL ENGINEERING DEPARTMENT.  OCTOBER 22,1985
C
      CHARACTER*3 SNO
      CHARACTER*10 DATFN
      REAL M,L,A,RO,E,FREQ(40),AR,ALPHA(40),ALH,ALL,XIH,XIL
      REAL XI(40),PHAS,MTR,PHTR,ERR,ERXL,ERXH,ERAL,ERAH
      COMPLEX Z1,Z2,W,PHI,THETA,TR,CAR
      INTEGER I,K
C
C  OPEN DATA FILES FOR EASY PLOTTING OF THE MAGNITUDE OF THE
C  MEASURED ACCELERATION RATIO VERSUS EXCITATION FREQUENCY, AND
C  THE MEASURED PHASE LAG OF THE TOP ACCELERATION BEHIND THE
C  BOTTOM ACCELERATION VERSUS EXCITATION FREQUENCY.
C
      OPEN(UNIT=1,FILE='A:ALPHA.DAT')
      OPEN(UNIT=2,FILE='A:XI DAT')
      OPEN(UNIT=3,FILE='A:ARMAG DAT')
      OPEN(UNIT=4,FILE='A:PHASE DAT')
      OPEN(UNIT=9,FILE='LPT1')
C
C  M IS THE MASS OF THE ATTACHED ACCELEROMETER AND DISK AT THE TOP
C  OF THE SOIL SAMPLE DURING THE VIBRATION TESTS
C
      M=0.0413
C
C  INPUT THE SAMPLE DATA
C
      PRINT *,' ENTER SAMPLE NUMBER AS ''XXX'' '
      READ *,SNO
      WRITE(9,10)SNO
   10 FORMAT(' SECOND VISCOELASTIC MODEL FOR SAMPLE ',A3)
      PRINT *,' ENTER SAMPLE LENGTH (m) '
      READ *,L
      PRINT *,' ENTER SAMPLE CROSS SECTIONAL AREA (m**2) '
      READ *, A
      PRINT *,' ENTER SAMPLE WET BULK DENSITY (kg/m**3) '
      READ *,RO
      PRINT *,' ENTER SAMPLE ELASTIC MODULUS (Pa) '
      READ *,E
C
C  OUTPUT SAMPLE DATA TO PRINTER FOR HARDCOPY OF RESULTS
C
      WRITE(9,11)L,A,RO,E
   11 FORMAT('                  LENGTH = ',F7.4,' m',/,
     $ ' CROSS SECTIONAL AREA = ',E10.3,' m**2',/,
     $ '     WET BULK DENSITY = ',F7 1,' kg/m**3',/,
     $ '      ELASTIC MODULUS = ',E10 3,' Pa')
      WRITE(9,12)
   12 FORMAT('    FREQ',8X,'AR',8X,'TR',6X,'PH(AR)    PH(TR)',
     $ 5X,'ALPHA',10X,'XI')
C
C  GET THE FILENAME OF THE DYNAMIC TEST DATA
C
      PRINT *,' ENTER DYNAMIC TEST DATA FILENAME AS ''A:XXX.DAT'' '
      READ *,DATFN
      OPEN(UNIT=8,FILE=DATFN,STATUS='OLD')
C
C  READ THE NUMBER OF FREQUENCIES AT WHICH THE SAMPLE WAS TESTED
C
      READ(8,*)I
C
C  INITIAL GUESSES FOR XI AND ALPHA
C
      XI(1)= -100 0
      ALPHA(1)=10000.0
C
C  START ITERATION PROCESS FOR A PARTICULAR FREQUENCY
C  GET THE DATA FOR THIS FREQUENCY
C
      DO 300 K=1,I
      READ(8,*)FREQ(K),AR,PHAS
      IF(K .EQ. 1) GO TO 500
      XI(K)=XI(K-1)
      ALPHA(K)=ALPHA(K-1)
C
C  SECOND-ORDER VISCOELASTIC STRESS-STRAIN MODEL EQUATIONS FOR
C  THE ACCELERATION RATIO
C
  500 Z1=CSQRT(CMPLX(E-XI(K)*FREQ(K)**2 0,ALPHA(K)*FREQ(K)))
      Z2=M*FREQ(K)/(A*SQRT(RO)*Z1)
      W=CLOG((CMPLX(0.0,1.0)+Z2)/(CMPLX(0.0,1.0)-Z2))
      PHI=CMPLX(0 0,0.5)*W
      THETA=L*FREQ(K)*SQRT(RO)/Z1
      TR=CCOS(THETA)+CSIN(THETA)*CSIN(THETA+PHI)/
     $ CCOS(THETA+PHI)
C
C  CALCULATE THE ERROR FROM THE INITIAL GUESS
C
      CAR=CMPLX(AR*COS(PHAS),AR*SIN(PHAS))
      ERR=CABS(CAR-TR)
C
C  INITIAL STEP SIZES FOR CHANGES IN XI AND ALPHA
C
      SX=1.0
      SA=1000 0
C
C  CALCULATE HIGHER AND LOWER POSSIBILITIES FOR XI
C
  100 XIH=XI(K)-SX
      XIL=XI(K)+SX
C
C  STOP ITERATING FOR XI AND ALPHA AT THIS FREQUENCY IF THE
C  ERROR IS ACCEPTABLE
C
```

```
      IF(ERR .LE. 1.0E-7) GO TO 900
C
C  ACCEPT THE EXISTING ERROR AND STOP ITERATING FOR XI AND ALPHA
C  AT THIS FREQUENCY IF THE STEP SIZES ARE RIDICULOUSLY SMALL
C
      IF(SX  GT. 0 0001) GO TO 400
      IF(SA  GT. 0.1) GO TO 400
      GO TO 900
C
C  CALCULATE THE ACCELERATION RATIO AND ERROR USING THE LOWER
C  XI POSSIBILITY
C
  400 Z1=CSQRT(CMPLX(E-XIL*FREQ(K)**2 0,ALPHA(K)*FREQ(K)))
      Z2=M*FREQ(K)/(A*SQRT(RO)*Z1)
      W=CLOG((CMPLX(0 0,1 0)+Z2)/(CMPLX(0.0,1.0)-Z2))
      PHI=CMPLX(0 0,0 5)*W
      THETA=L*FREQ(K)*SQRT(RO)/Z1
      TR=CCOS(THETA)+CSIN(THETA)*CSIN(THETA+PHI)/
     * CCOS(THETA+PHI)
      ERXL=CABS(CAR-TR)
C
C  CHECK THE HIGHER XI POSSIBILITY IF THE LOWER XI POSSIBILITY
C  HAS A HIGHER ERROR
C
      IF(ERXL  GT. ERR) GO TO 110
C
C  THE LOWER XI POSSIBILITY HAS A LOWER ERROR SO MOVE XI TO THIS
C  VALUE, RESET THE ERROR VALUE AND GO BACK TO TRY NEW XI
C  POSSIBILITIES
C
      ERR=ERXL
      XI(K)=XIL
      GO TO 100
C
C  THE LOWER XI POSSIBILITY HAS A HIGHER ERROR SO TRY THE HIGHER
C  XI POSSIBILITY
C
  110 Z1=CSQRT(CMPLX(E-XIH*FREQ(K)**2 0,ALPHA(K)*FREQ(K)))
      Z2=M*FREQ(K)/(A*SQRT(RO)*Z1)
      W=CLOG((CMPLX(0 0,1 0)+Z2)/(CMPLX(0 0,1.0)-Z2))
      PHI=CMPLX(0.0,0 5)*W
      THETA=L*FREQ(K)*SQRT(RO)/Z1
      TR=CCOS(THETA)+CSIN(THETA)*CSIN(THETA+PHI)/
     * CCOS(THETA+PHI)
      ERXH=CABS(CAR-TR)
C
C  IF THE HIGHER XI POSSIBILITY HAS A HIGHER ERROR, DECREASE
C  THE XI STEP SIZE AND TRY SOME POSSIBILITIES FOR ALPHA
C
      IF(ERXH .GT. ERR) GO TO 120
C
C  THE HIGHER XI POSSIBILITY HAS A LOWER ERROR, SO MOVE XI TO THIS
C  VALUE, RESET THE ERROR AND GO BACK TO TRY NEW XI POSSIBILITIES
C
      ERR=ERXH
      XI(K)=XIH
      GO TO 100
  120 SX=SX/2.0
C
C  CALCULATE HIGHER AND LOWER POSSIBILITIES FOR ALPHA
C
  200 ALH=ALPHA(K)+SA
      ALL=ALPHA(K)-SA
C
C  STOP ITERATING FOR XI AND ALPHA AT THIS FREQUENCY IF THE ERROR
C  IS ACCEPTABLE
C
      IF(ERR  LE. 1.0E-7) GO TO 900
C
C  CALCULATE THE ACCELERATION RATIO AND ERROR USING THE LOWER
C  POSSIBILITY FOR ALPHA
C
      Z1=CSQRT(CMPLX(E-XI(K)*FREQ(K)**2 0,ALL*FREQ(K)))
      Z2=M*FREQ(K)/(A*SQRT(RO)*Z1)
      W=CLOG((CMPLX(0 0,1 0)+Z2)/(CMPLX(0 0,1.0)-Z2))
      PHI=CMPLX(0 0,0 5)*W
      THETA=L*FREQ(K)*SQRT(RO)/Z1
      TR=CCOS(THETA)+CSIN(THETA)*CSIN(THETA+PHI)/
     * CCOS(THETA+PHI)
      ERAL=CABS(CAR-TR)
C
C  CHECK THE HIGHER ALPHA POSSIBILITY IF THE LOWER POSSIBILITY
C  HAS A HIGHER ERROR
C
      IF(ERAL  GT. ERR) GO TO 210
C
C  THE LOWER ALPHA POSSIBILITY HAS A LOWER ERROR SO MOVE ALPHA TO
C  THIS VALUE, RESET THE ERROR VALUE AND GO BACK TO TRY NEW
C  ALPHA POSSIBILITIES
C
      ERR=ERAL
      ALPHA(K)=ALL
      GO TO 200
C
C  THE LOWER ALPHA POSSIBILITY HAS A HIGHER ERROR, SO TRY THE
C  HIGHER ALPHA POSSIBILITY
C
  210 Z1=CSQRT(CMPLX(E-XI(K)*FREQ(K)**2 0,ALH*FREQ(K)))
      Z2=M*FREQ(K)/(A*SQRT(RO)*Z1)
      W=CLOG((CMPLX(0 0,1 0)+Z2)/(CMPLX(0.0,1.0)-Z2))
      PHI=CMPLX(0 0,0 5)*W
      THETA=L*FREQ(K)*SQRT(RO)/Z1
      TR=CCOS(THETA)+CSIN(THETA)*CSIN(THETA+PHI)/
     * CCOS(THETA+PHI)
      ERAH=CABS(CAR-TR)
C
C  IF THE HIGHER ALPHA POSSIBILITY HAS A HIGHER ERROR, DECREASE THE
C  ALPHA STEP SIZE AND TRY SOME MORE POSSIBILITIES FOR XI
```

```
C
      IF(ERAH  GT. ERR) GO TO 220
C
C  THE HIGHER ALPHA POSSIBILITY HAS A LOWER ERROR, SO MOVE ALPHA TO
C  THIS VALUE AND GO BACK TO TRY SOME MORE ALPHA POSSIBILITIES
C
      ERR=ERAH
      ALPHA(K)=ALH
      GO TO 200
  220 SA=SA/2 0
      GO TO 100
C
C  PREPARE THE OUTPUT DATA
C
  900 MTR=CABS(TR)
      PHTR=ATAN(AIMAG(TR)/REAL(TR))
      IF(PHTR  LE  0 0) GO TO 910
      PHTR=PHTR-3 141593
C
C  OUTPUT RESULTS TO THE PRINTER
C
  910 WRITE(9,13)FREQ(K),AR,MTR,PHAS,PHTR,ALPHA(K),XI(K)
   13 FORMAT(1X,F9 2,4F10 3,3X,F9 1,3X,F10 5)
C
C  OUTPUT RESULTS TO DISK FILES FOR EASY PLOTTING
C
      WRITE(1,14)FREQ(K),ALPHA(K)
   14 FORMAT(1X,F9 2,1X,F9 1)
      WRITE (2,15)FREQ(K),-1 0*XI(K)
   15 FORMAT(1X,F9 2,1X,F10 5)
      WRITE(3,16)FREQ(K),AR
   16 FORMAT(1X,F9 2,1X,F7 3)
      WRITE(4,16)FREQ(K),-1 0*PHAS
C
C  GO BACK TO ITERATE FOR ANOTHER FREQUENCY IF NECESSARY
C
  300 CONTINUE
C
C  CLOSE FILES THAT ARE NO LONGER ACTIVE
C
      CLOSE(UNIT=1)
      CLOSE(UNIT=2)
      CLOSE(UNIT=3)
      CLOSE(UNIT=4)
      CLOSE(UNIT=8)
      CLOSE(UNIT=9)
C
C  WRITE DATA FILES TO DISK FOR USE IN CURVE FITTING FOR XI AND
C  ALPHA
C
      OPEN(UNIT=7,FILE='A:XIREG DAT')
      OPEN(UNIT=8,FILE='A:ALPHAREG.DAT')
      WRITE(7,17)I
   17 FORMAT('2,',I2,',0')
      WRITE(7,18)
   18 FORMAT('"FREQUENCY"')
      DO 540 K=1,I
  540 WRITE(7,21)FREQ(K)
   21 FORMAT(1X,F9 2)
      WRITE(7,19)
   19 FORMAT('"XI"')
      DO 510 K=1,I
  510 WRITE(7,22)-1 0*XI(K)
   22 FORMAT(1X,F10 5)
      CLOSE(UNIT=7)
      WRITE(8,17)I
      WRITE(8,18)
      DO 520 K=1,I
  520 WRITE(8,21)FREQ(K)
      WRITE(8,20)
   20 FORMAT('"ALPHA"')
      DO 530 K=1,I
  530 WRITE(8,23)ALPHA(K)
   23 FORMAT(1X,F9 1)
      CLOSE(UNIT=8)
      STOP
      END
```

APPENDIX F

ACCELERATION RATIO DATA

ACCELERATION RATIO DATA

SAMPLE	FREQ. rad/s	BOTTOM PEAK ACC. m/s^2	TOP PEAK ACC. m/s^2	ACC. RATIO	PHASE ANGLE rad	ALPHA	XI
V1							
	1257	20.8	22.3	1.071	-0.005	6413	-68.777
	1890	19.4	21.8	1.126	-0.013	8315	-40.674
	2546	19.1	23.0	1.204	-0.019	6688	-26.835
	3216	16.5	22.3	1.356	-0.047	7631	-16.902
	3683	16.2	24.0	1.482	-0.055	6126	-13.597
	4078	14.4	23.0	1.602	-0.082	6935	-11.597
	4402	13.4	22.9	1.711	-0.102	7091	-10.394
	4697	13.4	24.5	1.825	-0.115	6758	-9.513
	5040	11.9	23.9	1.998	-0.131	6186	-8.566
	5355	10.7	23.5	2.190	-0.162	6225	-7.793
	5678	10.1	24.7	2.460	-0.194	5877	-7.072
	6019	8.2	22.9	2.780	-0.232	5635	-6.498
	6296	7.8	24.4	3.120	-0.281	5591	-6.059
	6630	6.6	24.2	3.700	-0.383	5706	-5.532
	7002	5.4	24.0	4.450	-0.498	5593	-5.121
	7320	4.0	21.5	5.330	-0.628	5391	-4.813
	7584	3.8	24.0	6.370	-0.852	5364	-4.510
	7953	2.9	21.8	7.400	-1.206	5345	-4.205
	8267	3.0	22.0	7.440	-1.600	5326	-3.946
	8434	3.3	23.1	6.990	-1.812	5302	-3.808
	8832	4.0	21.9	5.490	-2.190	5207	-3.510
	9240	5.0	22.0	4.410	-2.370	5270	-3.299
	9407	5.4	21.4	3.960	-2.450	5190	-3.190
	10016	7.3	21.7	2.970	-2.600	5156	-2.897
	10633	10.0	23.5	2.350	-2.710	4901	-2.637
	11249	12.0	22.8	1.904	-2.770	4872	-2.393
	11948	14.3	22.2	1.558	-2.820	4802	-2.146
	12601	17.2	22.9	1.329	-2.850	4822	-1.941

ACCELERATION RATIO DATA (Continued)

SAMPLE	FREQ. rad/s	BOTTOM PEAK ACC. m/s^2	TOP PEAK ACC. m/s^2	ACC. RATIO	PHASE ANGLE rad	ALPHA	XI
V2							
	1346	20.9	24.0	1.149	-0.029	8906	-30.094
	1893	17.2	22.7	1.317	-0.052	5734	-16.211
	2522	16.7	25.1	1.504	-0.036	2453	-12.059
	3191	13.1	25.0	1.904	-0.153	4961	-8.078
	3687	10.0	23.3	2.330	-0.202	4273	-6.682
	4071	7.8	22.5	2.900	-0.250	3568	-5.788
	4409	6.6	23.4	3.550	-0.356	3642	-5.183
	4757	4.8	23.6	4.900	-0.567	3478	-4.540
	5037	4.0	24.2	6.010	-0.767	3439	-4.242
	5393	3.1	23.4	7.520	-1.215	3396	-3.872
	5712	3.2	23.2	7.140	-1.825	3332	-3.515
	6030	4.2	21.7	5.160	-2.280	3241	-3.174
	6312	5.8	23.2	4.010	-2.470	3193	-2.951
	6657	6.5	21.1	3.250	-2.590	3155	-2.762
	6962	8.6	22.5	2.620	-2.670	3167	-2.556
	7284	11.1	24.2	2.180	-2.730	3146	-2.368
	7565	11.5	22.8	1.983	-2.770	3064	-2.267
	7824	12.8	22.7	1.781	-2.800	3032	-2.149
	8184	15.1	23.5	1.561	-2.830	3023	-2.000
	8459	15.5	22.4	1.445	-2.850	2994	-1.911
	8886	18.2	23.0	1.258	-2.880	2937	-1.744
	9176	19.7	23.2	1.178	-2.890	2973	-1.664
	9412	19.5	21.8	1.123	-2.900	2970	-1.606
	10022	22.3	21.9	0.983	-2.930	2899	-1.435
	10706	22.0	19.1	0.868	-2.950	2980	-1.271
	11317	22.6	18.1	0.799	-2.970	3017	-1.156
	11949	22.7	16.5	0.727	-2.990	3205	-1.018
	12579	24.2	16.3	0.672	-2.990	3882	-0.915

ACCELERATION RATIO DATA (Continued)

SAMPLE	FREQ. rad/s	BOTTOM PEAK ACC. m/s^2	TOP PEAK ACC. m/s^2	ACC. RATIO	PHASE ANGLE rad	ALPHA	XI
V3							
	1258	21.5	23.2	1.079	-0.005	4364	-51.067
	1894	17.8	20.4	1.142	-0.007	2996	-30.420
	2513	18.4	23.1	1.252	-0.036	7011	-18.256
	3222	15.9	22.5	1.414	-0.042	4448	-12.590
	3707	15.1	24.0	1.590	-0.088	5813	-9.666
	4064	13.8	24.3	1.759	-0.098	4774	-8.297
	4398	12.2	23.5	1.927	-0.132	5059	-7.347
	4697	11.6	24.8	2.130	-0.159	4825	-6.609
	5027	9.6	22.8	2.370	-0.187	4584	-6.026
	5343	8.9	24.0	2.700	-0.231	4421	-5.477
	5680	7.7	24.5	3.180	-0.314	4480	-4.941
	6005	6.3	24.0	3.810	-0.396	4235	-4.538
	6283	5.3	23.6	4.490	-0.516	4252	-4.230
	6636	4.1	23.1	5.610	-0.721	4176	-3.901
	6943	3.6	25.2	6.920	-1.108	4123	-3.564
	7246	3.3	23.6	7.240	-1.405	4160	-3.388
	7555	3.8	24.6	6.470	-1.832	4205	-3.143
	7876	4.6	24.7	5.420	-2.090	4276	-2.964
	8160	5.2	23.0	4.430	-2.280	4300	-2.788
	8491	6.2	23.0	3.730	-2.380	4465	-2.649
	8893	7.9	24.3	3.070	-2.490	4509	-2.479
	9213	8.2	22.5	2.760	-2.570	4339	-2.376
	9408	9.2	24.2	2.620	-2.600	4309	-2.327
	10007	11.6	24.5	2.110	-2.710	4023	-2.117
	10631	13.4	23.1	1.727	-2.790	3747	-1.916
	11290	17.2	24.7	1.440	-2.840	3611	-1.727
	11978	19.3	23.7	1.226	-2.880	3472	-1.554
	12566	20.8	22.7	1.092	-2.900	3470	-1.426

ACCELERATION RATIO DATA (Continued)

SAMPLE	FREQ. rad/s	BOTTOM PEAK ACC. m/s^2	TOP PEAK ACC. m/s^2	ACC. RATIO	PHASE ANGLE rad	ALPHA	XI
V4							
	1365	21.7	24.0	1.105	-0.007	4190	-41.778
	2087	19.5	23.1	1.184	-0.026	8153	-25.531
	2651	17.5	23.2	1.324	-0.042	6042	-16.063
	3123	15.8	22.9	1.448	-0.058	5612	-12.637
	3967	12.4	23.2	1.874	-0.125	5152	-8.132
	4366	11.2	23.9	2.140	-0.160	4852	-7.053
	4719	9.2	22.5	2.460	-0.203	4632	-6.264
	5093	7.9	23.1	2.930	-0.257	4284	-5.587
	5464	6.1	22.0	3.620	-0.366	4273	-4.984
	5818	5.0	23.2	4.640	-0.533	4192	-4.487
	6208	3.8	23.9	6.230	-0.850	4098	-4.034
	6631	2.9	22.3	7.620	-1.390	3944	-3.646
	6943	3.1	23.7	7.580	-1.548	4050	-3.566
	7247	3.3	23.5	7.060	-1.825	4080	-3.413
	7510	4.0	23.6	5.830	-2.110	4120	-3.214
	7805	4.7	22.7	4.880	-2.330	3949	-3.040
	8223	6.4	24.6	3.820	-2.500	3919	-2.831
	8683	8.1	23.3	2.860	-2.640	3835	-2.569
	9114	9.2	22.3	2.430	-2.710	3753	-2.411
	9385	10.8	23.5	2.170	-2.740	3780	-2.299
	10200	14.1	23.6	1.672	-2.810	3739	-2.023
	10746	15.7	22.6	1.437	-2.840	3755	-1.854
	11244	17.9	23.0	1.283	-2.870	3653	-1.723
	11893	22.2	24.8	1.116	-2.890	3720	-1.557
	12634	23.5	23.0	0.978	-2.920	3631	-1.395

ACCELERATION RATIO DATA (Continued)

SAMPLE	FREQ. rad/s	BOTTOM PEAK ACC. m/s^2	TOP PEAK ACC. m/s^2	ACC. RATIO	PHASE ANGLE rad	ALPHA	XI
V5							
	1267	22.4	24.0	1.072	-0.010	11920	-62.377
	1932	21.0	23.9	1.135	-0.011	6099	-36.086
	2523	19.3	23.0	1.195	-0.028	10063	-26.000
	3157	17.0	22.6	1.335	-0.050	8470	-16.642
	3751	15.8	24.0	1.521	-0.054	5190	-12.200
	4078	14.2	23.2	1.639	-0.076	5651	-10.599
	4391	13.1	23.1	1.768	-0.098	5827	-9.423
	4742	11.5	22.1	1.915	-0.117	5718	-8.515
	5030	11.5	23.9	2.080	-0.138	5562	-7.783
	5378	10.3	24.0	2.322	-0.165	5285	-7.044
	5661	9.2	24.1	2.611	-0.202	5126	-6.436
	6077	7.8	24.3	3.130	-0.274	5046	-5.745
	6307	6.6	23.2	3.539	-0.340	5087	-5.380
	6623	5.8	24.2	4.199	-0.434	4979	-4.996
	6919	4.6	23.4	5.083	-0.559	4808	-4.666
	7167	4.1	23.7	5.825	-0.694	4834	-4.452
	7543	3.2	23.6	7.280	-1.046	4797	-4.104
	7873	3.2	24.8	7.769	-1.432	4834	-3.853
	8179	3.4	23.3	6.889	-1.851	4908	-3.594
	8426	4.0	24.1	5.978	-2.110	4788	-3.414
	8862	5.5	25.0	4.556	-2.354	4842	-3.164
	9129	6.3	25.1	3.986	-2.450	4819	-3.040
	9402	6.1	21.3	3.503	-2.532	4756	-2.917
	10088	8.9	23.2	2.612	-2.670	4643	-2.625
	10627	11.0	23.4	2.124	-2.751	4447	-2.402
	11392	14.9	25.0	1.676	-2.823	4248	-2.132
	11902	15.8	23.3	1.477	-2.847	4274	-1.983
	12622	18.5	23.5	1.266	-2.892	4020	-1.792

ACCELERATION RATIO DATA (Continued)

SAMPLE	FREQ. rad/s	BOTTOM PEAK ACC. m/s^2	TOP PEAK ACC. m/s^2	ACC. RATIO	PHASE ANGLE rad	ALPHA	XI
V6							
	1329	22.5	24.5	1.090	-0.011	9232	-54.146
	1895	21.0	24.1	1.147	-0.017	8503	-35.219
	2495	19.7	24.5	1.243	-0.037	9437	-22.732
	3224	16.4	23.7	1.439	-0.049	5789	-14.539
	3730	15.0	24.6	1.643	-0.084	5975	-11.118
	4058	13.8	24.9	1.811	-0.101	5450	-9.644
	4372	11.7	23.3	1.992	-0.117	4967	-8.630
	4731	10.4	23.9	2.295	-0.156	4849	-7.516
	5042	9.3	24.4	2.633	-0.205	4845	-6.748
	5370	7.6	23.3	3.083	-0.248	4466	-6.144
	5646	6.2	22.3	3.588	-0.336	4691	-5.657
	6013	5.1	24.2	4.712	-0.498	4537	-5.057
	6240	4.2	22.6	5.440	-0.603	4457	-4.825
	6628	3.5	24.2	6.841	-0.896	4527	-4.460
	6943	3.0	23.8	7.861	-1.349	4515	-4.119
	7228	3.2	22.9	7.202	-1.822	4510	-3.821
	7556	3.8	22.9	6.055	-2.133	4444	-3.599
	7854	4.6	21.6	4.703	-2.358	4452	-3.358
	8203	6.5	24.7	3.784	-2.510	4369	-3.146
	8434	7.3	24.0	3.294	-2.602	4178	-3.001
	8826	8.7	23.8	2.724	-2.678	4166	-2.806
	9127	9.5	23.1	2.438	-2.714	4198	-2.688
	9404	11.2	24.5	2.187	-2.754	4116	-2.564
	10053	13.5	24.0	1.769	-2.808	4119	-2.315
	10639	16.1	24.2	1.508	-2.856	3926	-2.114
	11331	18.1	23.3	1.283	-2.879	4044	-1.906
	11903	21.1	24.2	1.147	-2.906	3944	-1.755
	12562	23.9	24.7	1.031	-2.928	3916	-1.608

ACCELERATION RATIO DATA (Continued)

SAMPLE	FREQ. rad/s	BOTTOM PEAK ACC. m/s^2	TOP PEAK ACC. m/s^2	ACC. RATIO	PHASE ANGLE rad	ALPHA	XI
V7							
	1261	22.3	24.4	1.094	-0.004	3129	-47.203
	1904	20.9	24.5	1.174	-0.015	5258	-27.895
	2494	18.3	24.7	1.347	-0.037	4770	-15.636
	3197	14.1	22.9	1.620	-0.084	5120	-10.293
	3733	12.0	23.1	1.923	-0.120	4562	-8.134
	4109	11.2	25.0	2.240	-0.159	4292	-6.975
	4500	9.0	24.2	2.700	-0.219	4106	-6.052
	4684	8.0	23.2	2.897	-0.243	4066	-5.805
	5094	6.2	24.2	3.896	-0.370	3792	-5.003
	5362	5.0	24.1	4.826	-0.523	3832	-4.590
	5686	3.8	24.0	6.391	-0.803	3753	-4.179
	5998	3.1	24.3	7.728	-1.334	3748	-3.784
	6252	3.1	22.9	7.326	-1.790	3680	-3.526
	6614	4.6	24.8	5.416	-2.210	3739	-3.219
	6916	4.9	22.6	4.580	-2.354	3786	-3.077
	7255	6.2	22.1	3.589	-2.516	3728	-2.858
	7539	8.4	25.1	2.987	-2.625	3565	-2.681
	7834	9.1	23.3	2.574	-2.681	3565	-2.538
	8160	11.2	24.8	2.222	-2.739	3469	-2.388
	8462	11.8	23.8	2.013	-2.772	3446	-2.286
	8833	13.5	23.7	1.755	-2.811	3378	-2.136
	9057	14.6	23.9	1.643	-2.832	3318	-2.062
	9425	15.7	23.3	1.487	-2.856	3292	-1.948
	10078	18.4	22.8	1.235	-2.893	3235	-1.725
	10717	21.4	23.2	1.082	-2.915	3262	-1.563
	11356	22.5	21.7	0.961	-2.937	3254	-1.409
	11901	24.0	21.3	0.891	-2.950	3309	-1.310
	12574	22.7	18.5	0.813	-2.974	3285	-1.182

ACCELERATION RATIO DATA (Continued)

SAMPLE	FREQ. rad/s	BOTTOM PEAK ACC. m/s^2	TOP PEAK ACC. m/s^2	ACC. RATIO	PHASE ANGLE rad	ALPHA	XI
V8							
	1268	22.6	24.0	1.060	-0.004	4594	-55.253
	1892	20.3	22.3	1.101	-0.002	1268	-34.950
	2492	19.7	22.8	1.156	-0.023	9052	-23.221
	3219	17.8	22.9	1.291	-0.020	3323	-13.992
	3685	17.1	22.9	1.341	-0.033	4768	-12.372
	4058	16.0	22.7	1.419	-0.039	4307	-10.608
	4405	16.1	24.4	1.516	-0.055	4642	-9.114
	4698	15.4	24.2	1.574	-0.090	6687	-8.344
	5036	14.5	24.5	1.696	-0.119	6830	-7.311
	5358	13.4	24.4	1.816	-0.145	6894	-6.612
	5729	12.7	24.5	1.920	-0.143	6096	-6.247
	6042	11.8	24.3	2.063	-0.177	6316	-5.742
	6297	10.9	24.1	2.205	-0.177	5528	-5.437
	6614	10.1	24.2	2.391	-0.207	5502	-5.069
	6960	9.3	24.8	2.672	-0.254	5429	-4.662
	7236	8.1	23.8	2.915	-0.294	5393	-4.404
	7541	7.3	24.0	3.281	-0.354	5285	-4.117
	7913	6.5	25.0	3.857	-0.456	5199	-3.800
	8182	5.8	25.2	4.372	-0.537	5031	-3.612
	8463	4.7	23.3	4.929	-0.628	4907	-3.460
	8850	4.1	24.3	5.985	-0.908	4925	-3.186
	9125	3.7	24.2	6.480	-1.139	4973	-3.034
	9409	3.7	24.6	6.618	-1.373	5040	-2.906
	10088	4.5	24.3	5.409	-1.958	5146	-2.583
	10679	5.7	23.0	4.040	-2.252	5257	-2.348
	11332	8.3	24.9	2.996	-2.471	5083	-2.108
	11893	10.0	24.3	2.422	-2.581	4969	-1.936
	12594	12.8	24.4	1.909	-2.657	5013	-1.739

ACCELERATION RATIO DATA (Continued)

SAMPLE	FREQ. rad/s	BOTTOM PEAK ACC. m/s^2	TOP PEAK ACC. m/s^2	ACC. RATIO	PHASE ANGLE rad	ALPHA	XI
V9							
	1323	21.1	23.4	1.110	-0.013	6229	-36.650
	1894	20.5	24.6	1.202	-0.026	5760	-21.771
	2512	17.7	24.1	1.359	-0.044	4644	-13.754
	3168	15.2	24.6	1.621	-0.094	4952	-9.241
	3731	12.5	24.1	1.921	-0.146	4808	-7.263
	4074	10.8	23.8	2.197	-0.169	4147	-6.374
	4418	9.6	24.5	2.556	-0.233	4192	-5.614
	4727	7.5	22.6	3.001	-0.296	4001	-5.066
	5033	6.5	23.7	3.665	-0.383	3722	-4.587
	5362	5.2	23.4	4.543	-0.550	3790	-4.170
	5712	3.9	22.9	5.920	-0.802	3620	-3.803
	6013	3.6	24.9	6.946	-1.247	3669	-3.469
	6283	3.3	22.7	6.858	-1.652	3638	-3.239
	6649	4.2	23.0	5.519	-2.047	3730	-2.984
	6972	5.5	22.7	4.152	-2.290	3855	-2.742
	7239	6.7	23.8	3.547	-2.392	3921	-2.608
	7552	6.6	22.8	3.440	-2.379	4241	-2.600
	7854	8.2	24.8	3.019	-2.419	4518	-2.494
	8185	9.1	24.5	2.704	-2.502	4421	-2.385
	8497	10.1	25.0	2.476	-2.558	4371	-2.299
	8816	10.3	23.4	2.278	-2.638	4057	-2.211
	9173	11.8	24.2	2.048	-2.709	3793	-2.103
	9437	12.5	23.9	1.916	-2.743	3680	-2.037
	10028	14.3	23.2	1.627	-2.819	3350	-1.868
	10649	17.3	24.0	1.388	-2.868	3164	-1.702
	11316	19.4	23.6	1.217	-2.919	2830	-1.558
	11959	20.9	23.1	1.105	-2.943	2745	-1.452
	12583	23.5	24.0	1.020	-2.973	2508	-1.362

ACCELERATION RATIO DATA (Continued)

SAMPLE	FREQ. rad/s	BOTTOM PEAK ACC. m/s^2	TOP PEAK ACC. m/s^2	ACC. RATIO	PHASE ANGLE rad	ALPHA	XI
V10							
	1341	21.6	24.1	1.117	-0.004	1891	-40.200
	1893	20.0	23.9	1.196	-0.039	10172	-24.747
	2494	18.0	24.7	1.374	-0.039	4382	-15.195
	3167	15.0	24.9	1.663	-0.094	5054	-10.091
	3733	12.2	24.7	2.027	-0.138	4452	-7.834
	4083	9.5	22.4	2.355	-0.179	4184	-6.826
	4405	8.8	24.3	2.754	-0.240	4177	-6.080
	4689	7.4	24.6	3.328	-0.322	4024	-5.447
	5040	5.6	24.3	4.322	-0.467	3851	-4.853
	5347	4.2	24.3	5.732	-0.742	3843	-4.354
	5661	3.4	24.2	7.140	-1.153	3780	-3.974
	5999	3.5	24.1	6.982	-1.687	3841	-3.636
	6315	3.9	21.9	5.612	-2.093	3839	-3.347
	6628	4.9	20.4	4.191	-2.339	3916	-3.073
	6974	7.7	24.9	3.229	-2.466	4111	-2.833
	7251	7.8	22.5	2.874	-2.516	4230	-2.721
	7564	9.8	24.8	2.522	-2.619	3939	-2.574
	7854	11.4	24.9	2.180	-2.698	3704	-2.413
	8191	12.4	23.9	1.932	-2.743	3640	-2.280
	8464	13.2	23.1	1.755	-2.774	3587	-2.171
	8899	15.5	23.7	1.531	-2.818	3479	-2.012
	9181	17.3	24.3	1.405	-2.837	3462	-1.910
	9407	17.8	23.7	1.329	-2.850	3457	-1.842
	10017	21.4	24.5	1.146	-2.887	3351	-1.657
	10705	23.9	23.8	0.993	-2.918	3295	-1.472
	11314	23.8	21.5	0.905	-2.935	3353	-1.350
	11890	23.7	19.8	0.835	-2.956	3332	-1.238
	12554	23.6	18.3	0.776	-2.984	3229	-1.131

ACCELERATION RATIO DATA (Continued)

SAMPLE	FREQ. rad/s	BOTTOM PEAK ACC. m/s^2	TOP PEAK ACC. m/s^2	ACC. RATIO	PHASE ANGLE rad	ALPHA	XI
V11							
	1265	20.8	22.8	1.096	-0.000	75	-49.240
	1890	21.1	24.7	1.168	-0.011	4444	-30.743
	2488	18.5	24.2	1.306	-0.036	6154	-18.480
	3161	15.3	23.5	1.534	-0.068	5662	-12.265
	3687	13.2	24.0	1.825	-0.102	4897	-9.308
	4033	11.9	24.7	2.083	-0.136	4711	-8.002
	4348	10.3	24.0	2.331	-0.156	4333	-7.267
	4662	8.9	24.5	2.754	-0.210	4213	-6.426
	4918	7.4	23.1	3.135	-0.265	4266	-5.946
	5208	6.5	24.8	3.793	-0.348	4121	-5.426
	5520	4.9	24.0	4.850	-0.500	4059	-4.930
	5806	4.0	25.1	6.339	-0.734	3939	-4.526
	6283	2.9	24.1	8.293	-1.245	3901	-4.113
	6649	3.1	23.9	7.660	-1.844	3929	-3.769
	6956	4.0	23.0	5.572	-2.288	3813	-3.431
	7243	5.4	24.5	4.569	-2.459	3716	-3.252
	7551	6.3	23.7	3.769	-2.580	3632	-3.077
	7829	7.5	23.8	3.193	-2.649	3651	-2.922
	8174	8.9	24.0	2.692	-2.715	3621	-2.752
	8452	10.6	25.3	2.377	-2.752	3623	-2.621
	8855	11.9	24.0	2.011	-2.813	3447	-2.433
	9172	13.8	24.7	1.791	-2.835	3471	-2.298
	9412	14.4	24.2	1.687	-2.850	3460	-2.228
	10049	17.3	24.5	1.416	-2.887	3413	-2.011
	10662	20.1	24.5	1.222	-2.924	3238	-1.820
	11305	22.0	23.8	1.081	-2.951	3137	-1.655
	11980	23.4	22.7	0.974	-2.974	3050	-1.509
	12546	24.0	21.6	0.902	-2.993	2958	-1.398

ACCELERATION RATIO DATA (Continued)

SAMPLE	FREQ. rad/s	BOTTOM PEAK ACC. m/s^2	TOP PEAK ACC. m/s^2	ACC. RATIO	PHASE ANGLE rad	ALPHA	XI
V12							
	1262	20.4	23.0	1.124	-0.018	7296	-37.128
	1893	18.7	23.0	1.231	-0.035	6920	-21.876
	2525	17.1	24.4	1.429	-0.050	4437	-13.639
	3164	13.5	23.7	1.761	-0.111	4734	-9.204
	3715	10.7	23.4	2.187	-0.144	3695	-7.280
	4083	9.4	24.9	2.632	-0.204	3630	-6.273
	4408	7.5	23.7	3.172	-0.257	3338	-5.627
	4707	6.0	24.4	4.060	-0.393	3397	-4.991
	5027	4.6	24.8	5.365	-0.577	3288	-4.521
	5393	3.4	24.8	7.360	-1.009	3307	-4.052
	5712	2.9	22.5	7.719	-1.675	3298	-3.648
	5984	3.7	23.3	6.387	-2.063	3303	-3.404
	6357	5.0	22.6	4.523	-2.377	3354	-3.099
	6640	6.1	22.7	3.730	-2.508	3317	-2.924
	6957	7.6	23.1	3.028	-2.641	3110	-2.722
	7246	9.6	24.5	2.558	-2.720	2972	-2.554
	7592	10.8	23.5	2.171	-2.785	2832	-2.384
	7864	12.1	23.3	1.926	-2.813	2837	-2.256
	8180	13.7	23.3	1.705	-2.848	2757	-2.120
	8463	15.9	24.5	1.544	-2.875	2673	-2.006
	8861	17.7	24.3	1.371	-2.893	2707	-1.867
	9114	18.4	24.0	1.304	-2.906	2673	-1.807
	9424	20.4	24.5	1.199	-2.928	2576	-1.704
	10060	22.6	23.6	1.043	-2.951	2560	-1.528
	10660	23.5	22.0	0.937	-2.976	2450	-1.388
	11273	22.0	18.8	0.856	-2.992	2470	-1.265
	11918	23.4	18.5	0.789	-3.003	2599	-1.150
	12604	23.6	17.3	0.736	-3.029	2523	-1.039

ACCELERATION RATIO DATA (Continued)

SAMPLE	FREQ. rad/s	BOTTOM PEAK ACC. m/s^2	TOP PEAK ACC. m/s^2	ACC. RATIO	PHASE ANGLE rad	ALPHA	XI
V13							
	1334	22.0	23.8	1.084	-0.011	7190	-37.816
	1892	21.4	24.5	1.146	-0.018	6261	-23.412
	2527	19.2	24.2	1.259	-0.048	7502	-14.161
	3169	17.2	24.2	1.409	-0.050	4433	-10.258
	3714	15.3	24.3	1.587	-0.094	5253	-7.868
	4060	13.6	23.9	1.758	-0.122	4941	-6.686
	4397	12.4	23.7	1.915	-0.143	4686	-6.017
	4731	11.2	24.1	2.145	-0.170	4295	-5.356
	5027	10.2	24.5	2.398	-0.206	4117	-4.866
	5311	9.0	24.1	2.693	-0.256	4089	-4.465
	5661	7.8	24.7	3.184	-0.318	3813	-4.056
	5991	6.4	24.4	3.793	-0.438	3899	-3.701
	6296	5.2	23.8	4.608	-0.564	3707	-3.429
	6614	4.1	23.2	5.645	-0.779	3651	-3.178
	6965	3.3	22.7	6.784	-1.148	3601	-2.927
	7222	3.4	23.6	6.967	-1.511	3580	-2.749
	7525	4.0	25.0	6.302	-1.926	3430	-2.558
	7819	4.5	23.9	5.279	-2.172	3407	-2.418
	8202	5.8	24.1	4.153	-2.387	3361	-2.252
	8464	6.6	23.0	3.472	-2.505	3294	-2.128
	8816	8.2	23.4	2.851	-2.604	3239	-1.988
	9122	9.9	25.1	2.537	-2.651	3242	-1.905
	9421	10.6	24.1	2.271	-2.691	3229	-1.822
	10059	13.3	23.7	1.782	-2.771	3114	-1.628
	10687	15.6	22.9	1.466	-2.823	3014	-1.464
	11274	18.7	23.7	1.269	-2.858	2940	-1.338
	11905	22.3	24.6	1.106	-2.892	2822	-1.215
	12609	23.7	22.9	0.969	-2.907	2904	-1.094

ACCELERATION RATIO DATA (Continued)

SAMPLE	FREQ. rad/s	BOTTOM PEAK ACC. m/s^2	TOP PEAK ACC. m/s^2	ACC. RATIO	PHASE ANGLE rad	ALPHA	XI
V14							
	1281	22.0	24.4	1.108	-0.010	5750	-44.465
	1889	20.6	24.6	1.197	-0.038	10580	-25.739
	2505	18.0	24.8	1.375	-0.039	4689	-15.812
	3173	15.5	25.2	1.625	-0.109	6767	-10.807
	3746	12.3	24.3	1.980	-0.156	5661	-8.309
	4085	10.9	25.0	2.282	-0.207	5442	-7.224
	4433	8.8	23.8	2.691	-0.262	5033	-6.395
	4724	7.6	24.4	3.233	-0.342	4751	-5.730
	5067	5.7	23.2	4.101	-0.462	4407	-5.150
	5357	4.4	22.8	5.192	-0.697	4459	-4.657
	5686	3.8	25.0	6.542	-1.118	4400	-4.190
	6029	3.7	24.3	6.566	-1.561	4521	-3.868
	6283	4.0	24.1	6.024	-1.801	4633	-3.696
	6624	5.2	24.7	4.734	-2.173	4540	-3.371
	6990	6.0	22.6	3.750	-2.371	4538	-3.124
	7256	6.8	22.2	3.250	-2.503	4274	-2.961
	7549	8.3	22.9	2.744	-2.612	4050	-2.775
	7811	10.0	24.0	2.398	-2.675	3943	-2.626
	8208	12.0	24.0	2.003	-2.746	3792	-2.420
	8501	13.5	24.2	1.791	-2.785	3693	-2.287
	8850	15.2	24.4	1.604	-2.819	3609	-2.153
	9133	16.4	24.0	1.466	-2.850	3462	-2.040
	9444	16.4	22.3	1.362	-2.867	3455	-1.948
	10003	21.0	24.7	1.179	-2.906	3284	-1.759
	10708	22.7	23.4	1.031	-2.936	3211	-1.577
	11321	23.9	22.5	0.940	-2.961	3102	-1.448
	11956	23.6	20.7	0.876	-2.982	3045	-1.345
	12529	23.5	19.5	0.832	-3.002	2932	-1.267

ACCELERATION RATIO DATA (Continued)

SAMPLE	FREQ. rad/s	BOTTOM PEAK ACC. m/s^2	TOP PEAK ACC. m/s^2	ACC. RATIO	PHASE ANGLE rad	ALPHA	XI
V15							
	1258	22.2	23.7	1.066	-0.005	7566	-75.084
	1883	21.1	23.7	1.127	-0.008	5086	-41.375
	2520	20.6	24.6	1.195	-0.018	6806	-28.395
	3156	17.7	23.7	1.334	-0.038	7031	-18.186
	3764	16.1	24.3	1.511	-0.066	6966	-13.208
	4080	15.1	24.2	1.605	-0.090	7650	-11.714
	4406	14.2	24.7	1.747	-0.109	7160	-10.238
	4745	12.5	24.1	1.919	-0.132	6746	-9.069
	5030	11.9	25.0	2.102	-0.154	6345	-8.229
	5383	10.2	24.0	2.367	-0.193	6204	-7.385
	5666	8.8	23.0	2.620	-0.229	6062	-6.837
	5978	8.2	24.6	3.007	-0.278	5753	-6.270
	6276	6.9	24.2	3.485	-0.364	5850	-5.767
	6597	5.7	24.1	4.215	-0.498	5834	-5.271
	6919	4.7	23.9	5.130	-0.635	5521	-4.916
	7222	4.0	24.9	6.195	-0.868	5451	-4.583
	7570	3.4	24.0	7.078	-1.193	5449	-4.289
	7868	3.4	25.1	7.287	-1.563	5343	-4.032
	8160	3.5	23.2	6.628	-1.915	5199	-3.797
	8534	4.5	24.1	5.317	-2.239	5031	-3.530
	8836	5.0	22.3	4.426	-2.389	5021	-3.350
	9106	6.5	24.5	3.804	-2.503	4873	-3.194
	9448	6.9	22.3	3.224	-2.588	4857	-3.026
	10045	9.5	23.8	2.506	-2.695	4761	-2.754
	10679	12.3	25.0	2.035	-2.772	4580	-2.511
	11933	15.3	22.8	1.493	-2.866	4269	-2.125

ACCELERATION RATIO DATA (Continued)

SAMPLE	FREQ. rad/s	BOTTOM PEAK ACC. m/s^2	TOP PEAK ACC. m/s^2	ACC. RATIO	PHASE ANGLE rad	ALPHA	XI
H1							
	1266	22.5	24.0	1.064	0.002	-3074	-73.457
	1908	20.4	22.6	1.111	0.001	-1053	-44.765
	2517	19.6	22.9	1.168	-0.005	2208	-31.094
	3192	18.7	23.8	1.270	-0.051	12663	-20.011
	3718	17.7	24.5	1.383	-0.044	7067	-15.625
	4059	16.1	23.6	1.470	-0.056	6910	-13.442
	4379	14.9	23.4	1.564	-0.069	6816	-11.820
	4701	14.6	24.4	1.671	-0.095	7490	-10.475
	4981	13.5	24.1	1.790	-0.101	6597	-9.511
	5358	11.8	23.1	1.965	-0.124	6389	-8.477
	5668	11.7	24.9	2.128	-0.142	6120	-7.808
	5989	9.4	24.3	2.364	-0.178	6109	-7.092
	6288	8.6	24.8	2.589	-0.205	5930	-6.625
	6602	7.3	24.8	2.899	-0.255	6008	-6.133
	6974	9.7	23.0	3.413	-0.324	5798	-5.609
	7181	6.3	22.8	3.614	-0.337	5607	-5.479
	7525	5.1	22.3	4.368	-0.458	5629	-5.041
	7792	4.7	24.6	5.227	-0.596	5518	-4.720
	8180	3.8	24.5	6.409	-0.829	5503	-4.399
	8491	2.9	22.6	7.481	-1.092	5364	-4.164
	8811	2.9	22.6	7.704	-1.540	5413	-3.876
	9194	3.3	24.8	7.018	-1.889	5372	-3.664
	9419	3.3	23.5	6.299	-2.094	5247	-3.524
	10053	3.6	22.6	4.365	-2.417	5275	-3.185
	10694	5.2	22.8	3.147	-2.605	5127	-2.870
	11258	7.2	22.8	2.490	-2.714	4856	-2.625
	11902	9.8	24.4	2.032	-2.778	4768	-2.401
	12597	11.9	24.3	1.677	-2.827	4688	-2.178

ACCELERATION RATIO DATA (Continued)

SAMPLE	FREQ. rad/s	BOTTOM PEAK ACC. m/s^2	TOP PEAK ACC. m/s^2	ACC. RATIO	PHASE ANGLE rad	ALPHA	XI
H2							
	1265	22.9	24.4	1.066	-0.003	3858	-72.832
	1892	20.8	23.4	1.125	0.002	-987	-40.947
	2504	21.0	25.0	1.189	-0.014	5741	-28.536
	3165	17.9	23.7	1.326	-0.051	9406	-17.790
	3714	16.3	24.1	1.483	-0.048	5401	-13.515
	4046	15.6	24.8	1.596	-0.074	6321	-11.620
	4409	14.0	24.6	1.756	-0.091	5821	-9.999
	4701	13.1	24.9	1.911	-0.114	5772	-8.948
	5047	11.4	24.2	2.113	-0.121	4901	-8.080
	5347	10.2	24.1	2.363	-0.157	5017	-7.291
	5965	7.6	24.1	3.181	-0.263	4819	-5.978
	5984	8.1	25.1	3.117	-0.256	4899	-6.047
	6283	6.7	24.8	3.695	-0.328	4762	-5.557
	6628	5.0	23.8	4.759	-0.473	4624	-5.024
	6978	3.9	24.1	6.208	-0.716	4611	-4.593
	7264	3.1	23.1	7.382	-0.953	4564	-4.348
	7551	3.1	24.8	8.109	-1.459	4604	-4.008
	7835	3.2	22.7	7.058	-1.829	4841	-3.771
	8198	4.1	23.1	5.696	-2.159	4827	-3.518
	8462	4.6	22.2	4.799	-2.343	4692	-3.341
	8827	6.1	23.4	3.817	-2.532	4402	-3.112
	9144	7.4	24.0	3.231	-2.616	4353	-2.950
	9421	8.5	24.1	2.821	-2.681	4228	-2.810
	10093	11.5	24.2	2.107	-2.795	3905	-2.490
	10734	13.8	23.5	1.703	-2.849	3794	-2.240
	11300	16.9	24.5	1.447	-2.888	3654	-2.038
	11899	16.9	24.5	1.262	-2.913	3617	-1.863
	12589	19.0	24.0	1.093	-2.931	3678	-1.673

ACCELERATION RATIO DATA (Continued)

SAMPLE	FREQ. rad/s	BOTTOM PEAK ACC. m/s^2	TOP PEAK ACC. m/s^2	ACC. RATIO	PHASE ANGLE rad	ALPHA	XI
H3							
	1883	22.3	23.3	1.083	-0.003	3867	-63.82
	1258	22.4	24.2	1.046	-0.006	17867	-110.35
	1883	21.2	24.0	1.083	-0.003	3873	-63.81
	2494	19.6	23.8	1.133	-0.006	5231	-41.74
	3191	18.0	24.2	1.216	-0.040	16196	-26.37
	3716	16.9	23.9	1.344	-0.037	7723	-18.53
	4046	16.2	24.2	1.417	-0.047	7734	-16.00
	4387	15.3	24.4	1.496	-0.062	8226	-14.07
	4696	14.3	24.3	1.593	-0.066	7002	-12.50
	5009	12.8	23.7	1.694	-0.081	7052	-11.27
	5360	11.6	23.4	1.854	-0.107	7213	-9.90
	5661	11.1	24.6	2.016	-0.131	7123	-8.96
	6004	9.9	23.8	2.209	-0.162	7193	-8.17
	6283	8.9	24.2	2.410	-0.184	6832	-7.59
	6591	7.6	24.5	2.711	-0.225	6659	-6.96
	6974	6.8	24.8	3.242	-0.290	6243	-6.27
	7230	5.6	24.5	3.642	-0.355	6311	-5.90
	7581	5.0	24.8	4.345	-0.453	6130	-5.48
	7781	3.7	23.0	4.935	-0.572	6262	-5.19
	8126	3.7	24.8	6.153	-0.857	6320	-4.76
	8473	3.4	22.5	6.717	-1.113	6556	-4.51
	8829	4.0	24.0	6.689	-1.530	6756	-4.18
	9106	4.3	23.5	5.979	-1.701	7304	-4.03
	9395	5.5	24.4	5.467	-1.890	7377	-3.86
	10053	6.9	23.3	4.462	-2.208	7177	-3.55
	10686	9.2	24.2	3.391	-2.523	6126	-3.19
	11292	11.1	23.9	2.640	-2.666	5720	-2.91
	11926	13.7	24.2	2.141	-2.753	5430	-2.65

ACCELERATION RATIO DATA (Continued)

SAMPLE	FREQ. rad/s	BOTTOM PEAK ACC. m/s^2	TOP PEAK ACC. m/s^2	ACC. RATIO	PHASE ANGLE rad	ALPHA	XI
H4							
	1264	23.7	24.9	1.050	0.003	-7285	-100.41
	1876	22.4	24.3	1.083	-0.004	5709	-62.40
	2495	20.7	23.3	1.125	-0.015	12960	-42.13
	3168	19.2	22.9	1.189	-0.033	16476	-28.89
	3719	18.7	24.2	1.290	-0.041	11248	-20.40
	4059	18.1	24.5	1.350	-0.043	9203	-17.72
	4442	16.7	24.0	1.441	-0.057	8979	-14.87
	4689	16.2	24.1	1.493	-0.064	8879	-13.73
	5029	15.5	24.8	1.596	-0.079	8579	-12.04
	5338	13.5	22.8	1.691	-0.099	8968	-10.90
	5679	12.8	23.2	1.815	-0.111	8238	-9.87
	6005	12.3	24.2	1.969	-0.135	8081	-8.93
	6283	11.6	24.6	2.117	-0.151	7677	-8.28
	6614	9.9	23.0	2.331	-0.177	7314	-7.59
	6955	9.1	23.5	2.583	-0.232	7770	-6.96
	7222	7.9	22.7	2.883	-0.268	7309	-6.48
	7554	7.4	24.4	3.296	-0.325	7054	-6.01
	7846	6.0	22.4	3.735	-0.392	6936	-5.65
	8201	5.2	23.0	4.453	-0.534	7051	-5.21
	8476	4.5	23.3	5.156	-0.678	7013	-4.91
	8841	3.9	23.4	6.027	-0.903	7023	-4.60
	9085	3.4	21.9	6.475	-1.206	7204	-4.32
	9434	3.9	24.4	6.180	-1.504	7629	-4.08
	10041	4.3	23.0	5.409	-1.863	7871	-3.77
	10603	5.4	24.8	4.623	-2.201	7217	-3.49
	11359	6.9	23.4	3.380	-2.489	6691	-3.12
	11978	9.0	23.9	2.643	-2.639	6233	-2.84
	12535	10.4	23.0	2.201	-2.701	6226	-2.63

ACCELERATION RATIO DATA (Continued)

SAMPLE	FREQ. rad/s	BOTTOM PEAK ACC. m/s^2	TOP PEAK ACC. m/s^2	ACC. RATIO	PHASE ANGLE rad	ALPHA	XI
H5							
	1893	22.2	24.7	1.110	-0.005	4860	-51.641
	2518	20.1	23.6	1.177	-0.005	2376	-34.053
	3171	18.0	23.5	1.308	-0.043	9783	-20.961
	3709	16.0	23.0	1.439	-0.058	8415	-16.068
	4080	14.8	23.0	1.555	-0.064	6947	-13.687
	4381	14.6	24.5	1.677	-0.087	7305	-11.951
	4686	13.8	25.0	1.810	-0.103	6905	-10.709
	5033	11.7	23.6	2.025	-0.122	6188	-9.392
	5313	11.1	24.3	2.197	-0.150	6312	-8.642
	5668	9.8	24.6	2.524	-0.183	5809	-7.722
	5973	8.4	24.1	2.870	-0.225	5654	-7.079
	6270	7.4	25.1	3.371	-0.295	5604	-6.460
	6648	5.7	24.3	4.243	-0.401	5314	-5.845
	6978	4.6	24.1	5.226	-0.545	5282	-5.419
	7238	3.6	23.1	6.421	-0.715	5081	-5.096
	7543	3.2	24.8	7.828	-1.117	5211	-4.700
	7903	2.9	23.6	8.284	-1.467	5228	-4.458
	8193	3.1	22.6	7.280	-1.965	5054	-4.127
	8472	3.5	21.4	6.157	-2.193	5047	-3.936
	8835	4.7	23.0	4.926	-2.409	4913	-3.702
	9173	6.0	23.4	3.885	-2.553	4852	-3.461
	9415	6.7	22.7	3.410	-2.625	4738	-3.320
	10071	8.6	21.9	2.552	-2.742	4594	-2.989
	10606	11.5	23.9	2.086	-2.800	4520	-2.740
	11239	13.8	23.9	1.727	-2.842	4515	-2.492
	11894	15.5	23.1	1.490	-2.879	4406	-2.288
	12561	16.8	21.9	1.305	-2.901	4453	-2.098

ACCELERATION RATIO DATA (Continued)

SAMPLE	FREQ. rad/s	BOTTOM PEAK ACC. m/s^2	TOP PEAK ACC. m/s^2	ACC. RATIO	PHASE ANGLE rad	ALPHA	XI
H6							
	1267	23.0	24.5	1.066	-0.000	283	-70.361
	1880	21.5	24.0	1.120	0.002	-1565	-40.900
	2487	21.0	24.5	1.168	-0.015	7293	-30.283
	3127	18.3	23.4	1.279	-0.050	11580	-19.224
	3718	16.8	24.0	1.431	-0.047	6150	-14.077
	4071	15.4	23.9	1.546	-0.072	6885	-11.824
	4412	14.6	24.5	1.678	-0.088	6420	-10.262
	4718	12.5	22.5	1.805	-0.113	6707	-9.199
	5007	11.9	23.5	1.979	-0.123	5767	-8.267
	5328	11.1	24.4	2.193	-0.147	5426	-7.461
	5665	9.8	24.4	2.485	-0.188	5366	-6.710
	5984	8.9	25.2	2.835	-0.246	5463	-6.107
	6277	7.6	24.7	3.257	-0.315	5486	-5.621
	6588	5.9	23.1	3.896	-0.403	5254	-5.166
	6915	5.0	24.4	4.844	-0.560	5150	-4.731
	7222	3.7	22.1	5.998	-0.765	4995	-4.397
	7559	3.4	23.5	6.920	-1.111	5185	-4.083
	7805	3.4	23.9	7.041	-1.467	5273	-3.836
	8160	3.3	21.6	6.460	-1.811	5311	-3.610
	8491	4.3	22.5	5.274	-2.094	5424	-3.375
	8801	5.2	22.2	4.285	-2.277	5504	-3.167
	9118	6.0	22.8	3.834	-2.386	5401	-3.046
	9434	6.7	22.7	3.377	-2.497	5169	-2.909
	10086	9.1	23.6	2.587	-2.651	4869	-2.630
	10649	11.4	24.6	2.149	-2.735	4634	-2.427
	11294	13.9	24.0	1.729	-2.811	4337	-2.177
	11928	16.2	23.8	1.465	-2.848	4297	-1.980
	12529	18.4	23.5	1.278	-2.874	4283	-1.810

ACCELERATION RATIO DATA (Continued)

SAMPLE	FREQ. rad/s	BOTTOM PEAK ACC. m/s^2	TOP PEAK ACC. m/s^2	ACC. RATIO	PHASE ANGLE rad	ALPHA	XI
H7							
	1266	22.5	24.3	1.084	-0.005	4794	-54.111
	1870	21.2	24.5	1.156	-0.016	6325	-30.945
	2494	19.3	24.6	1.275	-0.037	6884	-19.133
	3129	16.7	24.0	1.436	-0.061	6404	-13.437
	3756	14.5	24.7	1.710	-0.102	5716	-9.629
	4072	12.3	23.2	1.882	-0.130	5612	-8.443
	4406	11.5	24.6	2.132	-0.162	5178	-7.385
	4699	10.0	23.7	2.373	-0.195	5021	-6.720
	5033	8.9	25.1	2.810	-0.256	4747	-5.952
	5331	7.2	23.4	3.269	-0.323	4636	-5.454
	5668	5.6	23.1	4.134	-0.448	4395	-4.898
	6003	4.8	24.8	5.160	-0.643	4424	-4.483
	6283	3.5	22.3	6.384	-0.943	4381	-4.123
	6630	3.3	23.7	7.216	-1.349	4334	-3.822
	6905	3.3	22.5	6.755	-1.802	4243	-3.540
	7166	3.9	22.5	5.771	-2.089	4183	-3.340
	7540	5.8	25.1	4.323	-2.384	4040	-3.057
	7885	6.7	23.4	3.510	-2.521	3979	-2.864
	8206	8.4	24.3	2.894	-2.619	3895	-2.678
	8476	8.8	23.4	2.654	-2.652	3943	-2.595
	8856	10.3	24.1	2.344	-2.704	3906	-2.468
	9117	11.6	24.8	2.135	-2.730	3929	-2.371
	9427	10.4	20.6	1.982	-2.764	3845	-2.290
	10045	12.9	20.8	1.611	-2.823	3714	-2.055
	10678	17.6	23.7	1.344	-2.858	3710	-1.842
	11289	18.4	21.9	1.189	-2.871	3870	-1.694
	11905	20.5	22.0	1.073	-2.885	3986	-1.566
	12557	19.9	19.3	0.969	-2.898	4135	-1.436

ACCELERATION RATIO DATA (Continued)

SAMPLE	FREQ. rad/s	BOTTOM PEAK ACC. m/s^2	TOP PEAK ACC. m/s^2	ACC. RATIO	PHASE ANGLE rad	ALPHA	XI
H8							
	1265	23.1	24.3	1.051	0.003	-6297	-73.015
	1265	22.7	24.6	1.051	0.003	-6297	-73.015
	1887	20.3	23.0	1.083	-0.005	5884	-46.898
	2489	20.7	24.8	1.134	-0.009	5378	-30.299
	3134	19.0	24.7	1.197	-0.031	11127	-21.281
	3764	17.4	23.7	1.301	-0.044	8712	-15.086
	4046	16.6	23.8	1.363	-0.039	6143	-13.160
	4408	15.7	23.5	1.438	-0.054	6663	-11.414
	4677	15.3	24.4	1.498	-0.057	6039	-10.445
	5014	14.0	23.8	1.591	-0.083	6942	-9.216
	5352	13.2	24.0	1.699	-0.088	6040	-8.318
	5664	12.4	23.2	1.824	-0.111	6185	-7.501
	5988	11.9	24.1	1.875	-0.114	6123	-7.270
	6302	10.6	23.4	2.018	-0.135	6054	-6.676
	6624	9.9	23.6	2.202	-0.165	6047	-6.111
	6926	9.1	24.0	2.390	-0.188	5847	-5.704
	7247	8.3	24.4	2.649	-0.225	5732	-5.280
	7546	7.6	24.7	2.925	-0.281	5936	-4.931
	7854	6.0	22.6	3.267	-0.317	5588	-4.653
	8181	5.2	22.9	3.771	-0.389	5429	-4.344
	8491	4.5	22.9	4.368	-0.488	5382	-4.080
	8788	4.2	24.8	5.107	-0.607	5248	-3.856
	9089	3.5	24.5	5.887	-0.763	5223	-3.666
	9469	3.2	22.4	6.957	-1.098	5235	-3.405
	10030	4.3	24.1	7.070	-1.682	5170	-3.089
	10669	5.9	22.9	5.550	-2.129	5158	-2.824
	11290	8.3	23.9	3.915	-2.437	4992	-2.543
	11980	10.0	24.2	2.886	-2.583	5037	-2.301

ACCELERATION RATIO DATA (Continued)

SAMPLE	FREQ. rad/s	BOTTOM PEAK ACC. m/s^2	TOP PEAK ACC. m/s^2	ACC. RATIO	PHASE ANGLE rad	ALPHA	XI
H9							
	1286	21.7	23.7	1.093	-0.011	8178	-51.563
	1929	20.2	23.6	1.166	-0.007	2874	-31.625
	2559	17.9	23.0	1.281	-0.043	8459	-19.911
	3123	16.9	24.1	1.425	-0.054	6277	-14.648
	3771	13.1	22.4	1.716	-0.085	5066	-10.292
	4088	12.4	23.8	1.915	-0.126	5530	-8.827
	4422	11.2	24.3	2.182	-0.150	4850	-7.732
	4731	9.7	24.3	2.490	-0.220	5362	-6.849
	5027	8.6	24.9	2.879	-0.273	5093	-6.212
	5370	6.9	24.0	3.481	-0.366	4954	-5.591
	5661	5.5	23.3	4.230	-0.510	4979	-5.094
	5949	4.4	22.9	5.242	-0.743	4994	-4.642
	6221	4.1	24.5	5.977	-1.160	5259	-4.194
	6579	3.9	23.1	5.867	-1.531	5454	-3.889
	6905	4.5	22.3	4.967	-1.821	5856	-3.620
	7234	5.6	23.1	4.102	-2.061	6005	-3.355
	7534	6.2	23.6	3.787	-2.195	5845	-3.229
	7884	6.3	21.9	3.482	-2.349	5434	-3.095
	8168	7.7	23.1	2.996	-2.481	5136	-2.913
	8505	9.1	23.0	2.532	-2.596	4814	-2.715
	8823	10.6	23.7	2.242	-2.655	4713	-2.574
	9083	12.1	24.7	2.048	-2.704	4529	-2.466
	9454	14.1	25.1	1.778	-2.749	4455	-2.296
	10051	16.4	24.3	1.485	-2.823	4077	-2.069
	10699	18.4	23.1	1.255	-2.862	4008	-1.853
	11305	21.8	24.1	1.106	-2.895	3885	-1.684
	11937	22.9	22.4	0.978	-2.923	3796	-1.514
	12613	23.6	20.9	0.885	-2.944	3815	-1.371

ACCELERATION RATIO DATA (Continued)

SAMPLE	FREQ. rad/s	BOTTOM PEAK ACC. m/s^2	TOP PEAK ACC. m/s^2	ACC. RATIO	PHASE ANGLE rad	ALPHA	XI
H10							
	1261	22.9	24.7	1.078	-0.007	7540	-65.585
	1890	21.7	25.0	1.154	-0.010	4894	-35.657
	2498	18.9	24.4	1.289	-0.044	8335	-20.461
	3120	16.3	24.1	1.476	-0.064	6405	-14.109
	3758	13.9	24.9	1.788	-0.112	5973	-10.099
	4080	12.3	24.7	2.008	-0.135	5367	-8.797
	4416	10.5	24.2	2.316	-0.168	4867	-7.698
	4720	8.6	23.0	2.664	-0.220	4847	-6.908
	5021	7.1	23.0	3.244	-0.301	4651	-6.128
	5339	5.9	24.2	4.092	-0.435	4592	-5.481
	5676	4.2	22.5	5.302	-0.666	4618	-4.939
	5971	3.7	24.5	6.662	-1.031	4580	-4.495
	6252	3.4	23.7	7.004	-1.498	4620	-4.133
	6579	3.8	22.4	5.946	-1.880	4853	-3.836
	6905	5.2	24.5	4.688	-2.179	4901	-3.539
	7252	5.7	22.6	3.991	-2.346	4816	-3.348
	7552	6.6	23.0	3.509	-2.473	4592	-3.195
	7854	8.1	24.2	2.996	-2.595	4285	-3.011
	8186	9.5	23.7	2.485	-2.693	4036	-2.795
	8502	11.4	24.7	2.168	-2.741	3983	-2.635
	8803	11.9	22.7	1.902	-2.786	3856	-2.474
	9122	13.0	23.3	1.788	-2.803	3885	-2.399
	9448	14.2	23.0	1.612	-2.836	3769	-2.266
	10087	18.1	24.6	1.360	-2.870	3768	-2.042
	10681	19.4	23.0	1.184	-2.913	3510	-1.849
	11305	22.1	23.4	1.059	-2.939	3432	-1.691
	11929	23.3	22.5	0.965	-2.972	3152	-1.553
	12541	24.1	21.5	0.895	-2.990	3112	-1.436

ACCELERATION RATIO DATA (Continued)

SAMPLE	FREQ. rad/s	BOTTOM PEAK ACC. m/s^2	TOP PEAK ACC. m/s^2	ACC. RATIO	PHASE ANGLE rad	ALPHA	XI
H11							
	1268	22.9	25.0	1.092	-0.010	7131	-46.298
	1890	21.0	24.4	1.161	-0.011	3821	-28.611
	2523	18.7	24.8	1.326	-0.034	4581	-15.800
	3143	15.7	23.5	1.495	-0.068	5481	-11.539
	3774	13.1	23.8	1.821	-0.127	5365	-8.253
	4093	12.1	24.8	2.049	-0.146	4620	-7.242
	4406	10.4	24.3	2.339	-0.182	4317	-6.418
	4711	8.8	23.8	2.701	-0.226	4092	-5.776
	5017	7.7	25.1	3.248	-0.321	4147	-5.150
	5347	6.1	25.0	4.078	-0.434	3901	-4.646
	5645	4.5	22.9	5.095	-0.604	3838	-4.267
	5984	3.8	24.4	6.453	-0.902	3824	-3.916
	6283	3.3	24.2	7.418	-1.357	3777	-3.600
	6629	3.4	23.6	6.861	-1.855	3698	-3.321
	6932	4.9	24.8	5.025	-2.242	3708	-3.023
	7264	5.3	22.6	4.226	-2.412	3602	-2.866
	7525	6.0	21.3	3.555	-2.514	3601	-2.719
	7832	8.3	23.7	2.856	-2.618	3546	-2.521
	8160	9.7	24.0	2.476	-2.678	3515	-2.386
	8518	10.9	23.5	2.151	-2.726	3495	-2.249
	8832	12.1	23.3	1.927	-2.760	3478	-2.137
	9126	14.1	25.0	1.768	-2.793	3383	-2.047
	9467	15.3	24.8	1.624	-2.805	3489	-1.958
	10046	17.0	23.7	1.397	-2.849	3364	-1.791
	10694	19.9	24.0	1.205	-2.877	3372	-1.624
	11320	22.6	24.1	1.063	-2.902	3346	-1.476
	11941	22.6	21.8	0.963	-2.918	3392	-1.358
	12579	23.4	20.6	0.880	-2.943	3304	-1.246

ACCELERATION RATIO DATA (Continued)

SAMPLE	FREQ. rad/s	BOTTOM PEAK ACC. m/s^2	TOP PEAK ACC. m/s^2	ACC. RATIO	PHASE ANGLE rad	ALPHA	XI
H12							
	1257	22.4	23.7	1.057	0.006	-11028	-80.587
	1891	21.4	23.6	1.102	0.004	-3651	-47.786
	2519	19.5	22.8	1.173	-0.012	5351	-29.811
	3127	18.2	22.8	1.255	-0.036	9871	-21.162
	3757	17.6	24.5	1.395	-0.044	6787	-15.115
	4095	16.3	24.4	1.492	-0.063	7274	-12.823
	4414	15.2	24.0	1.582	-0.074	6979	-11.434
	4704	14.1	23.6	1.679	-0.089	6929	-10.335
	5032	13.4	24.3	1.816	-0.107	6634	-9.230
	5335	12.4	24.3	1.956	-0.126	6522	-8.424
	5671	11.6	24.8	2.136	-0.153	6478	-7.674
	5998	10.1	24.0	2.362	-0.182	6246	-7.021
	6283	9.3	24.3	2.601	-0.217	6172	-6.519
	6573	8.1	23.6	2.917	-0.258	5966	-6.051
	6920	6.8	23.1	3.383	-0.322	5795	-5.578
	7273	6.0	24.1	4.008	-0.416	5716	-5.156
	7525	5.3	24.9	4.682	-0.553	5853	-4.814
	7885	4.0	22.6	5.715	-0.708	5556	-4.515
	8144	3.5	23.2	6.641	-0.967	5624	-4.238
	8455	3.1	23.0	7.304	-1.223	5590	-4.038
	8850	3.1	22.8	7.246	-1.632	5608	-3.778
	9106	3.5	22.8	6.546	-1.920	5533	-3.590
	9397	3.9	22.3	5.769	-2.082	5664	-3.458
	10069	5.1	21.6	4.273	-2.394	5513	-3.152
	10710	7.1	22.7	3.207	-2.585	5255	-2.868
	11319	9.7	23.9	2.462	-2.693	5138	-2.596
	11932	11.6	23.3	2.004	-2.765	4972	-2.368
	12537	14.2	24.1	1.700	-2.808	4911	-2.178

ACCELERATION RATIO DATA (Continued)

SAMPLE	FREQ. rad/s	BOTTOM PEAK ACC. m/s^2	TOP PEAK ACC. m/s^2	ACC. RATIO	PHASE ANGLE rad	ALPHA	XI
H13							
	1261	22.0	23.3	1.059	-0.009	16196	-83.432
	1884	21.3	23.8	1.114	-0.006	4889	-46.334
	2521	20.6	24.3	1.181	-0.008	3637	-30.918
	3148	18.0	23.5	1.303	-0.043	9283	-19.728
	3759	16.4	24.1	1.467	-0.048	5964	-14.391
	4077	15.3	23.9	1.561	-0.070	6864	-12.587
	4409	14.1	24.0	1.708	-0.096	6968	-10.764
	4715	12.4	22.8	1.833	-0.108	6515	-9.774
	5047	11.3	22.8	2.014	-0.123	5893	-8.778
	5386	10.5	23.6	2.244	-0.162	6070	-7.866
	5674	9.5	23.3	2.442	-0.181	5801	-7.349
	6000	7.7	21.7	2.827	-0.233	5635	-6.626
	6264	7.8	24.7	3.177	-0.307	5994	-6.144
	6598	6.5	24.5	3.747	-0.378	5689	-5.678
	6915	5.2	24.0	4.611	-0.479	5265	-5.247
	7264	4.2	23.8	5.732	-0.671	5255	-4.858
	7525	3.3	23.1	6.982	-0.930	5149	-4.543
	7834	3.1	24.5	7.808	-1.306	5174	-4.255
	8160	3.1	23.5	7.585	-1.731	5097	-3.986
	8472	3.5	22.6	6.544	-2.063	4982	-3.760
	8803	4.6	24.1	5.279	-2.285	5020	-3.547
	9159	5.3	22.9	4.358	-2.440	4961	-3.359
	9461	6.0	22.0	3.651	-2.545	4906	-3.183
	10079	8.2	22.5	2.737	-2.680	4763	-2.879
	10678	10.4	22.4	2.162	-2.758	4690	-2.610
	11314	13.7	24.6	1.791	-2.817	4520	-2.380
	11939	15.2	23.4	1.538	-2.855	4438	-2.186
	12628	18.3	24.3	1.334	-2.882	4450	-1.999

ACCELERATION RATIO DATA (Continued)

SAMPLE	FREQ. rad/s	BOTTOM PEAK ACC. m/s^2	TOP PEAK ACC. m/s^2	ACC. RATIO	PHASE ANGLE rad	ALPHA	XI
H14							
	1253	22.4	23.5	1.052	-0.002	4853	-98.304
	1890	19.6	21.4	1.090	-0.000	575	-59.157
	2521	20.6	23.6	1.145	-0.005	3204	-38.457
	3113	19.4	23.3	1.199	-0.036	16386	-28.292
	3740	17.8	23.8	1.337	-0.040	8871	-18.741
	4095	16.1	22.9	1.419	-0.047	7734	-15.914
	4398	15.9	23.8	1.492	-0.064	8538	-14.090
	4699	15.7	24.8	1.579	-0.083	8987	-12.541
	5024	14.1	23.9	1.698	-0.092	7899	-11.151
	5351	12.9	23.5	1.818	-0.110	7834	-10.104
	5650	12.0	23.6	1.960	-0.132	7730	-9.203
	6004	11.1	24.0	2.159	-0.142	6711	-8.373
	6274	10.3	24.2	2.353	-0.186	7256	-7.703
	6603	9.3	24.8	2.647	-0.223	6912	-7.051
	6880	8.3	24.0	2.902	-0.268	7047	-6.620
	7230	7.1	23.7	3.352	-0.327	6737	-6.117
	7534	6.2	24.6	3.947	-0.418	6580	-5.660
	7843	5.3	24.4	4.564	-0.539	6715	-5.308
	8171	4.6	24.5	5.320	-0.697	6760	-4.992
	8434	4.1	24.6	6.020	-0.903	6871	-4.719
	8768	3.4	22.8	6.682	-1.142	6832	-4.481
	9106	3.4	23.5	6.987	-1.438	6771	-4.249
	9477	3.4	23.3	6.805	-1.689	6757	-4.072
	10037	3.9	22.7	5.858	-2.139	6172	-3.752
	10682	5.1	21.9	4.333	-2.424	6025	-3.433
	11289	7.7	24.5	3.172	-2.617	5688	-3.102
	11935	9.1	22.7	2.487	-2.723	5446	-2.828
	12516	11.1	23.4	2.101	-2.774	5401	-2.628

ACCELERATION RATIO DATA (Continued)

SAMPLE	FREQ. rad/s	BOTTOM PEAK ACC. m/s^2	TOP PEAK ACC. m/s^2	ACC. RATIO	PHASE ANGLE rad	ALPHA	XI
H15							
	1256	22.4	23.7	1.058	-0.005	9607	-80.411
	1256	22.1	24.4	1.058	-0.005	9607	-80.411
	1888	20.1	23.5	1.105	-0.001	629	-47.028
	2521	19.9	24.6	1.169	-0.003	1324	-30.762
	3124	16.1	22.3	1.237	-0.043	13300	-22.311
	3770	16.9	24.9	1.386	-0.054	8638	-15.352
	4093	15.3	23.7	1.473	-0.058	7186	-13.312
	4405	14.9	25.1	1.551	-0.072	7421	-11.955
	4747	13.2	23.9	1.677	-0.093	7349	-10.404
	5067	12.4	24.0	1.807	-0.101	6513	-9.382
	5337	11.1	23.3	1.933	-0.125	6748	-8.598
	5655	10.6	24.9	2.097	-0.144	6421	-7.887
	6017	9.1	23.4	2.362	-0.172	5966	-7.095
	6272	8.4	24.7	2.580	-0.214	6210	-6.603
	6591	7.2	24.3	2.927	-0.258	5966	-6.081
	6897	6.0	23.7	3.350	-0.320	5871	-5.640
	7203	5.3	24.7	3.935	-0.401	5687	-5.234
	7525	4.0	22.5	4.699	-0.526	5640	-4.871
	7836	3.6	23.6	5.604	-0.730	5797	-4.534
	8196	3.4	23.7	6.642	-1.052	5855	-4.198
	8491	3.4	22.7	7.014	-1.373	5885	-3.959
	8828	3.6	22.6	6.756	-1.656	5957	-3.771
	9106	4.3	22.9	6.260	-1.938	5718	-3.586
	9450	6.0	23.3	5.351	-2.182	5573	-3.394
	10050	8.3	23.9	3.903	-2.473	5268	-3.076
	10686	10.5	24.1	2.885	-2.642	5010	-2.773
	11301	13.1	24.8	2.295	-2.730	4877	-2.531
	11928	14.8	24.2	1.894	-2.796	4680	-2.314

APPENDIX G

PREDSTRS.FOR

```
C  THIS PROGRAM PREDICTS THE THEORETICAL MAGNITUDE OF THE STRESS
C  AT THE TOP OF A SOIL SAMPLE FROM THE SECOND-ORDER
C  VISCOELASTIC STRESS-STRAIN MODEL FOR SOIL.  COEFFICIENTS FOR
C  THE PARAMETERS XI AND ALPHA USED IN THE STRESS PREDICTIONS
C  ARE TO BE INPUT FROM THE KEYBOARD   MICHAEL F  KOCHER
C  OKLAHOMA STATE UNIVERSITY AGRICULTURAL ENGINEERING DEPARTMENT
C  JANUARY 31, 1986
C
      REAL M,RO,L,A,FREQ,AR,ALPHA,MSTRS(40),PSTRS(40),BMAXA,TMAXA
      REAL E,XI,PHAS,LAMBDA,C1,C2,C3,C4
      COMPLEX Z0,Z1,Z2,W,PHI,THETA,STR,PSI
      INTEGER I,K
      CHARACTER*3 SNO
      CHARACTER*15 DATFN,DATFN2,DATFN3,DATFN4
C
C  READ IN THE FILENAMES FOR THE OUTPUT DATA
C
      PRINT *,' ENTER FILENAME OF DATA FOR GRAPHING '
      READ *,DATFN3
      PRINT *,' ENTER FILENAME OF DATA FOR REGRESSION '
      READ *,DATFN4
C
C  OPEN FILES FOR OUTPUT OF DATA TO DISK FOR EASY PLOTTING
C
      OPEN(UNIT=1,FILE=DATFN3)
      OPEN(UNIT=2,FILE=DATFN4)
      OPEN(UNIT=9,FILE='LPT1')
C
C  M IS THE MASS OF THE ATTACHED ACCELEROMETER AND DISK AT THE
C  TOP OF THE SOIL SAMPLE DURING VIBRATION TESTS
C
      M=0.0413
C
C  INPUT THE SAMPLE DATA
C
      PRINT *,' ENTER SAMPLE NUMBER AS ''XXX'' '
      READ *,SNO
      WRITE(9,10)SNO
   10 FORMAT(' SECOND VISCOELASTIC MODEL FOR SAMPLE ',A3,/)
      PRINT *,' ENTER SAMPLE LENGTH (m) '
      READ *,L
      PRINT *,' ENTER SAMPLE CROSS SECTIONAL AREA (m**2) '
      READ *,A
      PRINT *,' ENTER SAMPLE WET BULK DENSITY (kg/m**3) '
      READ *,RO
      PRINT *,' ENTER SAMPLE ELASTIC MODULUS (Pa) '
      READ *,E
      PRINT *,' ENTER MULTIPLIER FOR ALPHA '
      READ *,C1
      PRINT *,' ENTER EXPONENT FOR ALPHA '
      READ *,C2
      PRINT *,' ENTER MULTIPLIER FOR XI '
      READ *,C3
      PRINT *,' ENTER EXPONENT FOR XI '
      READ *,C4
C
C  OUTPUT SAMPLE DATA TO PRINTER FOR HARDCOPY OF RESULTS
C
      WRITE(9,11)L,A,RO,E,C1,C2,C3,C4
   11 FORMAT('                    LENGTH = ',F7 4,' m',/,
     $ ' CROSS SECTIONAL AREA = ',E10 3,' m**2',/,
     $ '     WET BULK DENSITY = ',F7 1,' kg/m**3',/,
     $ '      ELASTIC MODULUS = ',E10 3,' Pa',/,/,
     $ ' ALPHA = EXP(',F6 2,')/FREQUENCY**(',F6 3,')',/,
     $ ' XI = EXP(',F6 2,')/FREQUENCY**(',F6 3,')',/)
      WRITE(9,12)
   12 FORMAT('    FREQ',5X,'MSTRESS',3X,'PSTRESS')
C
C  GET THE FILENAME OF THE DYNAMIC TEST DATA
C
      PRINT *,' ENTER DYNAMIC TEST DATA FILENAME AS ''A:XXX.DAT'' '
      READ *,DATFN
      OPEN(UNIT=3,FILE=DATFN)
C
C  GET THE FILENAME OF THE MAXIMUM ACCELERATION DATA
C
      PRINT *,' ENTER MAX  ACCEL  DATA FILENAME AS ''A:XXXA.DAT'' '
      READ *,DATFN2
      OPEN(UNIT=4,FILE=DATFN2)
C
C  READ THE NUMBER OF FREQUENCIES AT WHICH THE SAMPLE WAS TESTED
      READ(3,*)I
C
C  START PREDICTION PROCESS FOR A PARTICULAR FREQUENCY
C  GET DATA FOR THAT FREQUENCY
C
      DO 300 K=1,I
      READ(3,*)FREQ,AR,PHAS
      READ(4,*)BMAXA,TMAXA
C
C  CALCULATE THE MAXIMUM DISPLACEMENT FROM THE MAXIMUM ACCELERATION
C
      LAMBDA=BMAXA/FREQ**2 0
C
C  USE THE APPROPRIATE REGRESSION EQUATIONS FOR XI AND ALPHA
C
      ALPHA=EXP(C1)/FREQ**C2
      XI=-1.0*EXP(C3)/FREQ**C4
C
C  SECOND-ORDER VISCOELASTIC STRESS-STRAIN MODEL EQUATIONS FOR THE
C  STRESS AT THE TOP OF THE SAMPLE
C
      Z0=CMPLX(E-XI*FREQ**2.0,ALPHA*FREQ)
      Z1=CSQRT(Z0)
      Z2=M*FREQ/(A*SQRT(RO)*Z1)
      W=CLOG((CMPLX(0 0,1 0)+Z2)/(CMPLX(0 0,1.0)-Z2))
      PHI=CMPLX(0 0,0 5)*W
      THETA=FREQ*SQRT(RO)/Z1
```

```
      PSI=LAMBDA*THETA*(CSIN(THETA*L+PHI)*CCOS(THETA*L)/
     * CCOS(THETA*L+PHI)-CSIN(THETA*L))
      STR=PSI*Z0
C
C  PREPARE RESULTS FOR OUTPUT
C
      MSTRS(K)=TMAXA*M/A
      PSTRS(K)=CABS(STR)
C
C  OUTPUT RESULTS TO PRINTER
C
      WRITE(9,13)FREQ,MSTRS(K),PSTRS(K)
   13 FORMAT(1X,F9 2,2F10 1)
C
C  OUTPUT RESULTS TO DISK FILE FOR EASY PLOTTING
C
      WRITE(1,14)MSTRS(K),PSTRS(K)
   14 FORMAT(1X,F8 1,1X,F8 1)
C
C  GO BACK TO ITERATE FOR ANOTHER FREQUENCY IF NECESSARY
C
  300 CONTINUE
C
C  WRITE STRESS DATA TO DISK FILE FOR REGRESSION
C
      WRITE(2,15)I
   15 FORMAT(1X,'2,',I2,',0')
      WRITE(2,16)
   16 FORMAT(1X,'"MSTRESS"')
      DO 200 K=1,I
  200 WRITE(2,17)MSTRS(K)
   17 FORMAT(1X,F8 1)
      WRITE(2,18)
   18 FORMAT(1X,'"PSTRESS"')
      DO 400 K=1,I
  400 WRITE(2,17)PSTRS(K)
C
C  CLOSE ALL FILES
C
      CLOSE(UNIT=1)
      CLOSE(UNIT=2)
      CLOSE(UNIT=3)
      CLOSE(UNIT=4)
      CLOSE(UNIT=9)
      STOP
      END
```

VITA

Michael Fred Kocher

Candidate for the Degree of

Doctor of Philosophy

Thesis: DYNAMIC STRESS-STRAIN MODELS FOR SOIL USING WAVE PROPAGATION

Major Field: Agricultural Engineering

Biographical:

Personal Data: Born in St. Joseph, Missouri, April 6, 1957, the son of Rev. Robert G. and Shirley L. Kocher. Married to Jodi E. Wolford on May 26, 1984.

Education: Graduated from Bertrand High School, Bertrand, Nebraska, in May 1975; received Bachelor of Science degree in Agricultural Engineering from the University of Nebraska-Lincoln in December, 1979; received Master of Science degree from the University of Nebraska-Lincoln in August, 1983; completed requirements for the Doctor of Philosophy degree at Oklahoma State University in May, 1986.

Professional Experience: Extension Project Engineer, Department of Agricultural Engineering, University of Nebraska-Lincoln, August, 1979 to April, 1983; Graduate Research Assistant, Department of Agricultural Engineering, University of Nebraska-Lincoln, May, 1983 to August, 1983; Graduate Teaching Assistant, Department of Agricultural Engineering, Oklahoma State University, August, 1983 to December, 1983; Graduate Research Assistant, Department of Agricultural Engineering, Oklahoma State University, January, 1984, to present. Passed Engineer in Training Exam, Spring 1980. Student Member of the American Society of Agricultural Engineers.